

PLANT UPTAKE AND IMPACT OF ENGINEERED METALLIC
NANOPARTICLES IN SOIL PLANT SYSTEMS

A Dissertation

by

XIAOXUAN WANG

Submitted to the Graduate and Professional School of
Texas A&M University
in partial fulfillment of the requirements for the degree of

DOCTOR OF PHILOSOPHY

Chair of Committee,	Xingmao Ma
Co-Chair of Committee,	Fugen Dou
Committee Members,	Qi Ying
	Virender Sharma
Head of Department,	Zachary Grasley

May 2022

Major Subject: Civil Engineering

Copyright 2022 Xiaoxuan Wang

ABSTRACT

Expanding applications of metallic nano-agricheicals have resulted in their increasing accumulation in agricultural soils. In addition to their potential uptake by agricultural crops, the effects of engineered nanoparticles (ENPs) on soil properties and the fate of co-contaminants in soil plant systems are still poorly understood.

The goal of this study was to gain better understanding on the impact of metallic ENPs on paddy soil health and their interactions with co-contaminants such as arsenic (As) and cadmium (Cd), as well as their plant uptake and accumulation. To achieve this goal, greenhouse experiments were performed to evaluate the effects of zinc oxide nanoparticles (ZnO NPs), copper oxide nanoparticles (CuO NPs), and silicon oxide nanoparticles (SiO₂ NPs), and their bulk and ionic counterparts on the properties of paddy soil, the formation and properties of iron plaque and As accumulation in rice. A pot experiment was also conducted to investigate the effect of SiO₂ NPs on the simultaneous uptake of As and Cd by rice seedlings with different water management schemes, because As and Cd co-contamination is common in paddy soils and both elements are hazardous to human health. Finally, machine learning was applied to predict plant uptake of metallic ENPs.

Our results showed distinctive effects of ENPs from their bulk and ionic counterparts on a range of soil properties, such as soil pH, redox potential, soil organic carbon (SOC), and cation exchange capacity (CEC). Highly intriguingly, our results for the first time showed that chemical amendments such as metallic ENPs affected iron

plaque formation on rice root surface and consequently As accumulation in rice tissues. The impact of chemical amendments on iron plaque formation varied with the composition of ENPs and the growth stage of rice plants. Our results also showed that simultaneous reduction of As and Cd in rice shoots could potentially be achieved by proper combination of SiO₂ NPs and water management. Furthermore, machine learning accurately predicted plant uptake and translocation of ENPs based on a set of input parameters that include representative properties of ENPs, plant species and soil properties. Overall, this study provided insight into safe and sustainable applications of ENPs in agriculture.

ACKNOWLEDGEMENTS

I would like to express my most profound appreciation to my committee chair, Dr. Ma. The completion of my dissertation would not have been possible without the support and nurturing of him. I would also like to extend my deepest gratitude to my co-chair Dr. Dou for his kindly help and valuable advice. I am also grateful to my committee members, Dr. Ying, Dr. Sharma, and a previous committee member Dr. Schwab, for their guidance and support throughout the course of this research.

Thanks also go to all my colleagues and friends for their kind help and care. I would like to recognize the help that I received from Cheyenne, Weilan, Yinghao, Binglin and Jieming throughout my research. Thanks also go to the department faculty and staff for making my time at Texas A&M University a great experience.

Finally, many thanks to my family, especially my dad, for his constant encouragement and selfless love. Special thanks to my boyfriend, Brandon, for his continuous understanding and love, as well as his families for their unending support and inspiration. Thanks also to my dogs for their companionship and comfort during my research and writing process.

CONTRIBUTORS AND FUNDING SOURCES

Contributors

Part 1, faculty committee recognition

This work was supervised by a dissertation committee consisting of Professor Xingmao Ma (advisor) and Professors Fugen Dou (co-advisor) and Professor Qi Ying of the Department of Civil and Environmental Engineering, and Professor Virender Sharma of the Department of Public Health.

Part 2, student/collaborator contributions

All work for the dissertation was completed by the student, in collaboration with Dr. Fugen Dou of the Texas A&M AgriLife Research Center at Beaumont, Dr. Jiechao Jiang at the University of Texas Arlington and Liwei Liu at the National Pingtung University of Science and Technology.

Funding Sources

Graduate study was supported by an excellence fellowship from Zachry Department of Civil Engineering. This work was also made possible in part by National Science Foundation Grant under Grant Number 1900022.

TABLE OF CONTENTS

	Page
ABSTRACT	ii
ACKNOWLEDGEMENTS	iv
CONTRIBUTORS AND FUNDING SOURCES.....	v
TABLE OF CONTENTS	vi
LIST OF FIGURES.....	x
LIST OF TABLES	xvi
CHAPTER I INTRODUCTION	1
Research hypothesis and goal	7
CHAPTER II ELUCIDATING THE IMPACT OF THREE METALLIC NANOAGRICHEMICALS AND THEIR BULK AND IONIC COUNTERPARTS ON THE CHEMICAL PROPERTIES OF BULK AND RHIZOSPHERE SOILS IN RICE PADDIES	10
Introduction	10
Materials and Methods	14
Chemicals	14
Nanoparticles Characterization	14
Soil Collection and Characterization.....	15
Experimental Setup	15
Preparation of Bulk and Rice Rhizosphere Soil	16
Soil Sampling and Analysis	17
Statistical Analysis	19
Results and Discussion.....	20
Particles characterization.....	20
Soil pH.....	22
Soil Eh	25
Soil CEC.....	29
Plant-available As.....	31
Conclusions	35

CHAPTER III EFFECTS OF ZINC FERTILIZERS ON ARSENIC ACCUMULATION AND SPECIATION IN RICE (ORYZA SATIVA L.): FORMATION OF IRON PLAQUE	37
Introduction	37
Materials and Methods	40
Nanoparticles and other chemicals	40
Soil collection and characterization	41
Treatment setup	42
Plant growth and harvest	42
Plant tissue sampling	43
Dithionite-citrate-bicarbonate (DCB) extraction of iron plaque	44
X-ray Diffraction analysis of iron plaque.....	44
Total elements in rice tissues.....	45
As speciation in plant tissues.....	45
Fe(II) and Fe(III) in soil	46
Statistical Analysis	46
Results and Discussion.....	46
Rice biomass and yield.....	46
Impacts of Zn amendments on the total As in rice tissues	48
Effects of Zn amendments on As speciation	51
Impacts of Zn fertilizers on iron plaque formation	54
Characterization of iron plaque with X-ray diffraction.....	57
Conclusions	57
 CHAPTER IV IMPACT OF SOIL COPPER AMENDMENTS ON ARSENIC ACCUMULATION AND SPECIATION IN RICE (ORYZA SATIVA L.) IN A LIFE-CYCLE STUDY	 59
Introduction	59
Materials and Methods	61
Nanoparticles Characterization	61
Soil Characterization and Preparation	62
Rice Growth and Sampling	63
Iron Plaque Extraction.....	64
Total Elements in Rice Tissues and Grains.....	64
As Speciation in Rice Tissues and Grains.....	65
Statistical Analyses.....	65
Results and Discussion.....	66
Effects on Rice Plant Growth and Yield	66
Effects of Cu amendments on As Accumulation in Rice	69
Effects of Cu amendments on As Speciation in Rice.....	70
Effects of Cu amendments on iron plaque formation.....	74
Conclusions	76

CHAPTER V SIMULTANEOUS MITIGATION OF ARSENIC AND CADMIUM ACCUMULATION IN RICE (ORYZA SATIVA L.) SEEDLINGS BY SILICON OXIDE NANOPARTICLES UNDER DIFFERENT WATER MANAGEMENT SCHEMES	78
Introduction	78
Materials and Methods	82
Chemicals and Nanoparticles Characterization.....	82
Pot Experiment	83
Sampling and Analysis of the Soil Solution.....	85
Total Elements in Rice Plants	85
Statistical Analysis	86
Results	86
SiO ₂ Nanoparticle Characterization	86
Soil Redox Potential (Eh) and pH	87
Rice Plant Biomass.....	89
Accumulation of As in Rice Tissues	90
Accumulation of Cd in Rice Tissues.....	91
Accumulation of Si in Rice Tissues	92
Soil solution Chemistry	93
SEM of Rice Root	95
Discussion	97
SiO ₂ NPs and Cd Accumulation in Rice Tissues	99
SiO ₂ NPs and As Accumulation in Rice Tissues	100
Conclusions	103
CHAPTER VI PREDICTION OF PLANT UPTAKE AND TRANSLOCATION OF ENGINEERED METALLIC NANOPARTICLES BY MACHINE LEARNING.....	105
Introduction	105
Materials and Methods	108
Data collection and processing.....	108
Back propagation neural network (BPNN)	111
Sensitivity analysis (SA)	112
Results and Discussion.....	114
BPNN simulation on the plant uptake of ENPs in hydroponic systems	114
BPNN simulation on the plant uptake of ENPs in soil systems	116
Sensitivity analysis on the input variables	118
Conclusion.....	122
CHAPTER VII CONCLUSIONS AND RECOMMENDATIONS.....	124
Conclusions	124
Recommendations	125

REFERENCES.....127

LIST OF FIGURES

	Page
Figure I-1. Illustration of the primary goal and specific objectives of this dissertation. (Created with BioRender.com).....	7
Figure II-1. The effects of different soil amendments on soil pH at (a) Day 47 and (b) Day 104 of the bulk soil, and (c) Day 47 and (d) Day 104 of the rhizosphere soil. Different letters indicate significant differences ($p \leq 0.05$) according to one-way ANOVA followed by Tukey's test. All reported values represent mean \pm standard deviation (n=3).	23
Figure II-2. The effects of different soil amendments on soil Eh at (a) Day 47 and (b) Day 104 of the bulk soil, and at (c) Day 47 and (d) Day 104 of the rhizosphere soil. Different letters indicate significant differences ($p \leq 0.05$) according to one-way ANOVA followed by Tukey's test. All reported values represent mean \pm standard deviation (n=3).	26
Figure II-3. The effects of different soil amendments on SOC at (a) Day 47 and (b) Day 104 of the bulk soil, and at (c) Day 47 and (d) Day 104 of the rhizosphere soil. Different letters indicate significant differences ($p \leq 0.05$) according to one-way ANOVA followed by Tukey's test. All reported values represent mean \pm standard deviation (n=3).	28
Figure II-4. The effects of different soil amendments on soil cation exchange capacity (CEC) at (a) Day 47 and (b) Day 104 of the bulk soil, and (c) Day 47 and (d) Day 104 of the rhizosphere soil. Different letters indicate significant differences ($p \leq 0.05$) according to one-way ANOVA followed by Tukey's test. All reported values represent mean \pm standard deviation (n=3).	30
Figure II-5. The effects of different soil amendments on total plant-available As at (a) Day 47 and (b) Day 104 of the bulk soil, and (c) Day 47 and (d) Day 104 of the rhizosphere soil. Different letters indicate significant differences ($p \leq 0.05$) according to one-way ANOVA followed by Tukey's test. All reported values represent mean \pm standard deviation (n=3).	33
Figure II-6. The Pearson correlation networks between plant-available As at different stages and other soil chemical properties (pH, Eh, SOC (soil organic carbon), CEC (cation exchange capacity)). Green lines indicate positive correlation (correlation coefficient > 0.20). Red lines indicate negative correlation (correlation coefficient < 0.20).	34
Figure III-1. The biomass of (a) root and (b) shoot of rice at the maximum tillering and mature stage; and the biomass of (c) husk and (d) de-husked grains at	

the mature stage. Values represent mean \pm SD ($n = 4$), with different letters indicating significant differences ($p \leq 0.05$) according to one-way ANOVA followed by Tukey's test. Asterisks (*) indicate significant differences between two growth stages according to t-test.	48
Figure III-2. Total As in rice (a) root and (b) shoot at the maximum tillering and mature stages; and in rice (c) husk and (d) de-husked grains at the mature stage. Values represent mean \pm SD ($n = 4$), with the different letters indicating significant differences ($p \leq 0.05$) according to one-way ANOVA followed by Tukey's test. Asterisks (*) indicate significant differences between two different growth stages according to t-test.	49
Figure III-3. As speciation in rice root and shoot at the maximum tillering (a and b) and the mature stage (c and d), and in (e) husks, and (f) de-husked grains. Reported values represent mean \pm SD ($n = 4$), with different letters indicating significant differences ($p \leq 0.05$) according to one-way ANOVA followed by Tukey's test.	50
Figure III-4. The impacts of different Zn amendments on As(III) to total As ratio in rice (a) root and (b) shoot at the maximum tillering and mature stage; and the As(III) to total As ratio in rice (c) husk and (d) de-husked grains at the mature stage. Values represent mean \pm SD ($n = 4$), with different letters indicating significant differences ($p \leq 0.05$) according to one-way ANOVA followed by Tukey's test.	53
Figure III-5. (a) The amount of DCB-extractable Fe normalized by root dry weight and (b) the total mass of Fe in the iron plaque at maximum tillering and mature stages. Values represent mean \pm SD ($n = 4$), with different letters indicating significant differences ($p \leq 0.05$) according to one-way ANOVA followed by Tukey's test. Asterisks (*) indicate significant differences between two different growth stages according to t-test.	53
Figure III-6. Fe(II)/Fe(III) ratio (a) in the bulk soil and (b) in the rhizosphere soil at two growth stages. Values represent mean \pm SD ($n = 4$), with different letters indicating significant differences ($p \leq 0.05$) according to one-way ANOVA followed by Tukey's test. Asterisks (*) indicate significant differences between two different growth stages according to t-test.	55
Figure III-7. (a) The total mass of As in the iron plaque, (b) As content in the DCB extraction normalized by dry root weight, and (c) As/Fe ratio in the iron plaque at maximum tillering and mature stages. Values represent mean \pm SD ($n = 4$), with different letters indicating significant differences ($p \leq 0.05$) according to one-way ANOVA followed by Tukey's test. Asterisks (*) indicate significant differences between two different growth stages according to t-test.	55

Figure III-8. X-ray diffraction spectra of iron plaque from different treatments at (a) the maximum tillering stage and (b) the mature stage.....	57
Figure IV-1. The biomass of rice (a) root and (b) shoot at the maximum tillering and mature stage; and the biomass of rice (c) husk and (d) de-husked grains at the mature stage exposed to arsenic and different Cu amendments in soil ($n = 4$). Different letters indicate significant differences between different treatments ($p < 0.05$). Asterisks (*) indicate significant differences between maximum tillering and mature stages according to t-test.....	66
Figure IV-2. The total As in rice (a) root and (b) shoot at the maximum tillering and mature stage; and the As accumulation in rice (c) husk and (d) de-husked grains at the mature stage exposed to arsenic and different Cu amendments in soil ($n = 4$). Different letters indicate significant differences between different treatments ($p < 0.05$). Asterisks (*) indicate significant differences between maximum tillering and mature stages according to t-test.....	67
Figure IV-3. The As speciation in rice (a)(c) root and (b)(d) shoot at the maximum tillering stage and mature stage, respectively; and the biomass of rice (e) husk and (f) de-husked grains at the mature stage exposed to arsenic and different Cu amendments in soil ($n = 4$). Different letters indicate significant differences between different treatments in each As species group ($p < 0.05$).....	68
Figure IV-4. The total Cu in rice (a) root and (b) shoot at the maximum tillering and mature stage; and in rice (c) husk and (d) de-husked grains at the mature stage exposed to arsenic and different Cu amendments in soil ($n = 4$). Different letters indicate significant differences between different treatments ($p < 0.05$). Asterisks (*) indicate significant differences between maximum tillering and mature stages according to t-test.....	71
Figure IV-5. The As(III)/total As ratio in rice (a) root and (b) shoot at the maximum tillering and mature stage; and the As accumulation in rice (c) husk and (d) de-husked grains at the mature stage exposed to arsenic and different Cu amendments in soil ($n = 4$). Different letters indicate significant differences between different treatments ($p < 0.05$).....	72
Figure IV-6. The (a) total mass of Fe and (b) amount of Fe normalized by root dry weight in the iron plaque at the maximum tillering and mature stage exposed to arsenic and different Cu amendments in soil ($n = 4$). Different letters indicate significant differences between different treatments ($p < 0.05$). Asterisks (*) indicate significant differences between maximum tillering and mature stages according to t-test.....	73

Figure IV-7. The (a) total mass of As, (b) amount of As normalized by root dry weight in the iron plaque, and (c) As/Fe ratio in the iron plaque at the maximum tillering and mature stage exposed to arsenic and different Cu amendments in soil ($n = 4$). Different letters indicate significant differences between different treatments ($p < 0.05$). Asterisks (*) indicate significant differences between maximum tillering and mature stages according to t-test.....74

Figure V-1. SiO₂ NPs characterization. (a) HRTEM image, showing the size and shape of average SiO₂ NPs, (b) EDS spectrum of SiO₂ NPs at the selected area in red box, and (c) electron diffraction pattern of SiO₂ NPs.....87

Figure V-2. Redox potential (a and b) and pH (c and d) of soil in different water management: CF (a and c) and AWD (b and d) exposed to 1 mg/kg of As with 5 mg/kg of Cd alone or As and Cd with 150 mg/kg, 500 mg/kg or 2000 mg/kg of SiO₂ NPs.....88

Figure V-3. Dry biomass of rice tissues under different level of SiO₂ NPs treatment and different water management schemes. Root biomass (a) and shoot biomass (b) of rice plants treated with different combination of 1 mg/kg of As with 5 mg/kg of Cd and 150 mg/kg, 500 mg/kg or 2000 mg/kg of SiO₂ NPs under two different water managements: CF and AWD. Values represent mean \pm SD ($n=3$). Different letters indicate significant differences ($p \leq 0.05$) according to one-way ANOVA followed by Tukey's test.89

Figure V-4. Total arsenic in rice root (a) and shoot (b) exposed to 1 mg/kg of As with 5 mg/kg of Cd alone or As and Cd with 150 mg/kg, 500 mg/kg or 2000 mg/kg of SiO₂ NPs under two different water managements: CF and AWD. Values represent mean \pm SD ($n=3$). Different letters indicate significant differences ($p \leq 0.05$) according to one-way ANOVA followed by Tukey's test. Asterisks (*) indicate significant differences between water management at a particular Si concentration level, according to t-test.91

Figure V-5. Total cadmium in rice root (a) and shoot (b) exposed to 1 mg/kg of As with 5 mg/kg of Cd alone or As and Cd with 150 mg/kg, 500 mg/kg or 2000 mg/kg of SiO₂ NPs under two different water managements: CF and AWD. Values represent mean \pm SD ($n=3$). Different letters indicate significant differences ($p \leq 0.05$) according to one-way ANOVA followed by Tukey's test. Asterisks (*) indicate significant differences between water management at a particular Si concentration level, according to t-test.92

Figure V-6. Concentration of element Si in rice root (a) and shoot (b) exposed to 1 mg/kg of As with 5 mg/kg of Cd alone or As and Cd with 150 mg/kg, 500 mg/kg or 2000 mg/kg of SiO₂ NPs under two different water managements: CF and AWD. Values represent mean \pm SD ($n=3$). Different letters indicate

significant differences ($p \leq 0.05$) according to one-way ANOVA followed by Tukey's test. Asterisks (*) indicate significant differences between water management at a particular Si concentration level, according to t-test.93

Figure V-7. Concentration of element As (a), Cd (b) and Si (c) in soil solution and pH (d) of soil solution extracted from the soil exposed to 1 mg/kg of As with 5 mg/kg of Cd alone or As and Cd with 150 mg/kg, 500 mg/kg or 2000 mg/kg of SiO₂ NPs under two different water managements: CF and AWD. Values represent mean \pm SD (n=3). Different letters indicate significant differences ($p \leq 0.05$) according to one-way ANOVA followed by Tukey's test. Asterisks (*) indicate significant differences between water management at a particular Si concentration level, according to t-test.94

Figure V-8. Scanning electron micrographs (SEM) of rice root under various condition: (a) control under CF (b) control under AWD (c) As and Cd without SiO₂ NPs under CF, (d) As and Cd without SiO₂ NPs under AWD. (e) As and Cd with 150 mg/kg SiO₂ NPs under CF, (f) As and Cd with 150 mg/kg SiO₂ NPs under AWD. (g) As and Cd with 500 mg/kg SiO₂ NPs under CF, (h) As and Cd with 500 mg/kg SiO₂ NPs under AWD. (i) As and Cd with 2000 mg/kg SiO₂ NPs addition under CF, (j) As and Cd with 2000 mg/kg SiO₂ NPs addition under AWD.96

Figure V-9. (a) SEM of rice root in the presence of 500 mg/kg SiO₂ NPs under CF. (b and c) Energy dispersive X-ray (EDX) spectra taken from the point A and B in figure 8a.97

Figure VI-1. Frequency of (a) ENPs composition for RCF; (b) Plant subclass for RCF; (c) ENPs composition for TF; and (d) Plant subclass for TF in the hydroponic systems. Included refers to the dataset used in the modeling after cleaning. Excluded refers to the raw dataset that was not included in the modeling. 110

Figure VI-2. Frequency of (a) ENPs composition for RCF; (b) Plant subclass for RCF; (c) ENPs composition for TF; and (d) Plant subclass for TF in the soil system. Included refers to the dataset used in the modeling after cleaning. Excluded refers to the raw dataset that was not included in the modeling. 111

Figure VI-3. ANN simulation correlation in model training/CV/testing stage of (a) RCF, and (b) TF in hydroponic system. 114

Figure VI-4. ANN simulation correlation in model training/CV/testing stage without input "ENPs initial concentration" of (a) RCF, and (b) TF; and with input "ENPs initial concentration" of (c) RCF, and (d) TF in soil system. 117

Figure VI-5. Sensitivity analysis index of each input descriptor for (a) RCF model and (b) TF model in hydroponic system; and (c) RCF model and (d) TF model in soil system. 118

Figure VI-6. Boxplot of cleaned dataset showing (a) RCF by ENPs composition; (b) RCF by plant subclass; (c) TF by NPs composition; and (d) TF by plant subclass in hydroponic system. The cross marker represents the data means and the lines indicated data medians. 120

Figure VI-7. Boxplot of cleaned dataset showing (a) RCF by ENPs composition; (b) RCF by plant subclass; (c) TF by ENPs composition; and (d) TF by plant subclass in soil system. The cross marker represents the data means and the lines indicated data medians. 122

LIST OF TABLES

	Page
Table II-1. The hydrodynamic diameter and zeta potential of three metallic nanoparticles (NPs) and bulk particles (BPs). All reported values represent mean \pm standard deviation (n=3). NA: not available.....	21
Table II-2. P-values of three-way ANOVA on soil pH, Eh, SOC (soil organic carbon), CEC (cation exchange capacity) and plant available-As (top) and p-values of Treatment*Soil*Stages effects sliced by 'Soil' (bottom).....	22
Table III-1. Soil characteristics of Topsoil (0-15 cm) from Eagle Lake, TX by the Soil, Water and Forage Testing Laboratory at Texas A&M University.....	41
Table V-1. Results of two-way ANOVA test. P-values of significant effects of different concentration of SiO ₂ NPs and/or different water management and interaction between them are highlighted in bold.....	89
Table VI-1. Characteristics of input and output numerical variables in the dataset.	113

CHAPTER I

INTRODUCTION

Engineered nanoparticles (ENPs) have attracted considerable attention over the past few decades due to their unique properties and growing applications in agriculture as slow-releasing fertilizers, antimicrobial agents, and nanocarriers of essential nutrients (Parada, et al. 2019). As a primary component of nano-agrichemicals, metallic nanoparticles played critical roles in advancing modern agriculture (Mishra, et al. 2017). For example, zinc oxide nanoparticles (ZnO NPs) have been explored as a novel fungicide, pesticide, and slow-releasing nano-fertilizer (Elhaj Baddar and Unrine 2018; Sun, et al. 2018a; Zabrieski, et al. 2015). Likewise, copper oxide nanoparticles (CuO NPs) have exhibited the potential to be a slow-releasing source of Cu, which also improve contents of nutrient elements such as Ca, Fe, Mg, and Mn in green onion (Wang, et al. 2020). Silicon oxide nanoparticles (SiO₂ NPs) have been synthesized as a carrier and slow releasing fertilizer of N, P, and K (Mushtaq, et al. 2018). Due to the rapid increase in nano-agrichemical applications, their accumulation in agricultural soils is unavoidable (Hochella, et al. 2019). A previous report on nanoparticle exposure indicated that between 8% and 28% of commercially manufactured metallic nanoparticles would end up in agriculture soils (Tolaymat, et al. 2017). The close interactions between ENPs and soil particles, and co-present contaminants in a soil and plant system necessitate a solid understanding of the impact of metallic nanoparticles on

soil health, as well as the plant uptake of ENPs and co-contaminants (Deng, et al. 2017; Rai, et al. 2018; Tourinho, et al. 2012).

Chemical properties of a soil, such as the percentage of soil organic carbon (SOC), pH, and cation exchange capability (CEC), are critical because they affect soil fertility and ecosystem sustainability (Bünemann, et al. 2018). They also affect the availability of micronutrients and pollutants in soil; therefore, the modification of these soil properties can have important implications for the nutritional values of food products and food safety. However, while the effects of ENPs on biological aspects of soil health have been widely investigated, limited research has performed on the impact of ENPs on soil chemical properties (Chai, et al. 2015; Guan, et al. 2020; Rajput, et al. 2018b; Samarajeeva, et al. 2020; Simonin, et al. 2016; Xu, et al. 2015). One study reported that CuO NPs at concentrations of 10, 100, and 1000 mg/kg significantly increased the soil pH and Eh within 10 hours of exposure in a low organic matter soil, but these effects were only observed at the highest concentration of 1,000 mg/kg in the high organic matter soil (Shi, et al. 2018). Another study indicated that the addition of 10 g/kg CuO NPs and Fe₃O₄ NPs did not affect SOC but changed humic substances in soil (Ben-Moshe, et al. 2013).

The properties of paddy soil, a common agricultural farmland in the world, could potentially be affected by ENPs released into the soil. Arsenic (As) is a heavy metal commonly detected in paddy soils and is a global food safety concern in rice consuming populations (Islam, et al. 2016). Therefore, the plant-available As concentration in paddy soil is an important indicator of soil health (Islam, et al. 2016; Qaswar, et al. 2020).

Considerable studies have been conducted to address rice plant uptake of As, but only few studies have reported the potential impact of nano-agricheicals on the phytoavailability of As in soil (Duncan and Owens 2019). The properties of paddy soil are heavily affected by processes involved with rice roots (Chen, et al. 2016a; Lambers, et al. 2009). Root exudates, including amino acid and organic acid, could induce significant changes in soil pH, Eh, SOC, nutrient oxidation state and bioavailability, making rhizosphere soil quite different from the bulk soil (Huang, et al. 2020; Seshadri, et al. 2015). Therefore, a systematic study focusing on the impact of ENPs on soil chemical health for both bulk and rhizosphere soil is of great interest.

With the rapidly growing world population and food demand, rice (*Oryza sativa* L.) serves more than three billion people as a staple food (Hoang, et al. 2019). However, the high propensity of arsenic (As) accumulation in rice grains provides a significant pathway to expose this carcinogen to the rice consumption population (Chen, et al. 2017a). Dietary consumption of rice and rice-based products has been associated with various human diseases (Shrivastava, et al. 2020). Increasing studies have been conducted to seek for effective approaches to reduce As accumulation in rice crops. Adjustment of water and nutrient management schemes, and addition of soil amendments are common approaches for As control in rice paddies. Among them, nanoagrichemicals have showed great potential to alleviate As toxicity and accumulation in rice tissues (Cui, et al. 2020; Wu, et al. 2020b; Yan, et al. 2021). Our previous studies with ZnO NPs and CuO NPs indicated that both ENPs could potentially alleviate As accumulation in rice, but different ENPs have different impacts on the uptake of As by

rice plants, and their impacts also differed from the respective ionic form (Ma, et al. 2020b; Wang, et al. 2019b; Wang, et al. 2018). In addition to the total As accumulation, the effects of ENPs on the As speciation in rice tissues are of great interest since different As species do not have equal toxicity (Garg and Singla 2011; Hughes 2002). Several previous investigations have shown that nanoparticles have the potentials to affect As speciation in rice seedlings. For instance, Liu et al, reported that CuO NPs could increase As(V) fraction in 18-day-old rice seedlings by directly oxidizing As(III) to As(V) on the surface of CuO NPs (Liu, et al. 2019; Martinson and Reddy 2009). Our previous studies indicated that cerium oxide (CeO₂) NPs at 100 mg/L could inhibit the translocation of As(III) from root to shoot but somehow promoted As(V) transport, while ZnO NPs at the same concentration had a negative effect on the root uptake of both As(III) and As(V) (Wang, et al. 2018). Another study also suggested that 10-100 mg/L of the ZnO NPs significantly reduced the ratio of As(III) to total As in the rice shoot at early growth stages (Yan, et al. 2021). However, most previous studies only investigated the impact of ENPs on As accumulation in early growth stages in hydroponic systems, the effects of ENPs on As accumulation and speciation in rice grains in a soil system and the underlying mechanisms are still unknown (Wang, et al. 2018; Wu, et al. 2020a; Yan, et al. 2021).

In a soil system, the effects of ENPs on As uptake and speciation could be due to many different processes such as the altered biological activities in soil by ENPs and their direct interactions with plants (Rajput, et al. 2018a; Verma, et al. 2021; Zhao, et al. 2013). Iron plaque formed on rice root surface has been reported to play an important

role in the bioavailability of As (Lee, et al. 2013; Liu, et al. 2006). Iron plaque is formed when Fe^{2+} reacts with radially released oxygen from rice roots (Bacha and Hossner 1977; Chen, et al. 1980; Hansel, et al. 2001). An enhanced formation of iron plaque was observed in response to As addition due to the increased oxidative stress caused by As (Lee, et al. 2013). In addition, previous studies also suggested that iron plaque could sequester As and acted as a protective barrier for As uptake (Liu, et al. 2006; Syu, et al. 2013). However, none of the previous studies has investigated the impact of ENPs on the formation and properties of iron plaque and their effects on rice plant uptake and accumulation of As in a soil system extending to the life cycle of the plant.

Besides As, cadmium (Cd) is another typical contaminant in paddy soils, which could cause various human health problems such as kidney failure and cancer (Huff, et al. 2007). As and Cd co-contaminate many paddy soils worldwide (Khanam, et al. 2020; Palansooriya, et al. 2020). Practical approaches to simultaneously decrease both As and Cd accumulation in rice are essential. Water management is a popular strategy to lower As and Cd accumulation in rice grains. However, simultaneously reducing As and Cd with only water management is difficult due to the trade-off relationship between As and Cd availability. In fully flooded paddies, Cd uptake is often inhibited because of the decreased dissolution of cadmium sulfide (CdS), however, As uptake is enhanced because inorganic As(III) is more mobile and bioavailable than As(V) (Honma, et al. 2016b; Sun, et al. 2014b). Previous studies have indicated that SiO_2 NPs could potentially lower either As or Cd in rice and wheat separately through different mechanisms compared to conventional Si fertilizer (Ali, et al. 2019; Liu, et al. 2014). As

a result, it is critical to investigate whether SiO₂ NPs could reduce As and Cd accumulation simultaneously as a novel silicon amendment.

In addition to their interaction with co-contaminants, ENPs themselves could accumulate in plant tissues and become a food safety concern. Due to the rapid development and broad application of ENPs in a variety of industrial and commercial areas, especially in agriculture, agricultural soils have become a primary sink for ENPs (Acharya and Pal 2020; Chhipa 2017; Kah 2015; Kah, et al. 2018; Nikolova and Chavali 2020; Wang, et al. 2019a; Xin, et al. 2020). As a result, plants are very likely to be exposed to ENPs, which raises food safety concerns about ENPs uptake and accumulation. Many previous studies in the past decade have confirmed the uptake of ENPs and their dissolved ions by plants. However, significant variations between different studies can be found, likely due to the use of different ENPs, different plant species and different growth conditions in different studies. Due to the large array of ENPs and their properties, various plant types, and different conditions for plant growth, it is impossible to experimentally investigate the uptake and accumulation of ENPs by plants for all possible combinations of ENPs, plants and growing conditions. Some predictive models are critically needed to enable the estimation of ENP plant uptake based on ENPs properties and plant species at a specific growth condition. Conventional linear methods are ineffective to predict the uptake and translocation of ENPs by plants (Lv, et al. 2019). Machine learning (ML) has recently been applied to simulate plant uptake of contaminant (Bagheri, et al. 2020; Bagheri, et al. 2021; Jaskulak, et al. 2020; Rossi, et al. 2019). For example, artificial neural network (ANN) has been successfully

applied to predict root concentration factor (RCF) and transpiration stream concentration factor (TSCF) of organic contaminants in plants (Bagheri, et al. 2020). Therefore, machine learning was investigated as an effective tool to predict the plant uptake of ENPs and identify important factors governing this process.

Research hypothesis and goal

The primary goal of this dissertation was to evaluate the effects of engineered metallic nanoparticles on plant uptake of ENPs and their co-contaminants, and the soil property that indirectly affect the plant uptake of ENPs and other soil borne chemicals. A brief summary of the four objectives is presented in **Figure I-1**.

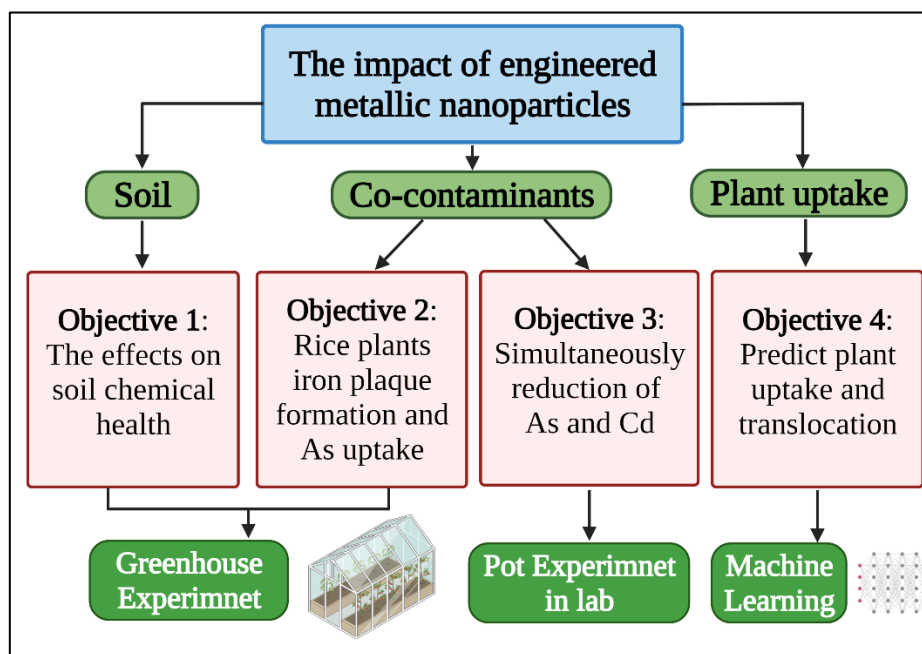


Figure I-1. Illustration of the primary goal and specific objectives of this dissertation. (Created with BioRender.com)

To achieve the overall goal, four hypotheses were formulated:

Hypothesis 1: ZnO NPs, CuO NPs and SiO₂NPs affect the chemical properties of bulk and rhizosphere paddy soil, and consequently the overall soil health.

Hypothesis 2: ZnO NPs, and CuO NPs affect the formation and properties of iron plaque and plant uptake of As.

Hypothesis 3: Combined water management and SiO₂ NPs amendment could simultaneously lower As and Cd accumulation in rice seedlings.

Hypothesis 4: Plant uptake of engineered metallic nanoparticles can be simulated by machine learning based on essential physicochemical properties of ENPs and plant species.

To test the above hypotheses, five studies were conducted and their objectives were listed below:

- (1) To determine the impact of three selected metal oxide nanoparticles and their bulk and ionic counterparts on the chemical properties of soil;
- (2) To elucidate the impact of ZnO NPs, and their ions and bulk equivalents on the formation and properties of iron plaques and the uptake and accumulation of As in rice tissues;
- (3) To determine the impact of CuO NPs, and their ions and bulk materials on the uptake and accumulation of As in rice;
- (4) To investigate the effect of SiO₂ NPs of the simultaneous control of As and Cd under different water management schemes.

(5) To predict the plant uptake and translocation of engineered metallic nanoparticles using machine learning.

CHAPTER II

ELUCIDATING THE IMPACT OF THREE METALLIC NANOAGRICHEMICALS
AND THEIR BULK AND IONIC COUNTERPARTS ON THE CHEMICAL
PROPERTIES OF BULK AND RHIZOSPHERE SOILS IN RICE PADDIES*

Introduction

As part of the effort to significantly enhance agricultural efficiency to meet the increasing global food demand through nanotechnology, metal oxide nanoparticles have been extensively explored in agriculture as slow-releasing fertilizers, antimicrobial agents, and nanocarriers of essential nutrients (Mishra, et al. 2017). For example, both zinc oxide nanoparticles (ZnO NPs) and copper oxide nanoparticles (CuO NPs) have been incorporated into pesticide formulas due to their antimicrobial property, and into slow-releasing fertilizers as a sustained source of Zn and Cu (Elhaj Baddar and Unrine 2018; Sun, et al. 2018a; Wang, et al. 2020; Zabrieski, et al. 2015), while silicon oxide nanoparticles (SiO₂ NPs) were used as a nanocarrier for essential plant nutrients (Mushtaq, et al. 2018). The expanding applications of metal oxide nanoparticles in agriculture have made it inevitable for them to accumulate in soil (Hochella, et al. 2019). Due to their intense interactions with soil particles, co-existing environmental pollutants, plant nutrients, and the soil microbial community, understanding how increasing metal

* Reprinted with permission from “Elucidating the impact of three metallic nanoagricheicals and their bulk and ionic counterparts on the chemical properties of bulk and rhizosphere soils in rice paddies.” by Wang, X., Li, X., Dou, F., Sun, W., Chen, K., Wen, Y. and Ma, X., *Environmental Pollution* 290 (2021): 118005, Copyright [2021] by Elsevier.

oxide nanoparticles affect soil health is imperative (Deng, et al. 2017; Dimkpa, et al. 2015; Joško, et al. 2019; Parada, et al. 2019; Rai, et al. 2018; Tourinho, et al. 2012).

Soil health is defined as “the continued capacity of soil to function as a vital living ecosystem that sustains plants, animals and humans” (Lehmann, et al. 2020a). Disturbance of soil health and its functions can significantly compromise soil ecosystem services and agricultural productivity. Because of the complexity of soil composition, soil health is defined by a range of physical, chemical, and biological parameters (Bünemann, et al. 2018; Lehmann, et al. 2020a). The relative importance of these parameters for soil health depends on the intended soil uses. For instance, biological parameters would be more important to monitor and control the growth of pathogens and predators in a soil, while chemical parameters indicating the availability of nutrients and heavy metals (e.g. arsenic availability in rice paddies) are essential for agricultural soil because these parameters affect agricultural production and food safety. Most previous studies on the impact of engineered nanoparticles on soil focused on the biological aspect of soil health, such as the enzymatic activities and soil microbial community (Chai, et al. 2015; Guan, et al. 2020; Rajput, et al. 2018b; Samarajeewa, et al. 2020; Simonin, et al. 2016; Xu, et al. 2015). Systematic evaluation of the impact of engineered nanoparticles on chemical properties of a soil is rare. Limited evidence suggested that the effect of nanoparticles on soil properties depends on the applied concentrations and soil organic matter content (Shi, et al. 2018; Waalewijn-Kool, et al. 2013). One study reported that adding ZnO NPs at 200-6,400 mg/kg to a loamy sand soil increased the soil pH by 0.1-0.8 unit dose-dependently but did not affect the soil pH at 100 mg/kg

(Waalewijn-Kool, et al. 2013). CuO NPs at 10, 100, and 1,000 mg/kg also significantly increased the soil pH and Eh within 10 hours after they were added to a low-organic matter soil. For high-organic matter soil, however, the increased soil pH and Eh were only observed at the highest concentration (Shi, et al. 2018).

Paddy soil represents one of the most common agricultural farmlands globally, yet the impact of engineered metallic nanoparticles on paddy soil health is rarely studied. Paddy soil distinguishes itself from upland soil by its generally reduced conditions during rice cultivation. One of the chief concerns with paddy soil is the elevated arsenic (As) bioavailability to rice (Islam, et al. 2016). The plant available As in the soil has shown a strong correlation with As in rice plants; therefore, it could be an important indicator for paddy soil health (Anawar, et al. 2008). Our previous studies showed that ZnO NPs could potentially lower As accumulation in rice seedlings both hydroponically and in soil (Ma, et al. 2020b; Wang, et al. 2018). However, detailed examination on the long-term impact of ZnO NPs on plant-available As in paddy soil has not been fully conducted. A recent study reported that 500 mg/kg of CeO₂ NPs and TiO₂ NPs did not affect the long-term plant-available As in soil, but both significantly altered the availability of N and P as well as some micronutrients even though their effect on plant-available nutrients varied with soil types (Duncan and Owens 2019).

Plants can significantly change the properties of soil adjacent to plant roots through the excretion of root exudates. The soil near plant roots, or the rhizosphere soil, has remarkably different chemical properties from the bulk soil (Huang, et al. 2020; Seshadri, et al. 2015). A previous study reported that 500 mg/kg of ZnO NPs

significantly increased the pH of both bulk and rhizosphere soil, but the impact was more remarkable for the bulk soil (Zhang, et al. 2019). A separate study indicated that bulk soil had a significantly lower pH compared to the rhizosphere soil at day 14 and day 42 after mixing with 500 mg/kg of CuO NPs (Gao, et al. 2018).

Agrichemicals containing Zn, Cu, and Si have been widely used in agriculture. With the growing enthusiasm for expanding nanotechnology applications in agriculture, ZnO NPs, CuO NPs, and SiO₂ NPs are increasingly explored as novel and more effective alternatives to conventional agrichemicals. However, concerns also grow for their potential adverse environmental impacts due to the general concern on nanotoxicity. Many previous studies have investigated the impact of metal oxide nanoparticles on plants, and micro- and macro-organisms in soil, and the results suggested significant differences between nanoparticles and their ionic and bulk particles (Castiglione, et al. 2016; Garcia-Gomez, et al. 2015; Landa, et al. 2016). Several previous studies reported that ZnO NPs and CuO NPs differently affected the uptake of As by rice seedlings from their ionic compounds (Ma, et al. 2020b; Wang, et al. 2019b; Wang, et al. 2018). CuO NPs at 500 mg/kg significantly increased the bulk soil pH by around 0.3 units, while ionic Cu significantly decreased the bulk soil pH by 0.5 units (Gao, et al. 2018). Shi et al. (Shi, et al. 2018) also reported that soil containing 1,000 mg/kg CuO bulk particles (BPs) had a significantly lower pH than the soil with the same concentration of CuO NPs after 30 days of mixing. These studies suggested that metallic nanoparticles and their ionic and bulk counterparts could have notably different impacts on soil health, which has to be considered in applying nanotechnology into agriculture

because the fundamental role of soil plays in agricultural production. The objectives of this study were to (1) investigate the effects of ZnO NPs, CuO NPs, and SiO₂ NPs on several key chemical properties of soil; (2) determine different impacts of three metal oxide nanoparticles and their bulk and ionic counterparts on soil health; and (3) assess the different responses of the bulk and rice rhizosphere soil to different types of agrichemicals.

Materials and Methods

Chemicals

ACS reagent-grade zinc sulfate heptahydrate (ZnSO₄·7H₂O >99%) and copper sulfate pentahydrate (CuSO₄·5H₂O >98%) were obtained from Acros Organics (Geel, Belgium). Certified sodium meta-silicate nonahydrate (Na₂SiO₃) was purchased from Fisher Chemical (Hampton, NH, USA). Certified ACS ZnO, CuO, and SiO₂ bulk particles were obtained from Alfa Aesar (Haverhill, MA, USA). Their corresponding nanoparticles were purchased from US Research Nanomaterials, Inc (Houston, TX, USA).

Nanoparticles Characterization

The size and shape of nanoparticles were determined using a Tecnai G2 F20 transmission electron microscope (TEM) (Wang, et al. 2019b; Wang, et al. 2018). The hydrodynamic size and zeta potential of the NPs in ultrapure water and soil extract water, a mimic of the soil pore water, at 100 mg/L were measured with three replicates for each NPs by a dynamic light scattering (DLS) instrument (Malvern Zetasizer Nano-

ZS90) right after sonication for 30 mins. The soil extract water was prepared by mixing 1 g of air-dried background soil with 50 mL ultrapure water. Then the mixture was shaken at 100 rpm for 24 hours before it was centrifuged at 3,000 rpm for 10 minutes to remove very large soil particles to avoid clogging of filter paper in the subsequent filtration. The filtrate of the supernatant through a 0.2 μm syringe filter was taken as the soil extract water which was expected to contain the introduced NPs but not natural colloids (Di Bonito, et al. 2008).

Soil Collection and Characterization

The soil used in this study was collected from the top layer (0-15 cm) of a rice paddy at the Texas A&M AgriLife Research Station near Eagle Lake, Texas, USA (N 29° 37', W 96° 22'). The soil was air-dried and passed through a 2-mm sieve before use. The soil was determined as a Hockley silt loam (fine, smectitic, hyperthermic Typic Albaqualfs) with 19% silt, 15% clay, 2.47% organic carbon, and pH 5.9 by the Soil, Water and Forage Testing Laboratory at Texas A&M University. The background soil contained around 6.36 mg/kg of As.

Experimental Setup

A three-way mixed factorial design with two between-group factors (bulk soil or rhizosphere soil and different treatments) and one within-subject factor (measurements at two different stages) was used for this greenhouse trial. The soil treatment consisted of 10 scenarios: one control (background soil without any amendments) and nine treatments containing one of the nine admendments: 100 mg/kg ZnO NPs, Zn²⁺, ZnO BPs, CuO NPs, Cu²⁺, CuO BPs, or 500 mg/kg SiO₂ NPs, SiO₃²⁻, and SiO₂ BPs. The

concentrations of ZnO NPs and CuO NPs and their corresponding bulk and ionic particles were selected based on previous studies that these agrichemicals at the chosen concentration did not exert overt phytotoxicity in similar growing conditions but could potentially modify soil chemical properties (Liu, et al. 2018b; Wang, et al. 2019b; Wang, et al. 2018). The concentration of Si was adopted following the guidance on rice Si demand (Datnoff and Rodrigues 2005). All concentrations of dosed chemicals were reported as concentrations as elements.

Preparation of Bulk and Rice Rhizosphere Soil

To prepare the bulk soil, soil amendments in pre-determined concentrations were mixed with 4.5 kg of dry soil in each pot to achieve the targeted concentration for each chemical. After the soil was homogenized, 1,386 mL of rainwater was added to each pot to obtain a 70% water holding capacity. The rainwater was collected from the roofs of the greenhouse and stored in large containers before irrigation. Rainwater harvest and reuse help release the pressure of stormwater drains and also help to solve water shortage problems, and is a common practice in rice production in Texas. Three replicates were prepared for each treatment. All pots were then placed in a greenhouse for 2 days to further homogenize the soil (e.g. even distribution of water in soil pores). Measurements on the impact of different treatments on soil properties started after soil homogenization, labeled as Day 0. The rhizosphere soil was prepared similarly. Compared with the bulk soil pots, the only difference in the rhizosphere soil pots was that seven pre-germinated rice seeds were evenly planted at 1.5-cm depth in each pot at Day 0. The rice cultivar used was XP753, a popular high-yielding long-grain hybrid

from RiceTec Inc. (Alvin, TX, USA). The seeds were pre-germinated at 30 °C for 36 hours before seeding. Seedlings in different treatments all started with similar sizes. Twenty-eight days after seeding, the emerged seedlings in each pot were thinned down to four, and each pot was considered one replicate. For the first 28 days, 100 mL rainwater was added to each pot every other day to keep surface moisture. All pots were permanently flooded at 9-cm depth on Day 29, and the water was maintained until rice harvest at Day 104 (maturity). A total of 250 kg ha⁻¹ urea (46-0-0) was applied to each pot in two splits: 50% (approximately 170 mg/kg) was applied at permanent flooding at Day 29, and the rest were applied at maximum tillering at Day 47. In addition, P fertilizer (Super Triple Phosphate, 0-45-0) and K fertilizer (Potassium Chloride, 0-0-60) were applied at 40 kg P₂O₅ ha⁻¹ (~ 56 mg/kg) and 60 kg K₂O ha⁻¹ (~63 mg/kg) respectively, at Day 60. The water and nutrient management were applied to the bulk soil similarly as to the rhizosphere soil.

Soil Sampling and Analysis

Soil sampling was carried out at Day 0, 47 (maximum tillering stage of rice), and 104 (maturing stage of rice). Soil property at Day 0 was assumed to be the same for both the bulk and rhizosphere soil because when the pre-germinated seeds were just transferred to the pots, the rhizosphere soil around rice roots has not been established. At each sampling event, soil redox potential (Eh) was first measured using a combined platinum and silver/silver chloride electrode system (HI 3230B. Hanna Instruments, Woonsocket, RI) by inserting the electrode at approximately 1 cm below the soil surface. Soil Eh was not measured at Day 0 due to the low water content.

For sampling, about 500 g (dry-weight equivalent) bulk soil was taken from each pot, while only 50 g of rhizosphere soil was taken from each pot using a sterilized spatula to minimize the impact on rice growth. The rhizosphere soil is defined as the soil attached to plant roots which exhibits different physical, chemical and biological properties from the bulk soil (Bowen and Rovira 1999). In this study, the rapidly growing rice roots fully filled the pot before the maximum tillering stage, therefore, the soil collected from the pots with rice was considered as the rhizosphere soil. The collected soil samples were air-dried and then sieved through a 2-mm screen before analyzing their pH, cation exchange capacity (CEC), soil organic carbon (SOC), and plant-available As.

Soil pH was determined in a 1:2 soil: water (w/v) extract. Briefly, 10 g of air-dried soil was mixed with 20 mL of deionized (DI) water in a 50 mL centrifuge tube. The mixture was then shaken on a shaker at 300 rpm for 30 mins and stood at room temperature for 1 hour. The pH of the supernatant was then measured with a pH meter.

SOC is an important indicator of soil fertility and was quantified following the loss-on-ignition method (Nelson and Sommers 1983; Shi, et al. 2018). First, 10 g of air-dried soil was placed in an oven at 105 °C for 24 h to obtain the initial dry weight. Then the oven-dried soil was heated in a muffle furnace at 400 °C for 8 h to remove the OC in soil, and the weight after the ignition was recorded as the final weight. SOC was then calculated as:

$$\text{SOC}(\%) = \frac{\text{Initial weight} - \text{Final weight}}{\text{Initial weight}} \times 100\%$$

Soil CEC measurement was performed following the CEC-7 method (Burt 2014). Briefly, the cation exchange sites of 1 g of air-dried soil were first saturated with NH_4^+ by mixing it with 30 mL of 1 N NH_4OAc . 20 mL of ethanol (95%) was then added to remove the excessive NH_4^+ . Afterward, the sample was rinsed with 40 mL of 1 N NaCl to displace the NH_4^+ adsorbed by the soil. The leachate was diluted to 50 mL, and 1 mL of the leachate was added to a micro-diffusion unit along with 3 mL of 12% (w/v) MgO suspension and 0.5 mL of boric acid indicator solution in the center. The units were wrapped with plastic wrap and kept at room temperature for 36 hours. The indicator solution in the center was then titrated with 0.005 N sulfuric acid to determine the adsorbed NH_4^+ . The CEC was calculated as:

$$CEC \text{ (cmol(+)/kg)} = A * 5 * B$$

Where A is the normality of sulfuric acid (0.005), and B is the volume of acid consumed in μL .

The plant-available As was determined following the mixed acid extraction protocol (Başar 2009; Woolson, et al. 1971). Briefly, 1 g of air-dried soil was added into a 50 mL centrifuge tube containing 30 mL of 0.05 M HCl and 0.025 M H_2SO_4 , and the tube was sealed and shaken for 30 min on a shaker table at 300 rpm. The mixture was then centrifuged at 5,000 rpm for 10 mins. Afterward, the supernatant was filtered through a 0.45- μm filter, and the filtrate was acidified to $\text{pH} < 2.0$ with concentrated HCl before the plant-available As was analyzed using an inductively coupled plasma-mass spectrometry (ICP-MS).

Statistical Analysis

Multi-way analysis of variance (ANOVA) was performed to assess the main and interaction effects of three factors on all the measured soil chemical properties. Due to significant interactions among the three factors, further analysis was performed to examine the effects of agricultural amendments and growth stages on soil properties for each soil type, and the effects of agricultural amendments on soil properties for each soil type and growth stage. Pearson correlation coefficient and p-value were calculated to reveal the relationship between plant available As and As content in rice plants and the association of plant-available As and different soil chemical properties. Sample averages with standard deviations were reported, and an effect was considered significant when $p < 0.05$. All statistical analyses were performed in Minitab 18 (Minitab Inc., State College, PA).

Results and Discussion

Particles characterization

The primary sizes of ZnO NPs, CuO NPs, and SiO₂ NPs were in the range of 15-137 nm, 9-22 nm, and 20-30 nm, respectively, as reported in our previous studies or by the manufacturer (Wang, et al. 2019b; Wang, et al. 2018). All three NPs were roughly spherical and exhibited significant aggregation in both DI water and soil extract water (**Table II-1**). The strong aggregation of these nanoparticles was expected from their zeta potentials because most of them fell within the range of -30 to +30 mV. Interestingly, the aggregation was generally less intense in the soil extract solution than in DI water. The

soil extract water contained higher contents of natural organic matter, and most of them carry negative charges.

Table II-1. The hydrodynamic diameter and zeta potential of three metallic nanoparticles (NPs) and bulk particles (BPs). All reported values represent mean \pm standard deviation (n=3). NA: not available.

Particles	Hydrodynamic diameter (nm)		Zeta potential (mV)	
	ultrapure water	soil extract water	ultrapure water	soil extract water
ZnO NPs	991 \pm 39	961 \pm 50	7.6 \pm 1.3	-16.6 \pm 0.2
ZnO BPs	N/A	N/A	6.0 \pm 1.9	-25.8 \pm 0.3
CuO NPs	1028 \pm 59	617 \pm 33	-27.9 \pm 4.5	-24.9 \pm 0.4
CuO BPs	N/A	N/A	-1.1 \pm 5.8	-23.8 \pm 2.9
SiO ₂ NPs	2590 \pm 442	2168 \pm 73	-26.4 \pm 2.4	-19.1 \pm 4.1
SiO ₂ BPs	N/A	N/A	-12.8 \pm 1.2	-35.0 \pm 3.7

Their adsorption on the surface of NPs and BPs is likely one of the reasons for the generally more negative zeta potential and greater stability of these particles in soil extract water (Cervantes-Avilés, et al. 2021). The hydrodynamic sizes of BPs were not determined because the BPs used in the study contained much larger particles than the optimal range of measurement by DLS used in this study, which could significantly skew the values of hydrodynamic size of BPs. Another possibility of the smaller hydrodynamic size of nanoparticles in the soil extract water could be the heteroaggregation between concerned nanoparticles and other colloidal particles (e.g., clay minerals), which could be retained in the filter due to their expected large sizes than nanoparticle homoaggregates, resulting in slightly smaller aggregates in the soil extract. The time-dependent ionic strength effect could also play a role here. A previous study

indicated that higher ionic strength did not affect TiO₂ NPs aggregation in the initial stage but resulted in a larger hydrodynamic size and broader size distribution of TiO₂ NPs aggregates after 100 hours (French, et al. 2009). Regardless of the reasons, the notably different behaviors of metal oxide nanoparticles in DI and the soil extract water underscored the importance of nanoparticle characterization in a more realistic condition.

Table II-2. P-values of three-way ANOVA on soil pH, Eh, SOC (soil organic carbon), CEC (cation exchange capacity) and plant available-As (top) and p-values of Treatment*Soil*Stages effects sliced by ‘Soil’ (bottom).

	pH	Eh	SOC	CEC	Plant available As
Treatments	<0.001	<0.001	<0.001	<0.001	<0.001
Soil	0.286	<0.001	<0.001	<0.001	<0.001
Stages	<0.001	<0.001	<0.001	<0.001	<0.001
Treatments*Soil	<0.001	0.017	<0.001	0.004	0.047
Treatments*Stages	<0.001	<0.001	<0.001	<0.001	<0.001
Soil*Stages	<0.001	<0.001	<0.001	<0.001	<0.001
Treatments*Soil*Stages	<0.001	0.033	<0.01	0.102	0.093
Bulk soil	<0.001	<0.001	<0.001	<0.001	<0.001
Rhizosphere soil	<0.001	<0.001	<0.001	<0.001	<0.001

Soil pH

ANOVA results showed significant interactions between treatment, soil type, and rice growth stage on soil pH (**Table II-2**), among which the treatment and rice growth stage were the main factors. For both the bulk and rhizosphere soil, the interactions between treatment and growth stage were significant, suggesting that the effect of treatment on soil pH could vary with soil types and growth stages. We therefore examined the effect of different treatments on soil pH for each soil type and at different growth stages separately (**Figure II-1**). The addition of different soil amendments

significantly affected soil pH at Day 0 compared with the background soil. In particular, Na_2SiO_3 significantly increased the soil pH from 6.41 to 10.46. All three forms of Cu, as well as the ZnO BPs and ZnO NPs, also significantly increased soil pH from 6.41 to around 7.

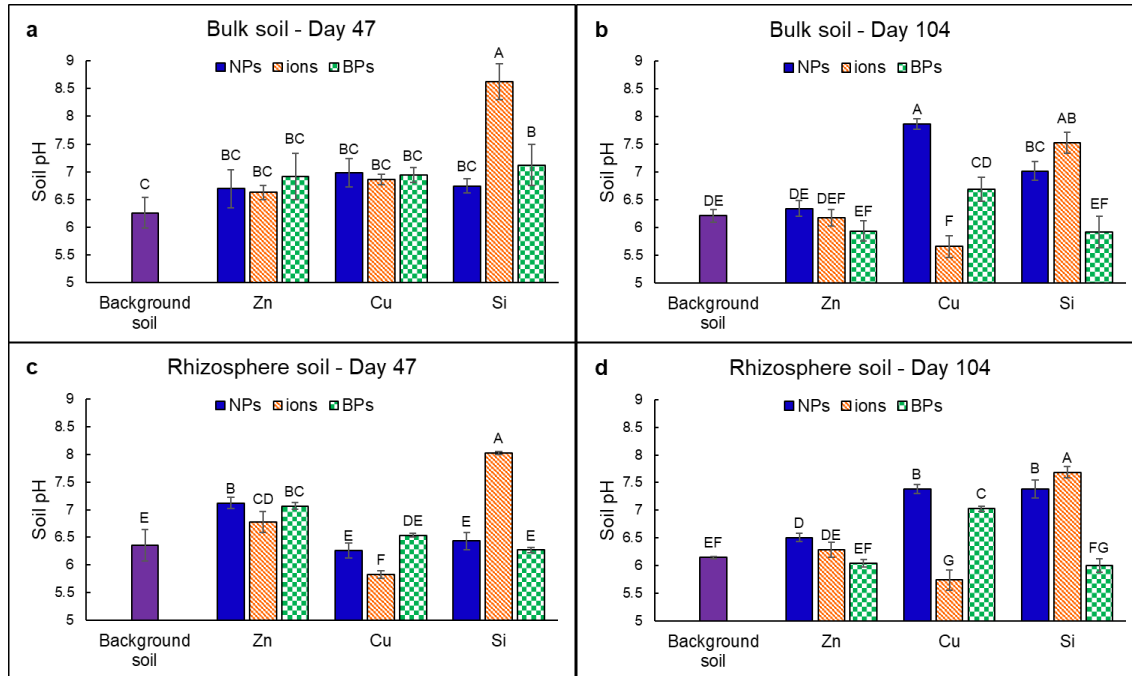


Figure II-1. The effects of different soil amendments on soil pH at (a) Day 47 and (b) Day 104 of the bulk soil, and (c) Day 47 and (d) Day 104 of the rhizosphere soil. Different letters indicate significant differences ($p \leq 0.05$) according to one-way ANOVA followed by Tukey's test. All reported values represent mean \pm standard deviation ($n=3$).

The bulk soil pH in the SiO_3^{2-} treatment dropped gradually over time, to 8.62 and 7.53 on Day 47 and 104, respectively. However, the soil pH in this treatment was still markedly higher than that in the background soil at both stages. A similar effect of SiO_3^{2-} on the rhizosphere soil pH was also observed. The increased soil pH by silicate was consistent with several previous studies (Bokhtiar, et al. 2012; Elisa, et al. 2016;

Greger, et al. 2018; Jianfeng and Takahashi 1991). For example, Greger et al.(Greger, et al. 2018) reported that the 1,000 kg/ha silicate significantly increased the soil pH by 0.29-0.47 units in clayey, sandy, alum shale, and submerged soil after 90 days. Similarly, the addition of sodium silicate at 470 mg/kg increased a paddy soil pH by 1 unit (Jianfeng and Takahashi 1991). Nevertheless, a 4-unit increase of the pH at Day 0 after the silicate addition was unusual. A pH of 10.5 was much higher than the desired pH (5-8) for rice production. Fortunately, the effect of silicate on bulk soil pH tapered off over time, and the pH change in the rhizosphere was generally milder than in bulk soil, **Figure II-1**, possibly due to the buffering capacity provided by the acidic root exudates in rhizosphere soil (Ding, et al. 2019; Vives-Peris, et al. 2020). The addition of SiO₂ BPs resulted in insignificant impacts on soil pH for both bulk and rhizosphere soils compared with background soil. In contrast, SiO₂ NPs led to a 1.0-unit increase in both soils at Day 104 compared to the control group. At present, few studies have investigated the effect of SiO₂ NPs on soil pH (Khan, et al. 2020). Our results suggest that SiO₂ NPs are more favorable Si amendments than SiO₃²⁻ to maintain a favorable pH for rice crops.

Cu amendments did not significantly alter the pH of the bulk soil at Day 47. However, the ionic Cu significantly lowered the pH of rhizosphere soil at Day 47 while the other two forms of Cu showed limited effect. For both bulk and rhizosphere soils, CuO NPs resulted in significantly higher pH while Cu²⁺ significantly lowered the pH at Day 104. The elevated soil pH by CuO NPs and, to a less extent, by CuO BPs agree with previous studies (Peng, et al. 2020; Peng, et al. 2017; Shi, et al. 2018). It is possible that

some H^+ were adsorbed on the surface of CuO NPs and BPs due to their negative surface charge. The generally more substantial effect of NPs than BPs can be explained by its greater surface area. No previous studies reported the effect of ionic Cu on soil pH. The lower pH caused by Cu^{2+} in both bulk and rhizosphere soils might be partially attributed to the ion exchange with H^+ on soil particles and the higher toxicity of Cu^{2+} to rice plants and soil microorganisms that led to the release of acidic root exudates.

Compared with the background soil, Zn amendments showed little effect on the bulk soil pH on both Day 47 and 104. In contrast, all Zn amendments significantly increased the rhizosphere soil pH at Day 47 compared with the background soil. However, only ZnO NPs treatment led to significantly higher rhizosphere soil pH at Day 104. The rhizosphere soil added with the other two forms of Zn had comparable pH as the background soil. Zhang et al. (Zhang, et al. 2019) also found that 500 mg/kg of ZnO NPs significantly increased the pH of bulk paddy soil and the rhizosphere soil. The hydrolyzation of ZnO NPs, which could release OH^- may be a reason for the elevated pH (Peng, et al. 2020). Unlike the other two NPs, the differences between the impact of ZnO NPs and Zn^{2+} on soil pH were less pronounced, likely due to the high dissolution rate of ZnO NPs (Domingos, et al. 2013).

Soil Eh

The effect of different amendments on soil Eh varied with soil types and growth stages, as shown in **Table II-2 and Figure II-2**. Interestingly, the differences between different amendments were minor. All soil amendments notably raised the Eh in both soils at Day 47, but the impact became insignificant at Day 104, suggesting that their

impact on soil Eh was temporary. The generally lower Eh in the bulk soil than in the rhizosphere soil at Day 104 is likely an artifact because the standing water above the soil surface of bulk soil pots was deeper than the rhizosphere pots due to the larger soil samples taken from the bulk soil pots at Day 47.

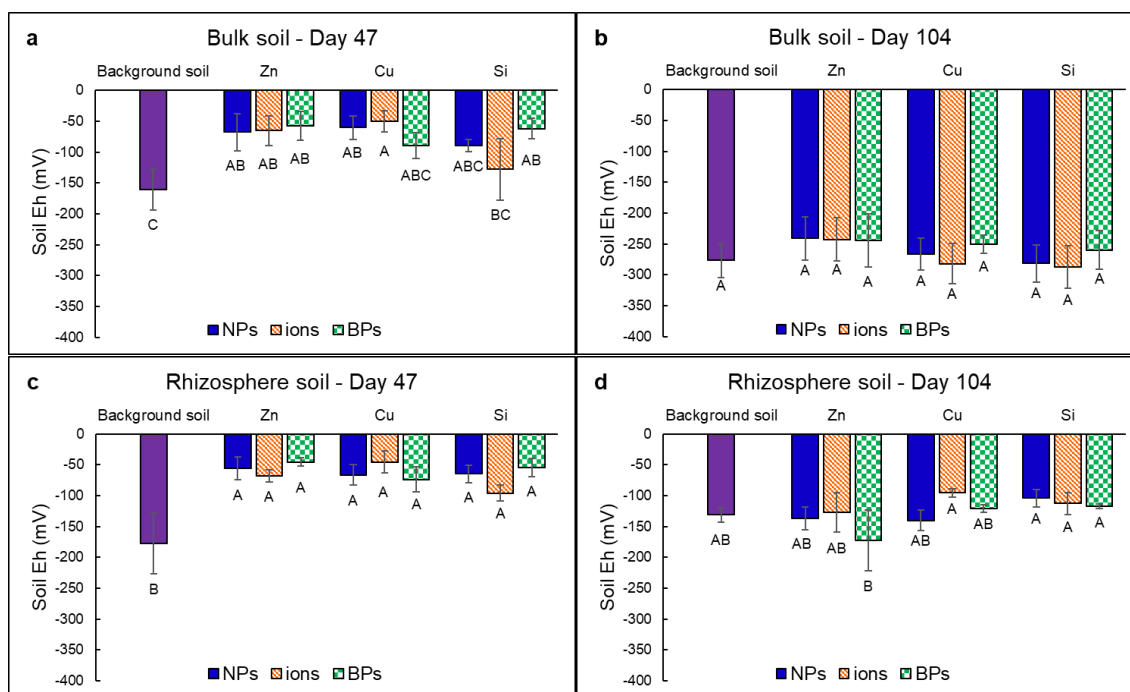


Figure II-2. The effects of different soil amendments on soil Eh at (a) Day 47 and (b) Day 104 of the bulk soil, and at (c) Day 47 and (d) Day 104 of the rhizosphere soil. Different letters indicate significant differences ($p \leq 0.05$) according to one-way ANOVA followed by Tukey's test. All reported values represent mean \pm standard deviation ($n=3$).

Several previous studies also reported a significant increase of soil Eh after the addition of metal oxide NPs (Peng, et al. 2020; Shi, et al. 2018). For example, Peng et al. (Peng, et al. 2020) found that 500 mg/kg of ZnO NPs, CuO NPs, or CeO₂ NPs significantly increased paddy soil Eh from -222.67 mV to -130 to -75 mV one day after mixing. After 30 days of flooding, the soil Eh with the nanoparticle amendments slightly

decreased to around -150 mV but was still higher than the control soil (-200 mV), consistent with our results. The increase of soil Eh by metal amendments might stem from their toxicity to soil microorganisms, which slowed down the oxygen depletion after mixing (Shen, et al. 2015; Xu, et al. 2015). With the gradual adaptation of soil microorganisms and continuous flooding, the impact of chemical amendments on soil Eh tapered off.

Soil organic carbon (SOC)

SOC affects a range of soil properties and functions such as soil aggregation, nutrient retention, carbon sequestration, and microbial diversity (Blanco-Canqui, et al. 2013). SOC is a relatively stable parameter, and noticeable changes in natural soil often occur in years to decades (Jobbágy and Jackson 2000; Lehmann, et al. 2020b). The generally consistent bulk soil SOC after the addition of different amendments, **Figure II-3**, agrees with the general observation and some previous studies which showed that Fe₃O₄ and CuO NPs had minimal impact on SOC (Ben-Moshe, et al. 2013; Shi, et al. 2018). However, ZnO BPs and SiO₃²⁻ did significantly lowered SOC by 14.6% and 13.8% in the bulk soil at Day 47. None of the soil amendments showed any impact on SOC in bulk soil at Day 104. A previous study indicated that the application of silicate fertilizer could increase the relative abundance of saprotrophic fungal, therefore promote organic matter decomposition in a short-term (120 days) (Das, et al. 2019). The lower SOC after the addition of ZnO BPs and SiO₃²⁻ in this study could be attributed to the increased microbial activity leading to negative effects on SOC storage (Das, et al. 2019).

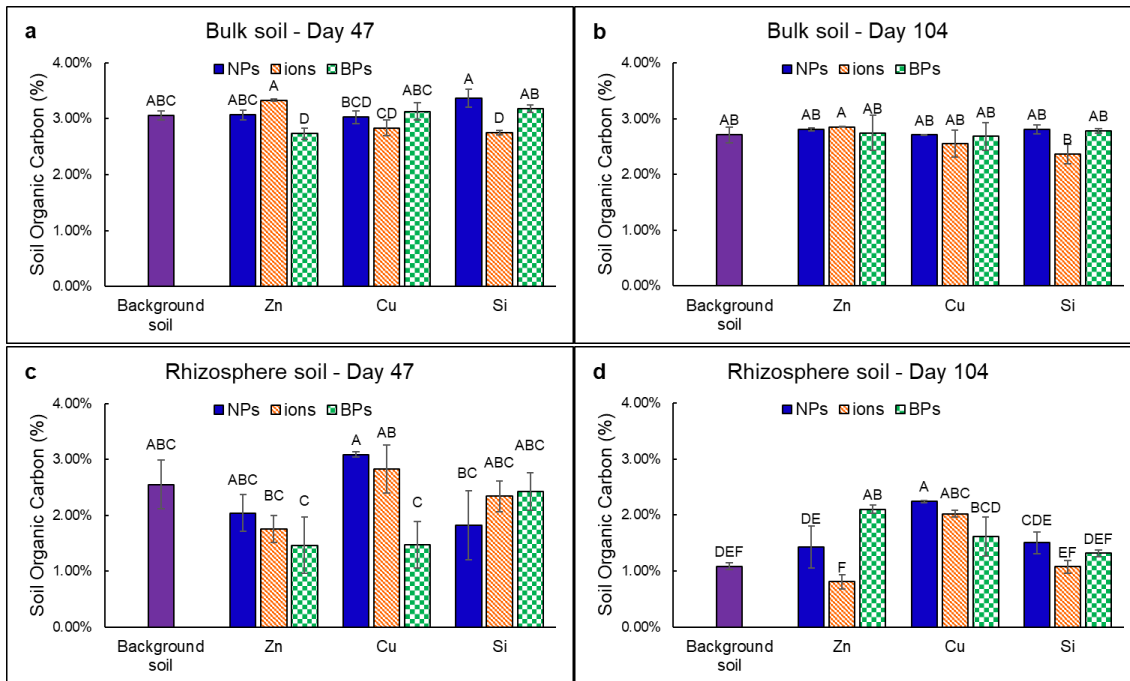


Figure II-3. The effects of different soil amendments on SOC at (a) Day 47 and (b) Day 104 of the bulk soil, and at (c) Day 47 and (d) Day 104 of the rhizosphere soil. Different letters indicate significant differences ($p \leq 0.05$) according to one-way ANOVA followed by Tukey's test. All reported values represent mean \pm standard deviation ($n=3$).

In comparison, the SOC in rhizosphere soil was much more susceptible to the impact of different amendments and was lower than that in bulk soil on both days for all treatments. The observation that the SOC in the rhizosphere soil was lower than in the bulk soil was somewhat unintuitive because plant roots generally excrete organic compounds to soil which would increase rhizosphere SOC. However, the lower molecular weight root exudates can stimulate microbial activity and be easily consumed by local microorganisms in the rhizosphere. The enhanced microbial activity in the rhizosphere would promote the decomposition of organic compounds, therefore, leading to a lower SOC in the rhizosphere soil compared to the bulk soil (Leifeld, et al. 2020; Nardi, et al. 2000; Torn, et al. 1997; Yang, et al. 2021). The varying effects of different

soil amendments on SOC in the rhizosphere soil could be ascribed to their substantially different impacts on plant root physiology and the release of plant-derived carbon (e.g., exudates) (Rastogi, et al. 2017). Both ZnO BPs and CuO BPs notably reduced the rhizosphere SOC by about 60% compared to the background soil at Day 47, while other amendments displayed less to insignificant effects, indicating that ZnO BPs and CuO BPs might promote the microorganism activity temporarily (Rousk, et al. 2012). The impact of soil amendments on rhizosphere SOC varied at Day 104 compared to Day 47. For instance, ZnO BPs significantly increased SOC in the rhizosphere soil by 93.5%, opposite to what was observed at Day 47, revealing potential long-term toxicity to microorganisms and enzyme activities of bulk ZnO (Kouhi, et al. 2015). The generally more significant impact of Cu amendments on soil SOC agrees with the observation that Cu amendments are usually more toxic to microorganisms than other agrichemicals. In addition, all three forms of Zn showed similar effects on rhizosphere SOC at Day 47, but Zn ions-treated soil showed significant lower rhizosphere SOC at Day 104 than ZnO NPs and then ZnO BPs, suggesting different forms of amendments could have significantly different time-dependent impacts on rhizosphere SOC. Overall, different amendments affected SOC differently for different soils and at different sampling time (**Table II-2**).

Soil CEC

Soil CEC indicates the ability of a soil to retain nutrients and environmental contaminants, and is closely related to various other soil parameters such as soil mineral content, SOC, and soil pH (Manrique, et al. 1991; Parfitt, et al. 1995; Seybold, et al.

2005). Three-way ANOVA results indicated insignificant three-way interactions between treatments, soil type, and stages (**Table II-2**). However, interactions between treatments and growth stages were significant for both soils. Soil CEC from different treatments at different stages is presented in **Figure II-4**.

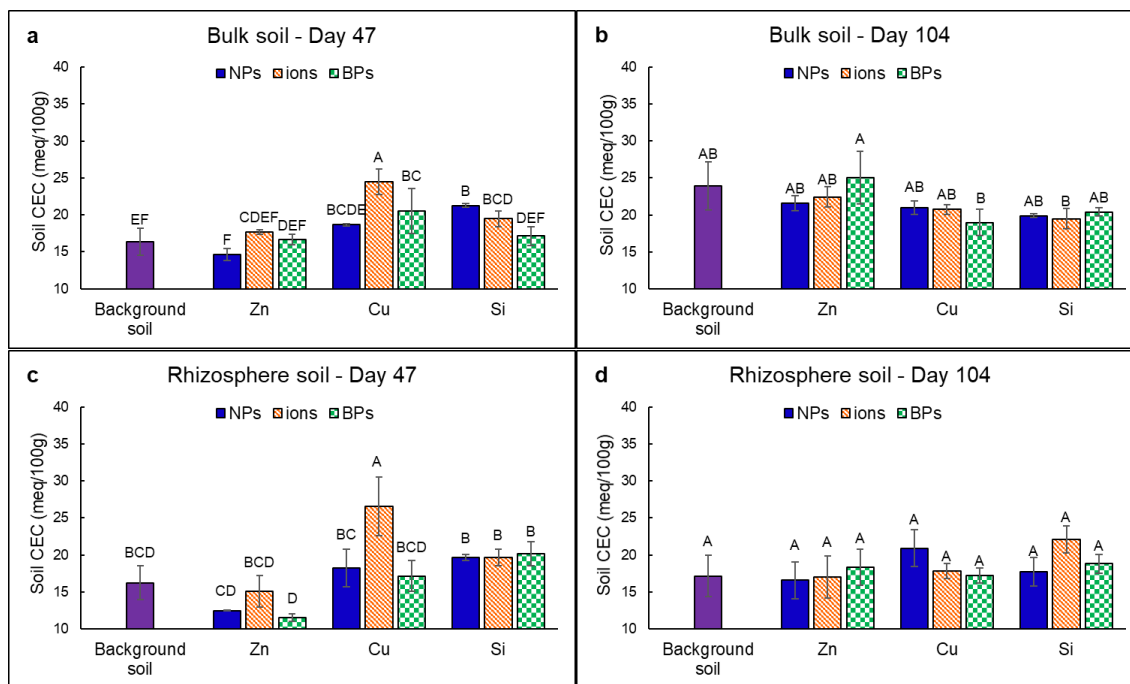


Figure II-4. The effects of different soil amendments on soil cation exchange capacity (CEC) at (a) Day 47 and (b) Day 104 of the bulk soil, and (c) Day 47 and (d) Day 104 of the rhizosphere soil. Different letters indicate significant differences ($p \leq 0.05$) according to one-way ANOVA followed by Tukey's test. All reported values represent mean \pm standard deviation ($n=3$).

A significant impact of soil amendments on CEC was only observed at Day 47 for both soils compared with the background soil, even though significant differences between different treatments (e.g., ZnO BPs vs. CuO BPs) were also observed for the bulk soil at Day 104. Cu^{2+} stood out as the most influential amendment that significantly increased the bulk soil CEC by 49.6% and the rhizosphere soil CEC by 63.5% at Day 47,

compared with the background soil. The altered CEC can reciprocally affect copper toxicity to plants (e.g. higher CEC leads to lower Cu phototoxicity) (Rooney, et al. 2006). All other amendments had a statistically insignificant impact on soil CEC. The interactions of soil amendments with clay minerals in the paddy soil could be a potential mechanism for the modified CEC of soils. Guo et al.(Guo, et al. 2019) reported that CeO₂ NPs interacted closely with kaolinite minerals and altered the surface charge of kaolinite. The paddy soil used in this study contained high contents of clay minerals. Overall, the soil CEC is a relatively stable parameter and is less susceptible to the impact of soil amendments.

Plant-available As

Arsenic (As) bioavailability has been a main food safety concern in rice production. Few previous studies have examined the effect of metallic nanoparticles on plant-available As in soil. Similar to soil CEC, the three-way interactions between treatments, soil and stages on plant-available As were not significant. However, significant interactions between treatments and sampling stages were detected in both bulk and rhizosphere soils (**Table II-2**). The effects of different amendments on the plant-available As at different stages are shown in **Figure II-5**.

The introduction of soil amendment did not significantly alter the plant-available As in the bulk soil, consistent with a previous study that 500 mg/kg of CeO₂ NPs and TiO₂ NPs had minimal impact on the phytoavailability of As in soil after 260 days of addition. (Duncan and Owens 2019) The same study also reported a temporary increase of plant-available As at the first 28 days after adding the nanoparticles. We also noticed

an initial increase in plant-available As from treatments exposed to ZnO NPs, Zn^{2+} and SiO_3^{2-} at Day 0. The higher plant-available As in the bulk soil at the initial mixing stage could be attributed to some of the significantly modified soil properties such as soil pH. Arsenic was predominantly in the form of arsenic acid (H_3AsO_4) at the soil pH and Eh on Day 0. With a first pK_a around 2.2, As was primarily in the form of the negatively charged As(V) at Day 0. Their adsorption on soil particles could be decreased due to competitive adsorption of hydroxyl ions, resulting in higher plant-available As (Marin, et al. 1993). The generally raised pH by different amendments, particularly the alkaline environment created by the addition of SiO_3^{2-} , could significantly lower As adsorption to soil particles, increasing the plant-available As (Pigna, et al. 2015). After the soils were fully flooded, As was reduced to the form of arsenous acid (H_3AsO_3), whose first pK_a is around 9.23. Therefore, its adsorption onto soil particles is less subjected to the impact of pH and other ions.

The plant-available As in the rhizosphere soil exhibited very different patterns from the bulk soil. The plant-available As was 134.9% and 143.8% higher in the treatments with CuO NPs and Cu^{2+} than the rhizosphere background soil at Day 47. A similar phenomenon was also observed for ZnO NPs treatment at Day 47, whose plant-available As was 74.2% higher than in background soil, while Zn^{2+} and ZnO BPs did not affect the plant-available As. All forms of Si amendments showed a minimal impact on plant-available As in the rhizosphere soil at both days. The different plant-available As in the rhizosphere soil may be resulted from either the altered soil chemical properties due to the added soil amendments, or the changed As sink because of plant uptake.

Direct adsorption of As on the particle amendments could also contribute to the altered As availability.

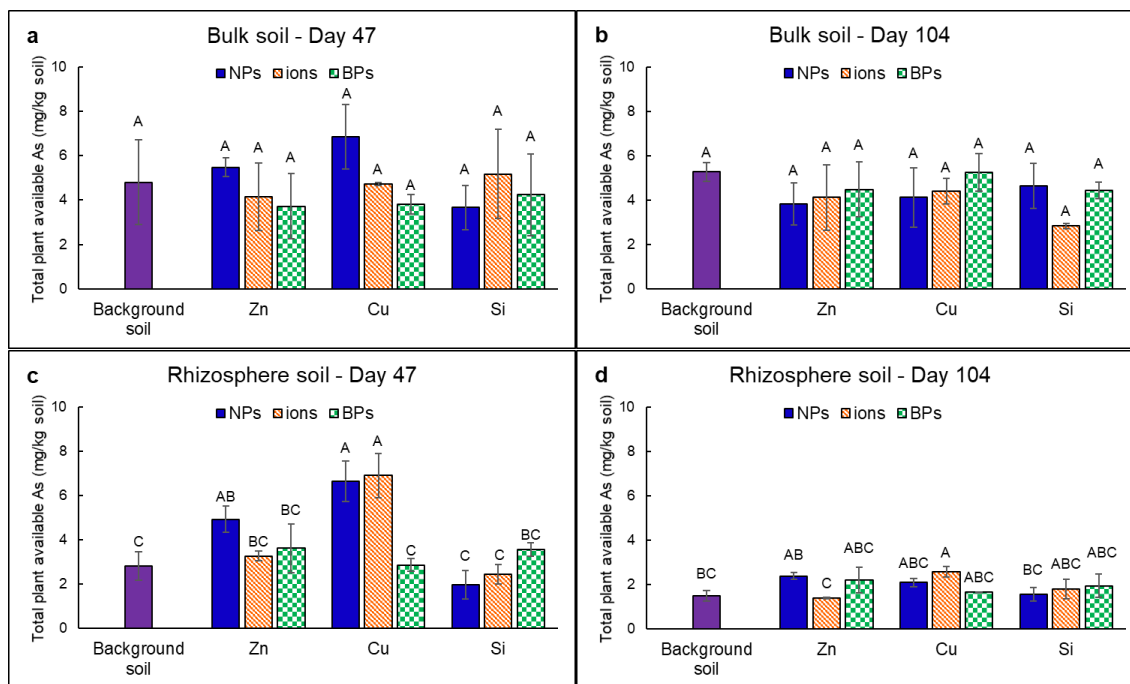


Figure II-5. The effects of different soil amendments on total plant-available As at (a) Day 47 and (b) Day 104 of the bulk soil, and (c) Day 47 and (d) Day 104 of the rhizosphere soil. Different letters indicate significant differences ($p \leq 0.05$) according to one-way ANOVA followed by Tukey's test. All reported values represent mean \pm standard deviation ($n=3$).

To elucidate how plant available As is affected by other soil properties, Pearson correlation analysis was conducted and strong correlations between plant-available As at different stages and other soil chemical properties were found (**Figure II-6**). These intertwined connections between plant-available As and other soil properties suggest that the impact of soil amendments on plant-available As is strongly dependent upon the unique soil properties and will likely vary from soil to soil. For instance, the positive correlation of soil Eh and plant-available As at Day 47 indicated that the elevated Eh

caused by the added soil amendments at early stages was one reason for the increased plant-available As content. Moreover, plant-available As was positively correlated with soil pH at Day 0 and Day 47 in bulk soil, which supports our postulation that the increased soil pH in the bulk soil at early stages lowered the adsorption of As onto soil particles, thus increasing plant-available As. However, plant-available As was negatively correlated with soil pH in the rhizosphere soil at all stages. The positive correlation between plant-available As and SOC in the rhizosphere soil at both stages suggests that plant root exudation could be an important factor in As availability.

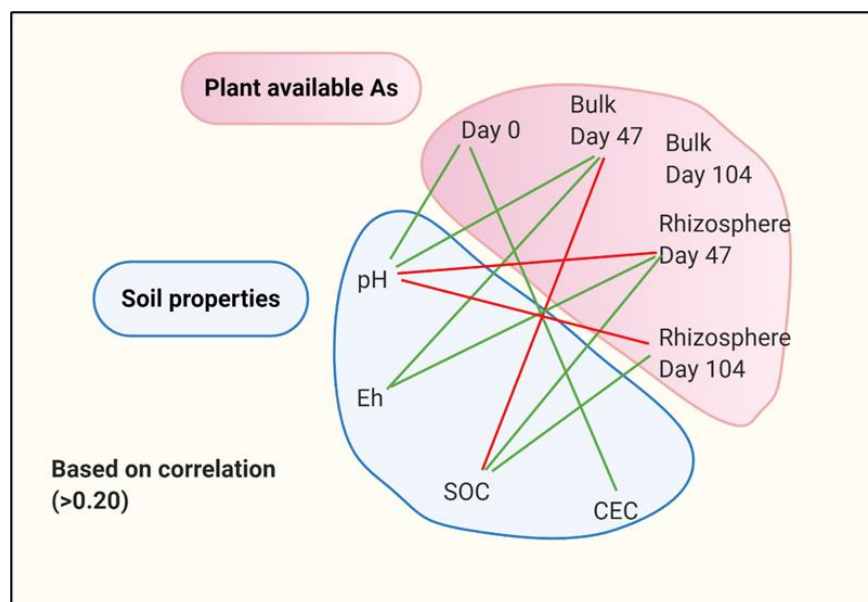


Figure II-6. The Pearson correlation networks between plant-available As at different stages and other soil chemical properties (pH, Eh, SOC (soil organic carbon), CEC (cation exchange capacity)). Green lines indicate positive correlation (correlation coefficient > 0.20). Red lines indicate negative correlation (correlation coefficient < 0.20).

Conclusions

In closing, this study represents one of the earliest studies on the impact of different soil amendments on the chemical properties of soil, which are critical for soil ecosystem services and sustainable agriculture. The results revealed the complex impacts of nanoagrichemicals and their corresponding bulk and ion materials on the chemical properties of rice paddy soils. As expected, bulk and rhizosphere soils displayed different responses to the addition of different amendments, suggesting that results obtained from the bulk soil studies could not be indiscriminately extrapolated to the rhizosphere. The relative stability of nanoagrichemicals in these two types of soil might have played a role due to the distinctive physicochemical properties of these two soils. Soil amendments with different compositions and those with the same primary metal element but different forms of amendments displayed markedly different impacts on the evaluated soil chemical properties. Cu-based agrichemicals generally had stronger effects on the examined chemical properties but silicate salt displayed the strongest effect on soil pH. Among the tested chemical properties, soil pH and SOC in the rhizosphere soil are more susceptible to the impacts of agrichemicals while soil Eh and CEC are more stable after agrichemical introduction. All of the examined chemical parameters could affect plant available As and have consequences in food safety. With the current efforts to broaden applications of nanotechnology in agriculture, this study adds a new layer of information for consideration. As indicated earlier, soil health is represented by an array of physical, chemical, and biological properties. Soil physical properties are unlikely to be dramatically affected by soil amendments at the level

typically used in agriculture according to previous studies (Sun, et al. 2020). However, biological properties are susceptible to environmental disturbance and comprehensive studies on how different soil amendments with different compositions and forms will affect soil biological health should be performed in the future. Future research should also evaluate the concentration effect of different amendments on soil health. In combination with the knowledge of the physiological needs of plants, this information may yield more accurate guidance on the applications of soil amendments to achieve sustainable agriculture and a healthy environment.

CHAPTER III

EFFECTS OF ZINC FERTILIZERS ON ARSENIC ACCUMULATION AND SPECIATION IN RICE (*ORYZA SATIVA L.*): FORMATION OF IRON PLAQUE

Introduction

Production of high-quality rice (*Oryza sativa* L.) has significant implications for global food safety and security because rice is a staple food for more than three billion people in the world (Hoang, et al. 2019). Nanotechnology has been hailed as a technical breakthrough that can substantially enhance agricultural production and avoid the negative consequences of conventional agrichemicals (Chhipa 2017; Duhan, et al. 2017; Kah, et al. 2019). In particular, some nanoparticle-containing soil amendments have displayed potential to alleviate arsenic (As) phototoxicity and accumulation in rice tissues (Cui, et al. 2020; Wu, et al. 2020b; Yan, et al. 2021), one of the major food safety concerns associated with rice consumption. Our previous studies suggested that zinc oxide nanoparticles (ZnONPs) significantly lowered As accumulation in rice seedlings in short-term hydroponic and soil studies (Ma, et al. 2020b; Wang, et al. 2018). However, the effect of ZnONPs on the accumulation of As in rice grains in more relevant growing conditions (e.g., in paddy soil) has not been studied, and the mechanisms for altered As accumulation in rice seedlings by Zn are poorly understood. ZnONPs is an appealing nanoagrchemical because Zn deficiency is common in rice paddy soils globally and ZnONPs can serve as a slow-releasing Zn source which improves Zn utilization efficiency. ZnONPs have also been widely used as pesticides

and fungicides in agriculture (Elhaj Baddar and Unrine 2018; Sun, et al. 2018a; Zabrieski, et al. 2015). Therefore, it is imperative to understand whether and how ZnONPs may affect the As accumulation in rice grains.

The bioavailability, speciation and accumulation of As in rice grains are governed by a range of factors, and many of them can be affected by ZnONPs, leading to altered As accumulation in rice. For instance, a previous study showed that ZnONPs changed the bioavailability of As in rice paddy soil by altering the critical physicochemical properties of soils such as the soil pH, Eh, cation exchange capacity and soil organic carbon (Wang, et al. 2021). ZnONPs can also modify the As speciation in paddy soil and affect its bioavailability. For example, ZnONPs-induced reactive oxygen species (ROS) could deplete the electrons needed for the reduction of As(V) to As(III) in the rhizosphere (Tu, et al. 2004; Xu, et al. 2007). ZnONPs may also interrupt the plant detoxification process, in which As(V) is reduced to As(III) before it is sequestered into the vacuole of rice root cells (Yan, et al. 2021). Several previous studies support these conjectures, showing that ZnONPs at 10-100 mg/L significantly lowered the ratio of As(III) to total As in rice shoot in a hydroponic study (Yan, et al. 2021). The result is significant because inorganic As(III) is the most hazardous As species and a lower As(III) to total As ratio can have strong implications for food safety. However, none of the studies has investigated the impact of ZnONPs on the total As uptake and the As speciation in rice grains. In view of the fact that conventional Zn salt remains the most dominant form of Zn agrichemicals, it is also critical to evaluate whether ZnONPs

is indeed more advantageous than conventional Zn salt in improving rice production and safety in terms of As accumulation.

Iron plaque formed on the root surface plays an essential role in plant As uptake (Lee, et al. 2013; Liu, et al. 2006). It is formed after Fe^{2+} in soil pore water is oxidized by oxygen released from rice roots and consists of primarily amorphous or crystalline iron (oxyhydr)oxides (Bacha and Hossner 1977; Chen, et al. 1980; Hansel, et al. 2001). Previous studies have identified the major component of iron plaque as ferrihydrite ($\text{Fe}_{10}\text{O}_{15}\cdot 9\text{H}_2\text{O}$), amorphous $\text{Fe}(\text{OH})_3$, goethite ($\alpha\text{-FeOOH}$) and lepidocrocite ($\gamma\text{-FeOOH}$) (Bacha and Hossner 1977; Chen, et al. 1980; Fu, et al. 2016; Hansel, et al. 2001; Wang and Peverly 1999). Iron plaque could act as a protective barrier against plant uptake of As because of its porous structure and high adsorption capacity (Liu, et al. 2006; Syu, et al. 2013; Yang, et al. 2018). Iron plaque is particularly effective in retaining inorganic As(V), likely due to the oxidation of As(III) to As(V) on the rice root surface (Chen, et al. 2005; Hansel, et al. 2002). Compared to the fine-ordered crystalline form, the amorphous iron (oxyhydr)oxides and weak crystalline ferrihydrite are more efficient in adsorbing As due to their relatively larger surface area (Duiker, et al. 2003; Frommer, et al. 2011). Thus, the amount of iron plaque formation on rice roots and its properties can markedly affect As accumulation in rice grains. A previous study reported that titanium oxide nanoparticles (TiO_2NPs) at 10-1,000 mg/L reduced iron plaque formation and decreased the arsenic retention in iron plaque in a short-term hydroponic experiment (Wu, et al. 2020b), however, the properties of iron plaque were not examined. In spite of the popularity of ZnONPs as a potential nanoagrichemical, no

information is available on the impact of ZnONPs, or its ionic counterpart, on the formation and properties of iron plaque and the subsequent effect on the As accumulation in rice grains in soil.

The objectives of this study were to (1) determine the effect of ZnONPs, Zn salt and ZnO bulk particles (ZnOBPs) on As accumulation and speciation in rice root, shoot, husk and grains over the life cycle of rice; and (2) ascertain their effect on the formation and properties of iron plaque and the subsequent impact on As accumulation in rice tissues. Zinc salt or ZnOBPs were included in the study because of the notably different impact of these different Zn forms on soil properties and plant growth, and the unsettled debate with regard to the advantages and disadvantages of nanoagrichemicals over conventional salt agrichemicals.

Materials and Methods

Nanoparticles and other chemicals

Sodium arsenite (NaAsO_2 >90%) was purchased from Sigma Aldrich (St. Louis, MO). ACS reagent-grade zinc sulfate heptahydrate ($\text{ZnSO}_4 \cdot 7\text{H}_2\text{O}$ >99%) was purchased from Acros Organics (Geel, Belgium). ZnONPs with an average size of 30 nm were obtained from US Research Nanomaterials, Inc (Houston, TX, USA). They are primarily spherical and their size ranged from 15 to 137 nm, as determined by A Tecnai G2 F20 transmission electron microscope (TEM) in our previous study (Wang, et al. 2021). Certified ACS grade ZnOBPs were purchased from Alfa Aesar (Haverhill, MA, USA) and had an average size of 172 nm. ZnOBPs consist of both spherical and rod particles.

The hydrodynamic size and zeta potential of ZnONPs in 100 mg/L solution prepared with ultrapure water were measured with a dynamic light scattering (DLS) (Malvern Zetasizer Nano-ZS90) and were 991 ± 39 nm and 7.6 ± 1.3 mV, respectively. The zeta potential of ZnOBPs was comparable to that of ZnONPs at 6.0 ± 1.9 mV. The hydrodynamic size of ZnOBPs was not attained due to their substantial aggregation, which made their hydrodynamic size out of the optimal range of DLS measurement.

Table III-1. Soil characteristics of Topsoil (0-15 cm) from Eagle Lake, TX by the Soil, Water and Forage Testing Laboratory at Texas A&M University.

Soil parameters	Units	Values
pH	/	4.63 ± 0.05
Conductivity	umho/cm	320.0 ± 91.4
Nitrate-N	mg/kg	42.0 ± 5.5
Phosphorus	mg/kg	19.3 ± 0.5
Potassium	mg/kg	59.0 ± 6.2
Calcium	mg/kg	343.5 ± 55.7
Magnesium	mg/kg	89.0 ± 4.8
Sulfur	mg/kg	88.5 ± 33.0
Sodium	mg/kg	16.0 ± 2.2
Iron	mg/kg	30.4 ± 0.8
Zinc	mg/kg	0.4 ± 0.07
Manganese	mg/kg	14.0 ± 2.0
Copper	mg/kg	0.28 ± 0.10
Silt	%	19
Clay	%	15
Organic carbon	%	2.47
Texture	/	Silt loam

Topsoil (0-15 cm) from a rice paddy field near Eagle Lake, Texas, USA (N 29° 37', W 96° 22') was collected and processed as reported in our previous publication (Wang, et al. 2021). Briefly, the collected soil was air-dried and sieved through a 2-mm sieve. The details of the soil properties are presented in **Table III-1**. The soil is characterized as a silt loam, containing 19% silt, 15% clay, and 2.47% organic carbon. The background As is around 1.36 mg/kg. The DTPA (diethylenetriaminepentaacetic acid) extractable Fe and Zn are around 30.4 and 0.4 mg/kg, respectively.

Treatment setup

Five treatments were prepared by mixing known amounts As and/or Zn amendments with 4.5 kg of dry soil in each pot. The treatments included one negative control (background soil without any amendments), one positive control with 5 mg/kg of freshly added As, and combinations of 5 mg/kg As with 100 mg/kg ZnONPs, Zn²⁺, or ZnOBPs as element Zn. For mixing, the soil was homogenized with a clean spatula by vigorously mixing it for ten minutes manually. 5 mg/kg of fresh As was added in treatments except for the negative control to raise the As concentration to the average As level in U.S. soil (Chou and Harper 2007; Punshon, et al. 2017). Four replicates were prepared for each treatment. Around 1.38 L of rainwater was added to each pot to achieve a 70% field water holding capacity. The use of harvested rainwater for rice cultivation is a common practice in Texas due to water shortage. The pots were then sat in a greenhouse for two days to further homogenize the soil before planting.

Plant growth and harvest

A popular high-yielding long-grain hybrid, XP753, from RiceTec Inc. (Alvin, TX, USA) was used in this study. Before planting, rice seeds were pre-germinated in an incubator at 30 °C for 36 hours. Seven similar-sized seeds were evenly placed about 1.5-cm beneath the soil surface in each pot and the moisture was maintained at 60% for the first 28 days. The seedlings were then thinned down to four in each pot and the pots were flooded by maintaining 9-cm water on top of the soil surface until harvest. The day of seed planting was considered as Day 0. Sampling took place at both the maximum tillering stage (Day 47) and mature stage (Day 104). In each stage, the fresh biomass of rice tissues, the amount and properties of iron plaque and the total As and different As species in plant tissues were determined as detailed below. The fertilizer management followed the same procedure as reported in our previous study (Wang, et al. 2021).

Plant tissue sampling

Two rice plants were gently removed from each pot at the maximum tillering stage, and then thoroughly cleaned with water and separated into roots and shoots manually. The roots and shoots of two sampled plants were pooled together as one replicate for each treatment. Plants were similarly sampled at the mature stage. Half of the shoots from each pot at both stages were oven-dried at 70 °C for 7 days and were used to determine the total As and Zn contents in these tissues. The other half was freeze-dried for As speciation analysis. Root biomass was collected by removing any visible soil particles first. Then they were thoroughly rinsed with deionized (DI) water, and the fresh biomass was measured. One replicate from each treatment was freeze-dried for the characterization of iron plaque and the other three replicates were dithionite-

citrate-bicarbonate (DCB) extracted to quantify the formation of iron plaque (Taylor and Crowder 1983). Rough rice was threshed manually. Half of the rough rice was air-dried for two to three days and weighed. Grain moisture content was determined with a digital moisture meter after weighing. The grain yield was expressed in grams per plant after adjusting the weight to 12% moisture content for the rough rice. The other half of the rough rice was freeze-dried for As speciation analysis. All rough rice was de-husked manually after drying, and separated into brown rice (grains) and husk for further analysis.

Dithionite-citrate-bicarbonate (DCB) extraction of iron plaque

Fresh rice roots from each replicate were put into a beaker with 300 mL of DCB solution (0.03 M sodium citrate, 0.125 M sodium bicarbonate and 0.6 g sodium dithionite). The mixture was incubated for 1 h at room temperature, and then the roots were rinsed with DI water three times. The washing solution was collected and added to the DCB extract. The extract was then made to 500 mL with DI water. Total Fe, As and Zn in the solution was then determined by an inductively coupled plasma-mass spectrometry (ICP-MS) to quantify the iron plaque, and its retainment of As and Zn (Hu, et al. 2005).

X-ray Diffraction analysis of iron plaque

About one-third of the root tissue unextracted with DCB from each treatment was vertically cut and ground to powder with a coffee grinder. The powder was sieved through a 2 mm sieve to remove large fibers. The sieved powder was directly examined

by an X-ray diffraction (XRD) to determine the composition and crystallinity of iron plaque.

Total elements in rice tissues

After DCB extraction, half of the rice root biomass from each pot was oven-dried at 70 °C for 7 days or until the biomass reached constant weight. The dried biomass (including the grains and husks) were ground and acid-digested to measure the total As, Zn, and Fe in these tissues following an established protocol (Wang, et al. 2019b). Briefly, about 1 g of dry biomass was added into 5 mL nitric acid solution (70% by volume) and sat overnight at room temperature for pre-digestion. They were further digested using a DigiPREP MS hot block digester (SCP science, Clark Graham, Canada) at 95 °C for 4 hours until all residual tissues were fully dissolved. The digestate was then cooled to room temperature and mixed with 3 mL of 30% (w/v) H₂O₂ and heated in the hot block again at 95 °C for another two hours. This solution was then analyzed by ICP-MS to determine the total As, Zn, and Fe.

As speciation in plant tissues

The other half of the rice tissues including husks and grains from each pot were freeze-dried and ground for As speciation analysis, following the modified EPA method 3050b (Wang, et al. 2018). Briefly, 0.1 g of the freeze-dried biomass was added into 20 mL of 0.15 mol/L nitric acid and 5 mg/L of Ag⁺. The mixture was sat overnight at room temperature for pre-digestion and then digested using a DigiPREP MS hot block digester at 100 °C for 2 hours until all residual tissues were fully dissolved. Afterward, the solution was transferred to a 50 mL centrifuge tube and centrifuged at 4,000 rpm for 10

min. The liquid phase was filtered through a 0.45 μm membrane filter and the filtrate was analyzed by a coupled high performance liquid chromatography ICP-MS (HPLC/ICP-MS).

Fe(II) and Fe(III) in soil

The concentration of Fe(II) and Fe(III) in the soil was determined by adding 1 g of freeze-dried soil into a 15 mL centrifuge tube with 3 mL of 0.05 M CaCl_2 under an anaerobic environment. 10 mL of 1 M NH_4OAc at pH 2.8 was then added to the tube. Afterward, the tube was sealed and shaken for 30 min on a shaker table. The extract was then centrifuged at 3,000 rpm for 10 mins, and all the solution phase was filtered through a 0.45- μm filter to determine Fe(II). Afterward, 10 mL of 2 M H_2SO_4 was added to the residue, and the processes of shaking, centrifugation and filtration were repeated to measure Fe(III) in the filtrate.

Statistical Analysis

One-way analysis of variance (ANOVA) with Tukey's comparison test was performed using Minitab 18 (Minitab Inc., State College, PA). The differences were considered significant when $p \leq 0.05$. All data were expressed as sample average with standard deviation (SD).

Results and Discussion

Rice biomass and yield

Plant root biomass was unaffected by the addition of As and Zn amendments at the tillering stage. However, joint As and Zn treatment significantly decreased the root

biomass at the mature stage compared with rice grown in the background soil or soil treated with As alone. The addition of 5 mg/kg of fresh As significantly lowered the rice shoot biomass at the tillering stage compared to plants grown in the background soil, even though the shoot biomass reached similar levels at the mature stage, **Figure III-1**. Interestingly, joint As and Zn treatments, irrespective of the Zn format, significantly increased the rice shoot biomass at the tillering stage but decreased the shoot biomass at the mature stage compared to As only treatment. The opposite effect of Zn amendments on rice shoot biomass at two growth stages emphasized the necessity of long-term studies. Our results shed light on the seemingly contradictory results in the literature with regard to the impact of ZnONPs on plant growth and suggest that the experimental duration is a significant consideration in the interactions of plants and nanoparticles (Chen, et al. 2018; Rameshraddy, et al. 2017; Wang, et al. 2018; Wu, et al. 2020a; Yan, et al. 2021). Notably, the grain yield in the As alone treatment was 86.3% lower than that from the background soil treatment. However, Zn fertilization markedly alleviated the impact of As and improved the grain yield to statistically comparable levels of the background rice, with the Zn salt demonstrating the greatest beneficial effect. The result agrees with previous studies that Zn could alleviate As stress and promote rice yields (Bala, et al. 2019; Muthukumararaja and Sriramachandrasekharan 2012; Wu, et al. 2020a; Yan, et al. 2021).

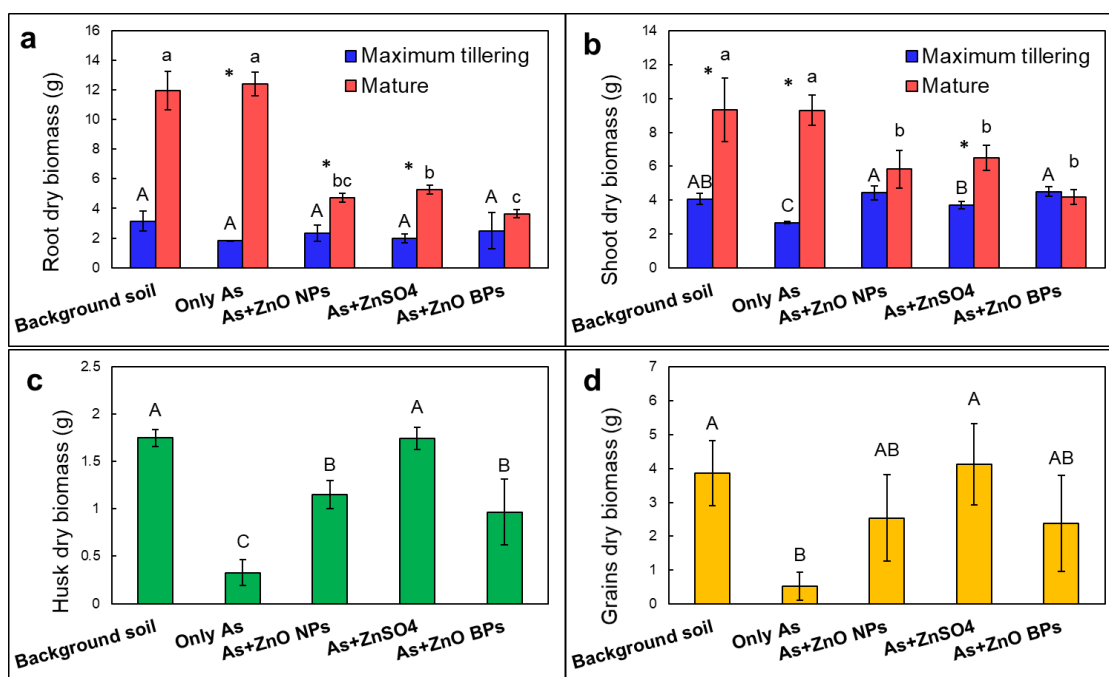


Figure III-1. The biomass of (a) root and (b) shoot of rice at the maximum tillering and mature stage; and the biomass of (c) husk and (d) de-husked grains at the mature stage. Values represent mean \pm SD ($n = 4$), with different letters indicating significant differences ($p \leq 0.05$) according to one-way ANOVA followed by Tukey's test. Asterisks (*) indicate significant differences between two growth stages according to t-test.

Impacts of Zn amendments on the total As in rice tissues

The impact of the Zn amendment on the total As varied with the specific rice tissue, the growth stage and Zn form (**Figure III-2**). ZnONPs and ZnOBPs significantly lowered the root As concentration in the mature stage by 25.3% and 18.3%, respectively, while Zn²⁺ significantly increased it by 61.9% compared to the treatment with As alone. The total As concentration in rice shoots was significantly lower in Zn-exposed plants at the tillering stage, with Zn²⁺ and ZnOBPs resulting in even lower total As in rice shoots than the ones treated with ZnONPs. The results at the maximum tillering stage agree with our previous studies that ZnONPs and Zn²⁺ both lowered As concentration in rice

shoots at the early stage of rice growth, with Zn²⁺ demonstrating greater effect (Ma, et al. 2019; Wang, et al. 2018). However, the total As concentration in rice shoots was statistically the same from all treatments at the mature stage, suggesting that studies extending to the whole life cycle of rice are necessary to reveal the long-term effect of Zn amendments. Interestingly, while the total As in rice grains and husk was unaffected by either ZnONPs or ZnOBPs, Zn²⁺ significantly decreased the total As in rice grains and husks by 31.0% and 42.6%, respectively.

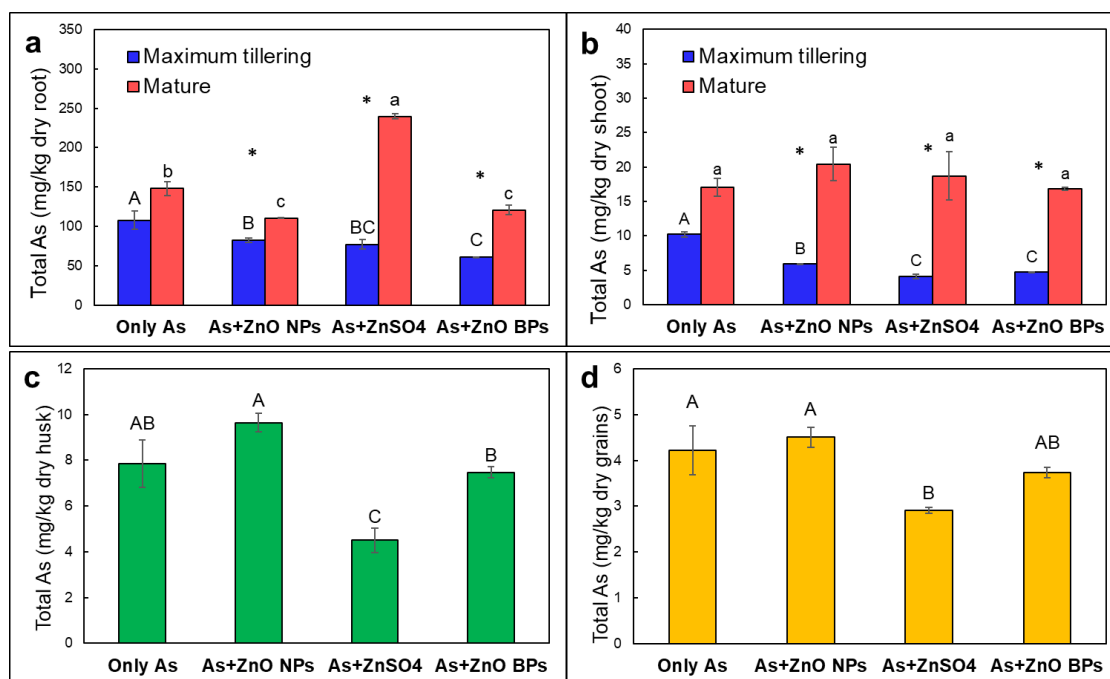


Figure III-2. Total As in rice (a) root and (b) shoot at the maximum tillering and mature stages; and in rice (c) husk and (d) de-husked grains at the mature stage. Values represent mean \pm SD ($n = 4$), with the different letters indicating significant differences ($p \leq 0.05$) according to one-way ANOVA followed by Tukey's test. Asterisks (*) indicate significant differences between two different growth stages according to t-test.

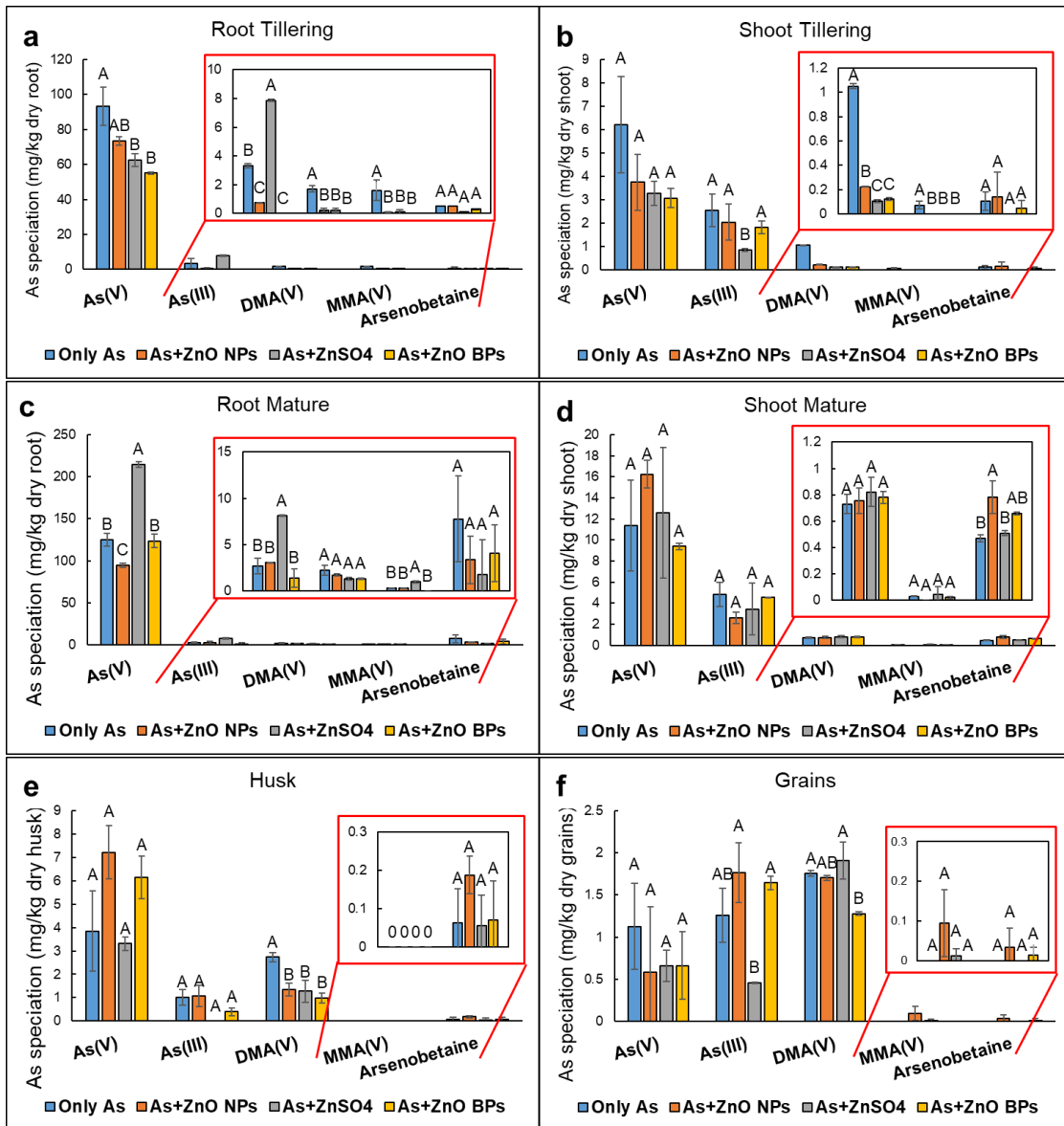


Figure III-3. As speciation in rice root and shoot at the maximum tillering (a and b) and the mature stage (c and d), and in (e) husks, and (f) de-husked grains. Reported values represent mean \pm SD ($n = 4$), with different letters indicating significant differences ($p \leq 0.05$) according to one-way ANOVA followed by Tukey's test.

Effects of Zn amendments on As speciation

Inorganic As(V) is the dominant species in rice roots in all treatments (**Figure III-3**). In rice shoots, inorganic As (V) and As(III) were notably higher than other species. Interestingly, Zn²⁺ displayed remarkably different impact on the As speciation in rice tissues than the two particulate Zn amendments. In rice roots, Zn²⁺ significantly increased the concentrations of both As(V) and As(III) in rice roots at the mature stage while the particulate Zn amendments either did not affect the concentrations of either species or lowered their concentrations. Similarly, only Zn²⁺ significantly lowered the As(III) concentration in rice shoots at the maximum tillering stage while other two amendments showed minimal impact on As speciation in rice roots at both stages. In rice husks, while As(V) remained the dominant species, more DMA(V) was detected, followed by As(III). All forms of Zn led to significantly lower DMA(V) in husks but showed no significant impact on the other two species. In rice grains, DMA(V) become the most dominant As species, followed by the two inorganic As species, consistent with the As speciation in USA rice grains (Zavala, et al. 2008). Importantly, while all Zn fertilizers insignificantly lowered As(V) by 41.1% to 48.2%, only Zn²⁺ significantly lowered the As(III) concentration in rice grains.

To gain further insight into the effect of Zn amendments on As speciation, the As(III)/total As ratio was calculated (**Figure III-4**). Most notably, Zn²⁺ significantly lowered As(III)/total As in rice grains, while ZnOBPs significantly increased this ratio. ZnONPs showed no effects on this ratio in the grains. The dramatically increased As(III) retention on the rice root by Zn²⁺ at the early stage may contribute to the lower

As(III)/total As ratio in the husk and grains. Previous studies reported that Zn^{2+} could form Zn-As(III) complex and stabilize in the rice root, similar to the Zn-silicate complex (Imtiaz, et al. 2016; Kaya, et al. 2009). While ZnONPs have displayed benefits in the early stage of rice, our results showed that the conventional Zn salt fertilizer led to relatively higher albeit insignificant rice yield and significantly lower As(III) content in rice grains, which has strong implications for food safety and public health. Therefore, it is prudent to be cautious in fully embracing nanotechnology in agriculture. ZnONPs holds the advantage over Zn salt in terms of Zn utilization rate because ZnONPs releases Zn slower than Zn salt. However, the argument that ZnONPs is more effective than Zn salt as a fertilizer needs to be more closely examined in rice paddies where As might be a food safety concern. As uptake and speciation in rice tissues are governed by many factors such as the speciation and bioavailability of As in rice rhizosphere, the expression of As transporters in rice roots and shoots, and the microbial activities in rice rhizosphere (Awasthi, et al. 2017; Jia, et al. 2014; Wang, et al. 2015). Among them, iron plaque plays a critical role in As uptake (Liu, et al. 2006). However, few studies have examined the impact of soil amendments on the formation and properties of iron plaque. It is postulated that Zn amendments modify the formation and properties of iron plaque on rice roots and subsequently affect the As uptake and accumulation in rice tissues. Thus, the formation and properties of iron plaque on rice roots were further investigated with different analytical and spectroscopic tools.

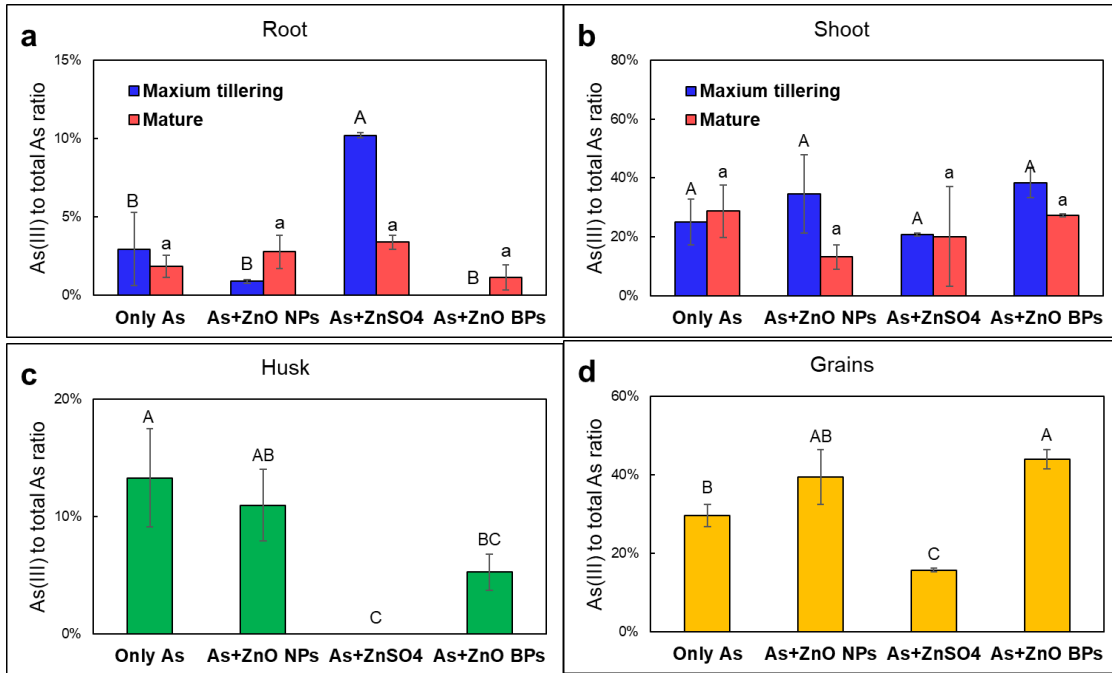


Figure III-4. The impacts of different Zn amendments on As(III) to total As ratio in rice (a) root and (b) shoot at the maximum tillering and mature stage; and the As(III) to total As ratio in rice (c) husk and (d) de-husked grains at the mature stage. Values represent mean \pm SD ($n = 4$), with different letters indicating significant differences ($p \leq 0.05$) according to one-way ANOVA followed by Tukey's test.

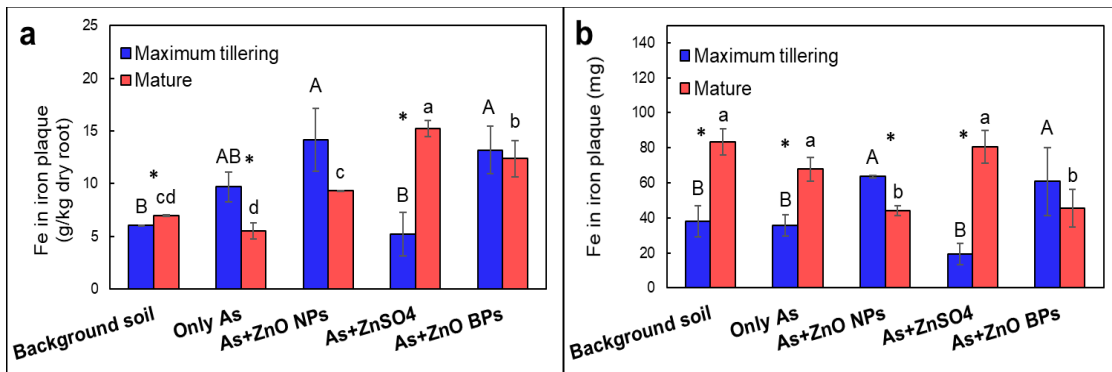


Figure III-5. (a) The amount of DCB-extractable Fe normalized by root dry weight and (b) the total mass of Fe in the iron plaque at maximum tillering and mature stages. Values represent mean \pm SD ($n = 4$), with different letters indicating significant differences ($p \leq 0.05$) according to one-way ANOVA followed by Tukey's test. Asterisks (*) indicate significant differences between two different growth stages according to t-test.

Impacts of Zn fertilizers on iron plaque formation

As alone did not appreciably affect the formation of iron plaque at both growth stages. However, co-exposure to As and Zn markedly affected the formation of iron plaque and the impact varied with the forms of Zn fertilizer and plant growth stages (**Figures III-5**). At the tillering stage, ZnONPs and ZnOBPs treated rice had substantially higher iron plaque (DCB extractable-Fe) than plants treated with Zn²⁺ (**Figures III-5a**). Even though all forms of Zn amendments increased the DCB-extractable Fe content compared to plants exposed to As alone, Zn²⁺ resulted in the greatest iron plaque formation in rice roots. Previous studies indicated that iron plaque is most effective in retaining As(V) (Frommer, et al. 2011; Liu, et al. 2006; Seyfferth, et al. 2010). Due to the varying root biomass from different treatments, iron plaque per pot (with two seedlings sampled at each stage) was calculated (**Figure III-5b**). Both ZnONPs and ZnOBPs led to lower iron plaque at the mature stage than at the maximum tillering stage, indicating that the iron plaque might have reductively dissolved in those treatments (Liu, et al. 2021b). It is not uncommon for iron plaques on aged rice roots to dissolve when the root oxygen release decreases, suggesting that ZnONPs and ZnOBPs might accelerate rice growth and shorten its life cycle (Chen, et al. 2016b; Zhang, et al. 2012). Dissolved iron plaque could release As initially retained in it and increase available As, which partially explains why the inhibition of rice As uptake by ZnONPs or ZnOBPs was only observed at the maximum tillering stage.

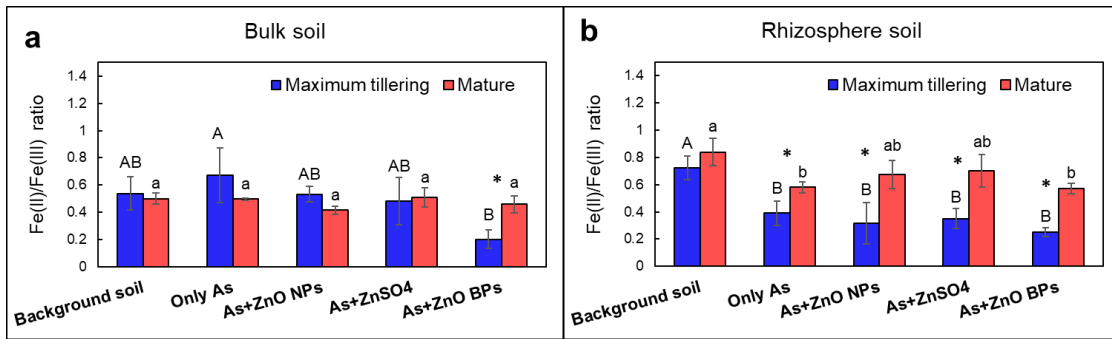


Figure III-6. Fe(II)/Fe(III) ratio (a) in the bulk soil and (b) in the rhizosphere soil at two growth stages. Values represent mean \pm SD ($n = 4$), with different letters indicating significant differences ($p \leq 0.05$) according to one-way ANOVA followed by Tukey's test. Asterisks (*) indicate significant differences between two different growth stages according to t-test.

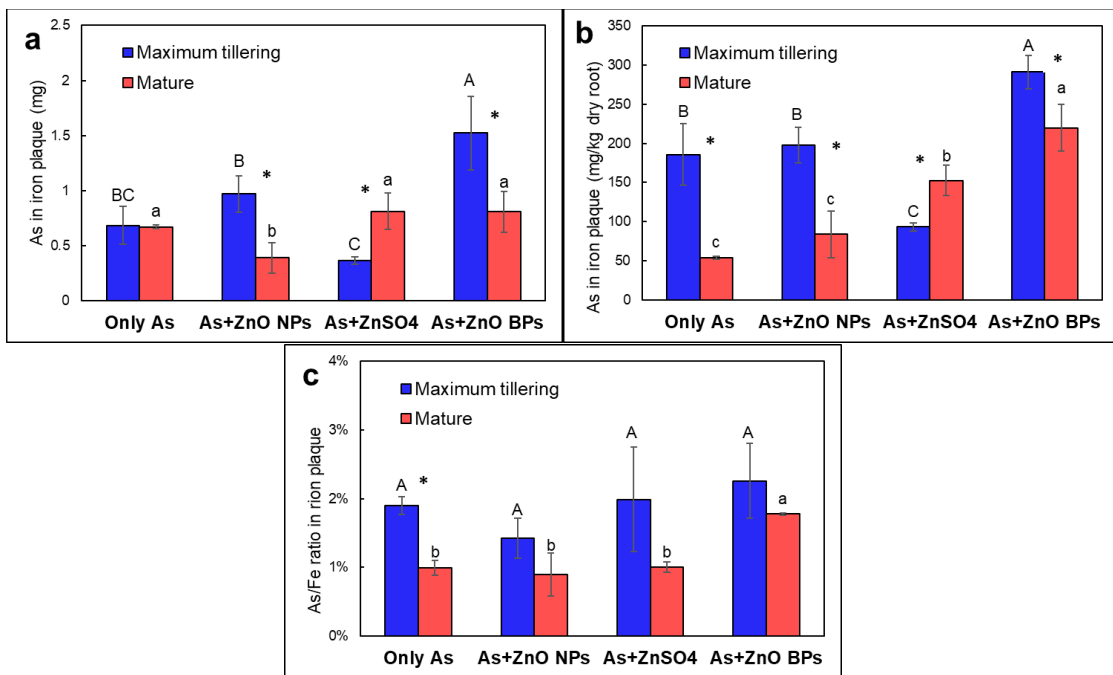


Figure III-7. (a) The total mass of As in the iron plaque, (b) As content in the DCB extraction normalized by dry root weight, and (c) As/Fe ratio in the iron plaque at maximum tillering and mature stages. Values represent mean \pm SD ($n = 4$), with different letters indicating significant differences ($p \leq 0.05$) according to one-way ANOVA followed by Tukey's test. Asterisks (*) indicate significant differences between two different growth stages according to t-test.

Because the formation of iron plaque depends on Fe(II) oxidation, Fe(II)/Fe(III) in the soil is considered an essential indicator of Fe(II) availability and iron plaque formation (Zhang, et al. 2020). The Fe(II)/Fe(III) ratio in both the bulk and rhizosphere soil are shown in **Figures III-6**. As and ZnOBPs together significantly lowered the Fe(II)/Fe(III) ratio in the bulk soil at the tillering stage. However, no differences were observed at the mature stage. In the rhizosphere soil, the Fe(II)/Fe(III) ratio was comparable among treatments with As alone or joint As and Zn amendments at both growth stages. The results indicated that Fe(II) availability from different treatments was not a governing factor for the varied formation of iron plaque in different treatments. Altered radial oxygen loss (ROL) from plant roots exposed to different treatments could contribute to the different formation of iron plaques because 50-150 mg/kg Zn²⁺ has been shown to increase ROL from rice roots in a hydroponic study under heavy metal stress (Cheng, et al. 2012; Ma, et al. 2020a). To confirm the role of iron plaque in As retainment, the total As in iron plaque at different growth stages is shown in **Figures III-7a and 7b**. The total As in iron plaque from different treatments followed a similar trend as the iron plaque itself, suggesting that iron plaque indeed played a role in As retainment. As accounted for about 1-2% of the total iron plaque from different treatments, **Figure III-7c**. However, observable differences can be seen from different treatments. For instance, the As/Fe ratio was noticeably higher in the Zn²⁺ and ZnOBPs treated plant roots. The result implied that Zn amendment would affect not only the formation of iron plaque, but also its properties such as the fractions of amorphous vs. crystalline Fe in the iron plaque, which was further explored below.

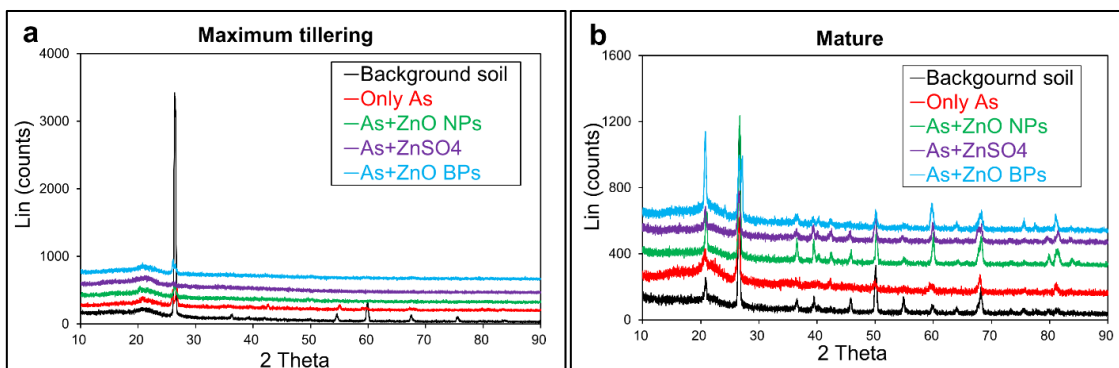


Figure III-8. X-ray diffraction spectra of iron plaque from different treatments at (a) the maximum tillering stage and (b) the mature stage.

Characterization of iron plaque with X-ray diffraction

The iron plaque contained substantial amount of silicon oxide (SiO_2) crystal structures. The result is not surprising considering the high levels of background Si in paddy soils. Highly intriguingly, however, the presence of As and the copresence of As and Zn amendments drastically slowed down the formation of SiO_2 crystals (**Figure III-8**). At the maximum tillering stage, only the iron plaque from the roots of the background soil had a clear spectrum of crystal SiO_2 . Fe oxide in the iron plaque was mostly X-ray amorphous for all treatments.

Conclusions

In closing, our results showed that the application of Zn amendments in As-contaminated paddy soils could improve rice yield and alter the As uptake and accumulation in rice grains. Different from previous short-term studies, our results showed that conventional Zn salt amendment appeared more effective to lower the total As, and the more hazardous As(III) in rice grains. Iron plaque formation and dissolution

at different stages could be a contributing factor in altering As accumulation in rice tissues including grains after the application of Zn amendments. Moreover, more complicated mechanism such as the formation of Zn-silicate were involved in the treatment with Zn ions which could stabilize As(III) in rice root. However, even though the properties of iron plaque were affected by the introduction of Zn amendments, its capability to retain As in the iron plaque did not change substantially. The results suggested that Zn amendment induced changes in iron plaque formation is one of the key factors regulating As uptake in rice. In addition, As and Zn amendments could alter the crystallization of iron plaque and SiO₂ on the root surface, subsequently affecting the As uptake in the rice. Our results provide a better understanding of the mechanisms involved in the uptake and speciation of As in the rice in a soil system during a life cycle of rice. Future studies should evaluate the effects of different Zn fertilizers on the microbial community and activities on the iron plaques to further understand their impact on the properties of iron plaques.

CHAPTER IV

IMPACT OF SOIL COPPER AMENDMENTS ON ARSENIC ACCUMULATION AND SPECIATION IN RICE (*ORYZA SATIVA L.*) IN A LIFE-CYCLE STUDY

Introduction

Due to its dual function as a slow releasing source of Cu micronutrient and an antimicrobial agent, copper oxide nanoparticles (CuONPs) have been used extensively as a nano-fertilizer, nano-pesticide, nano-fungicide and nano-herbicide. (Wang, et al. 2020; Zabrieski, et al. 2015). In addition, substantial amount of engineered nanoparticles including CuONPs are introduced into the agricultural soil with irrigation water and biosolids (Fayiga and Saha 2017; Malwal and Gopinath 2017). Therefore, studies of the interactions between CuONPs and plants or other soil contaminants are of great interest.

Rice (*Oryza sativa L.*) is an essential human food source for more than three billion people and is a critical food crop to feed the rapidly growing global population (Hoang, et al. 2019). Several factors affect the quality of rice, in which the accumulation of arsenic (As) in rice grains is the most serious food safety concern associated with rice consumption (Chen, et al. 2017a; Shrivastava, et al. 2020). A significant number of studies have been conducted and several nanoagrichemicals showed great potential to mitigate As toxicity and accumulation in rice (Cui, et al. 2020; Wu, et al. 2020b; Yan, et al. 2021). Our previous study indicated that 100 mg/L of CuONPs lowered the total As in rice root and shoot in a hydroponic system, and the decrease of As(III) was more significant than the decrease of As(V) (Wang, et al. 2019b). Liu et al.(Liu, et al. 2018a)

also reported that CuONPs at 50 and 100 mg/L, in a nutrient solution alleviated the adverse effect of As on rice seed germination and growth. A negative correlation was observed between the As concentration in rice shoots and the Cu concentration in the growth media (Liu, et al. 2018a). In a soil study concerning the effect of CuONPs on As uptake in rice grains, CuONPs in the irrigation solution decreased the As accumulation in rice grains (Liu, et al. 2019). However, detailed mechanisms for the inhibited As uptake by CuONPs were not provided.

Several studies indicated the adsorption of As(III/V) onto CuONPs is one of the main reasons causing As immobilization and decreased As bioavailability in the growth media (Liu, et al. 2021a; Wu, et al. 2021). Another important mechanism is the oxidation of As(III) to As(V) on the surface of CuONPs, which could lower the As availability and toxicity (Wang, et al. 2019b; Wu, et al. 2021). Furthermore, the addition of CuONPs can thicken the rice root cell wall and upregulate the expression of the *OsNIP1;1*, *OsHAC1;1*, and *OsHAC4* (Wu, et al. 2021). The upregulated *OsHAC1;1*, and *OsHAC4* as As(V) reductase could enhanced As(V) reduction and detoxification in rice root (Shi, et al. 2016; Xu, et al. 2017), while *OsNIP1;1* could decrease root-to-shoot translocation of As(III) (Sun, et al. 2018b).

Rice is usually cultivated in waterlogged soil in the field. Even though the soil is mostly anerobic during the growth period, oxygen released from the paracheyma of rice roots can create an oxidizing environment locally around rice roots where Fe^{2+} is oxidized to form iron plaque on the surface of rice roots (Bacha and Hossner 1977; Chen, et al. 1980; Hansel, et al. 2001). The formation of iron plaque affects the

phytoavailable As and its uptake by rice plants by sequestering As (Lee, et al. 2013; Liu, et al. 2006). A few previous studies also indicated that iron plaque could act as a barrier for the uptake of CuONPs by rice plants (Peng, et al. 2018; Yuan, et al. 2021). However, none of the previous studies has focused on the direct effects of CuONPs on iron plaque formation and the subsequent effects of iron plaque formation on As uptake and accumulation in the rice plants and grains.

This study investigated how the co-exposure of CuONPs and As during the whole life cycle of rice plants affected As uptake and accumulation in rice tissues. The objectives of this study were to (1) assess the impact of CuONPs and their ionic and bulk counterparts on the total As and As speciation in rice tissues over the life cycle of rice; and (2) determine the impact of CuONPs on the iron plaque formation on the rice root surface and the consequent effects on As uptake by rice plants.

Materials and Methods

Nanoparticles Characterization

CuONPs was purchased from US Research Nanomaterials Inc, (Houston, TX, USA) and was characterized using a transmission electron microscope (TEM, Tecnai G2 F20) for its primary size and size distribution (Wang, et al. 2019b; Wang, et al. 2018). Certified ACS CuO bulk particles (BPs) were obtained from Alfa Aesar (Haverhill, MA, USA). The hydrodynamic diameter and zeta potential of CuONPs and CuOBPs in ultrapure water were determined with a dynamic light scattering (DLS) instrument (Malvern Zetasizer Nano-ZS90). The primary sizes of the CuONPs were in the range of

9-22 nm, with an average diameter of 14 nm. The zeta potential and hydrodynamic diameter of the CuONPs were -27.9 ± 4.5 mV and 1028 ± 59 nm, respectively. The zeta potential of the CuOBPs was around neutral at -1.1 ± 5.8 mV, while the hydrodynamic size was not measurable because it was out of the measurement range of the DLS.

Soil Characterization and Preparation

The soil was collected from an agricultural site (N 29° 37', W 96° 22') in Eagle Lake, TX, USA. The soil was first air-dried, sieved through a 2 mm mesh and homogenized before characterization and use. The soil was classified as silt loam soil and has a pH of 4.63. The bioavailable Cu and Fe in the background soil is around 0.28 and 30.4 mg/kg, and the total As is around 1.36 mg/kg. The low bioavailability of Cu in the background soil allowed the accurate observation of the effects from the added Cu amendments.

The soil was prepared by adding As (0 and 5 mg/kg) in the form of NaAsO₂ (Sigma Aldrich, St. Louis, MO, USA) and 100 mg/L of CuONPs, Cu ions (in the form of CuSO₄·5H₂O, Acros Organics Geel, Belgium) or CuOBPs. Thus, there were five treatments, including one negative control with neither As nor Cu addition, one treatment that received only 5 mg/kg of As, and three treatments with the combination of As and 100 mg/kg of CuONPs, Cu ions or CuOBPs as element Cu. A total of 4 replicates was prepared for each treatment and each pot contained 4.5 kg dry soil each. After mixing, the air-dried soil was rewetted to 70% field capacity with rainwater and incubated for two days in the greenhouse for further homogenizing before seeding the rice.

Rice Growth and Sampling

Rice seeds (XP753, RiceTec Inc., Alvin, TX, USA) were germinated first at 30 °C for 36 hours before planting. Seven pre-germinated seeds were evenly planted right below the soil surface in each growth container and this date was recorded as Day 0. All pots were kept at 60% water holding capacity for the first 28 days to create a moisture condition for rice seedlings growth. On Day 29, only four rice seedlings of similar size were kept in each pot, and all growth pots were permanently flooded with rainwater. Urea, P fertilizer and K fertilizer were applied to soil during the rice growth following the general guidelines of nutrient management as reported in our previous study (Wang, et al. 2021). The experiment was conducted in a greenhouse for about 104 days until rice plants reached the mature stage. The sampling of plant tissues was carried out on Day 47 and Day 104 at the maximum tillering stage and maturing stage of rice.

On Day 47, two randomly selected plants were gently pulled out from each pot as one replicate for each treatment. The fresh biomass was obtained by cleaning the rice roots thoroughly with DI water and separating the root and shoot. At the mature stage, the fresh root and shoot biomass was similarly measured. After recording the fresh biomass, the shoots from both stages were freeze-dried for further analysis of total elements and As speciation, while the root was extracted using dithionite-citrate-bicarbonate (DCB) methods before freeze-dried. Rough rice was threshed manually and weighed to get fresh grain biomass. Exactly half weight of the rough rice was freeze-dried and de-husked manually into brown rice (grains) and husk for total elements and As speciation analysis. And the other half of the rough rice was air-dried to determine

the yield. After air-drying for 2-3 days, the rough rice was weighed and the moisture content was measured with a digital moisture meter. The yield was determined by calculating the weight at 12% moisture content of the rough rice.

Iron Plaque Extraction

DCB extraction was used to determine the iron plaque formation on rice roots at both growth stages (Liu, et al. 2004; Taylor and Crowder 1983). Fresh roots of each replicate were soaked in 300 mL solution containing 0.03 M sodium citrate, 0.125 M sodium bicarbonate and 6 g sodium dithionite at room temperature for about 1 hour. Afterward, the root was rinsed with ultrapure water three times. The extract solution was combined with the root washing solution and then made to 500 mL with ultrapure water. The mixture was then transferred to a centrifuge tube and centrifuged at 10,000 rpm for 10 mins. The total elements such as As, Fe and Cu in the supernatant were analyzed by an inductively coupled plasma-mass spectrometry (ICP-MS). The roots after DCB extraction were then freeze-dried for further analyses.

Total Elements in Rice Tissues and Grains

Total As, Fe and Cu concentrations in the root and shoot at both growth stages, and in husk and dehusked grains were determined by ICP-MS after acid digestion, following our previously reported method (Wang, et al. 2019b). Briefly, about 1 g of dried and ground rice tissues was weighed and incubated in 5 mL of 70% nitric acid solution in a 50 mL digestion tube overnight at room temperature. A DigiPREP MS hot block digester (SCP science, Clark Graham, Canada) was used for heat digestion. The mixture was heated at 95 °C until all residual tissues were fully dissolved and cooled to

room temperature. Three mL of 30% (w/v) H₂O₂ was added to each tube, and the digestate was then heated for another 2 hours in the hot block digester. The solution after digestion was made to 50 mL with ultrapure water and analyzed through an ICP-MS.

As Speciation in Rice Tissues and Grains

The As speciation in plant biomass was determined by a coupled high performance liquid chromatography ICP-MS (HPLC/ICP-MS) after digestion followed our previous study (Wang, et al. 2018). Firstly, 0.1 g of freeze-dried and ground rice tissues were mixed with a 20 mL solution containing 0.15 mol/L nitric acid and 5 mg/L of Ag⁺. The mixture was heated on a DigiPREP MS hot block digester at 100 °C for 4 hours after being incubated at room temperature overnight. The solution was then centrifuged at 4,000 rpm for 10 min and the supernatant was filtered through a 0.45 µm syringe filter for the HPLC/ICP-MS analysis.

Statistical Analyses

One-way analysis of variance (ANOVA) with Tukey's comparison test was conducted to determine the effects of As and Cu amendments. Means were considered significantly different when $p \leq 0.05$. All statistical analyses were performed using Minitab 18 (Minitab Inc., State College, PA).

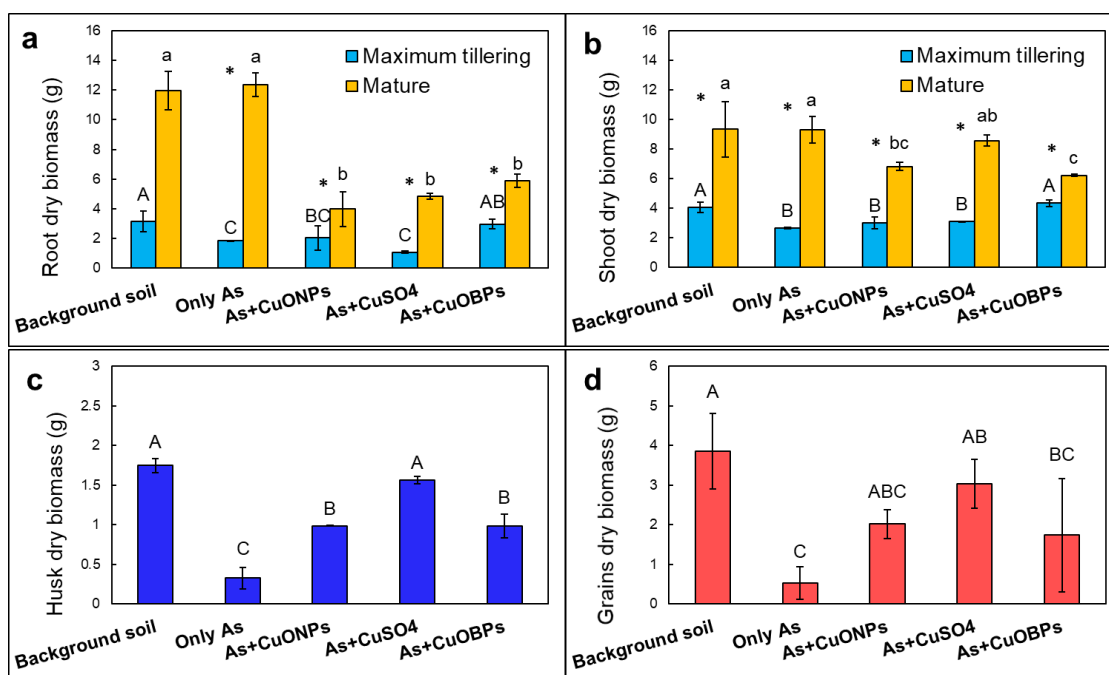


Figure IV-1. The biomass of rice (a) root and (b) shoot at the maximum tillering and mature stage; and the biomass of rice (c) husk and (d) de-husked grains at the mature stage exposed to arsenic and different Cu amendments in soil ($n = 4$). Different letters indicate significant differences between different treatments ($p < 0.05$). Asterisks (*) indicate significant differences between maximum tillering and mature stages according to t-test.

Results and Discussion

Effects on Rice Plant Growth and Yield

Arsenic at 5 mg/kg significantly decreased the root and shoot biomass at the maximum tillering stage compared to the background soil (**Figure IV-1**). Even though the root and shoot biomass reach similar levels at the mature stage as plants grown in background soil, the grains and husk biomass treated with only As was significantly decreased by 86% and 81%. The co-exposure of As and CuOBPs significantly increased the root and shoot biomass at the maximum tillering stage compared with plants receiving As alone, while the addition of the other two forms of Cu amendments did not

significantly increase the rice biomass at the maximum tillering stage. However, at the mature stage, all three forms of Cu amendments significantly decreased the root biomass by 53% - 68% and slightly lowered the shoot biomass by 8-33% compared to the plants treated with only As. Surprisingly, these adverse effects were not observed on the husk and grains biomass. Instead, all three forms of Cu fertilizer increased the husk biomass by 201% - 377% and increased the grains biomass by 284% - 475% compared to rice grown in soil with only As, with the Cu ions having the most beneficial effects.

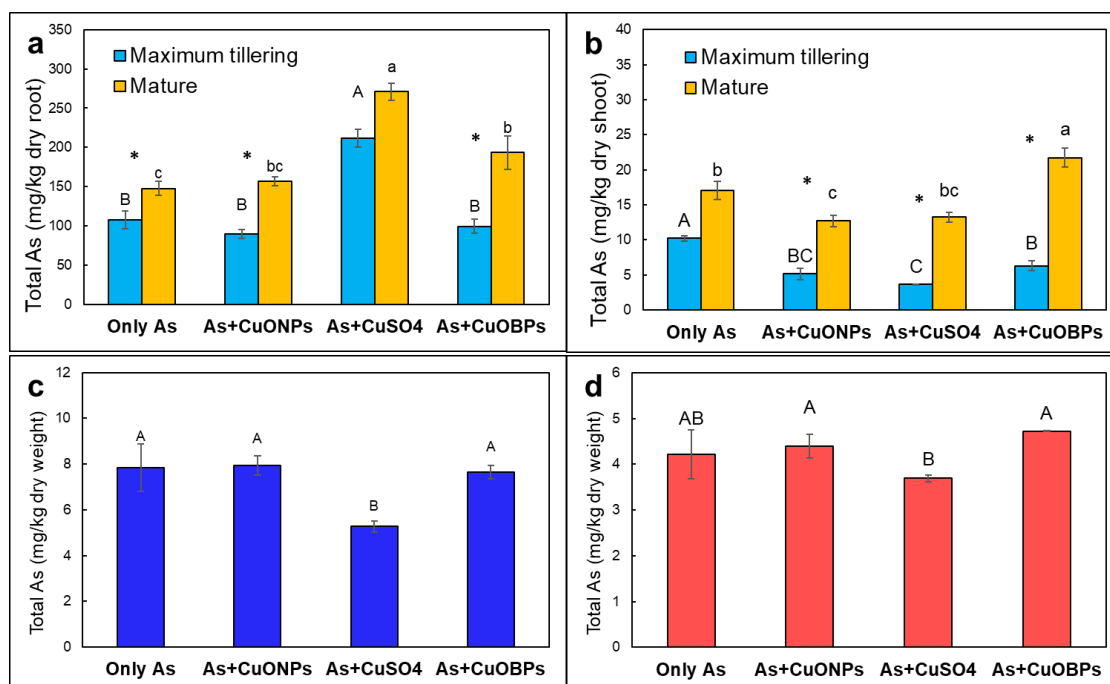


Figure IV-2. The total As in rice (a) root and (b) shoot at the maximum tillering and mature stage; and the As accumulation in rice (c) husk and (d) de-husked grains at the mature stage exposed to arsenic and different Cu amendments in soil ($n = 4$). Different letters indicate significant differences between different treatments ($p < 0.05$). Asterisks (*) indicate significant differences between maximum tillering and mature stages according to t-test.

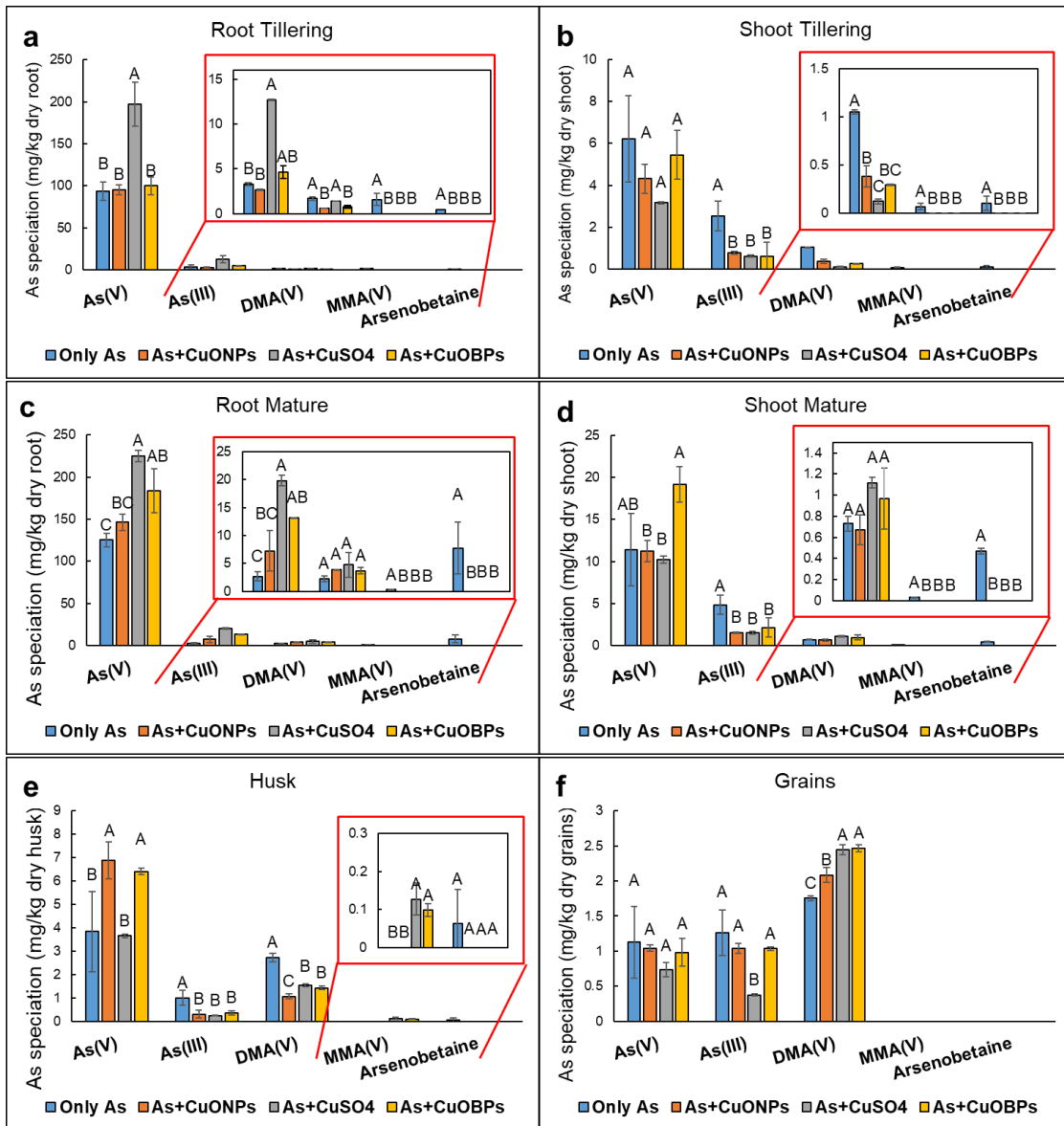


Figure IV-3. The As speciation in rice (a)(c) root and (b)(d) shoot at the maximum tillering stage and mature stage, respectively; and the biomass of rice (e) husk and (f) de-husked grains at the mature stage exposed to arsenic and different Cu amendments in soil ($n = 4$). Different letters indicate significant differences between different treatments in each As species group ($p < 0.05$).

Our results generally agreed with previous studies that CuONPs could mitigate the adverse effects of As to rice plants and improve rice yield and seedling growth (Liu,

et al. 2018a; Liu, et al. 2018b). In this study, traditional Cu salt fertilizer showed the best performance regarding the rice grains yields. The opposite effect of Cu amendments on the root and shoot biomass and grains at the mature stage might be because that the addition of Cu amendments shortened the growth period of rice plants, therefore, resulting in lower root and shoot biomass at the mature stage (Liu, et al. 2018b).

Effects of Cu amendments on As Accumulation in Rice

The total As in rice roots was significantly increased by 96% and 83% at the maximum tillering and mature stage by Cu ions compared to the As treatment (**Figure IV-2**). CuONPs did not affect the total As in rice roots at both stages, while CuOBPs significantly increased the As concentration in rice roots by 31% at the mature stage. The total As in rice shoots was significantly lowered by Cu amendments at the maximum tillering stage, but different forms of Cu fertilizer showed different effects on the As concentration in rice shoots at the mature stage. CuONPs significantly decreased the shoot As concentration by 25%, and Cu²⁺ also insignificantly lowered it by 22%. However, CuOBPs significantly increased the shoot As accumulation by 28% compared to the only As treated plants. The measured total As in plant tissues at the maximum tillering stage was generally consistent with our previous observations in a hydroponic study, which also showed that both CuONPs and Cu ions can lower As accumulation in rice shoot at the early stage (Wang, et al. 2019b). However, their different effects on As accumulation in rice shoots at the mature stage suggested that experiments extending to the whole life cycle of rice are necessary to reveal the long-term effect of Cu fertilizers. Interestingly, the addition of CuONPs and CuOBPs did not affect the total As in rice

husk and grains, but Cu^{2+} significantly lowered the total As in rice husk by 33% and slightly decreased As accumulation in rice grains by 13%. In contrast to some previous studies which suggested that CuONPs decreased the As accumulation in rice grains (Liu, et al. 2018b; Liu, et al. 2019), our results showed that traditional Cu salt fertilizer is more effective in reducing As accumulation in rice grains than CuONPs possibly due to the significantly increased As retention in rice root. However, the decreasing of As concentration in the rice grains was not significant, therefore, As speciation was measured to further evaluate the effects of Cu amendments.

Effects of Cu amendments on As Speciation in Rice

The As speciation in rice tissues is presented in **Figure IV-3**. Inorganic As(V) dominated in rice root and shoot from all treatments and at both growth stages. Cu ions significantly increased both inorganic As(III) and As(V) in rice root at both stages, while CuOBPs only significantly increased As(III) and As(V) in rice root at the mature stage. The addition of CuONPs showed minimum effect on the inorganic As species in rice roots compared with plants exposed to only As. All three forms of Cu significantly decreased As(III) and organic As species, especially monomethylarsonic acid (MMA(V)) and arsenobetaine in rice shoot tissues at both growth stages. The decreased As(III) in rice shoots was consistent with the result from previous short-term hydroponic studies with CuONPs (Wang, et al. 2019b; Wu, et al. 2021) Both CuONPs and CuOBPs display high adsorption capacity for As(III). It has been reported that As(III) could be oxidized to As(V) on the surface of CuONPs accompanied with the reduction of Cu^{2+} to Cu^+ , or by reactive oxygen species (ROS) induced by free Cu^+ (McDonald, et al. 2015;

Wang, et al. 2019b; Wu, et al. 2021). For Cu ions, the significantly higher As retention in rice root may be related to mechanisms to minimize the phytotoxicity of Cu ions in which excessive Cu ions form complexes with root exudates and are sequestered into vacuoles of root cells, together with As (Chen, et al. 2017b; Gong, et al. 2020; Printz, et al. 2016). This higher root As retention decreased As transfer from roots to shoots. The Cu distribution in rice different tissues further support this hypothesis and indicated that plant response to Cu toxicity in the early growth stage of rice contributed to lower As uptake (**Figure IV-4**).

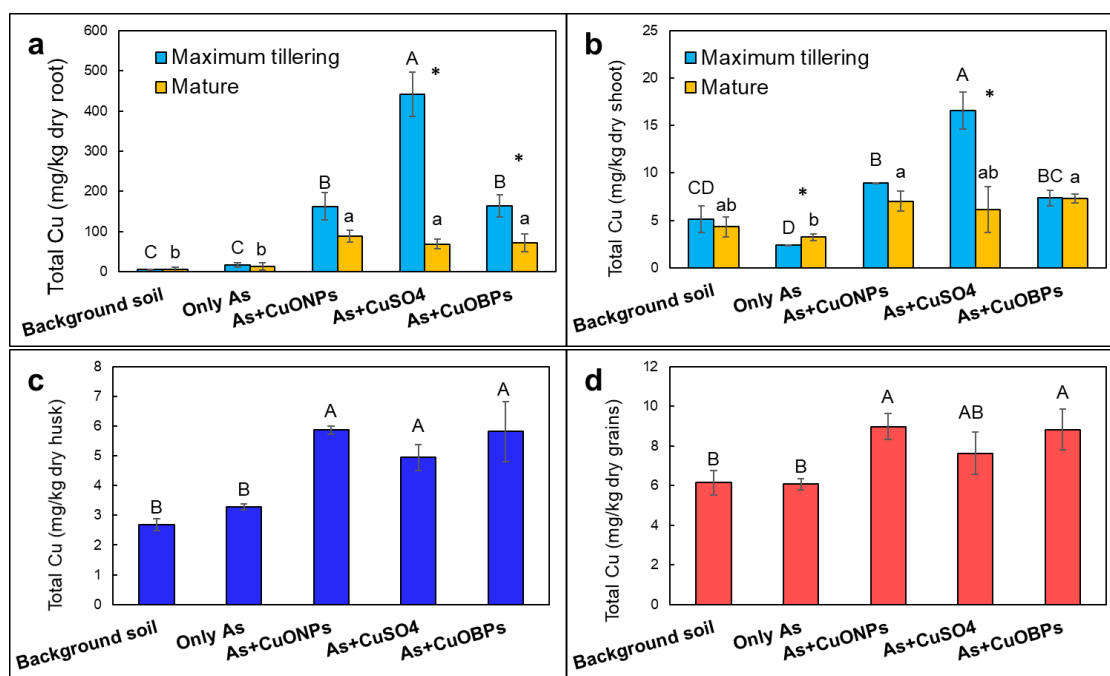


Figure IV-4. The total Cu in rice (a) root and (b) shoot at the maximum tillering and mature stage; and in rice (c) husk and (d) de-husked grains at the mature stage exposed to arsenic and different Cu amendments in soil ($n = 4$). Different letters indicate significant differences between different treatments ($p < 0.05$). Asterisks (*) indicate significant differences between maximum tillering and mature stages according to t-test.

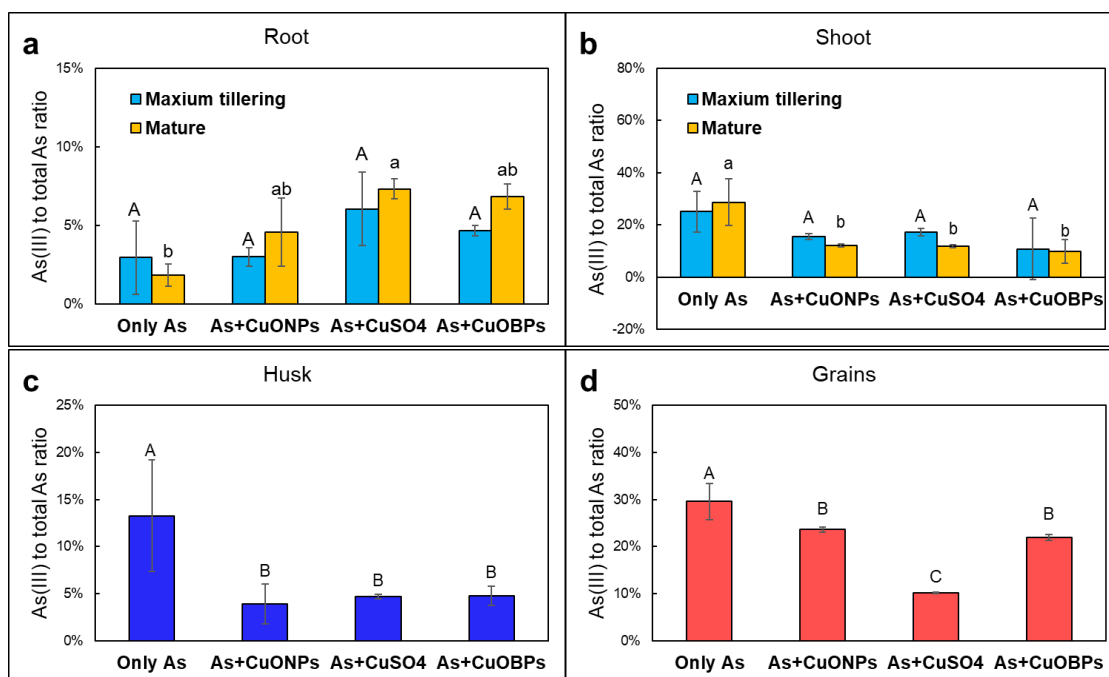


Figure IV-5. The As(III)/total As ratio in rice (a) root and (b) shoot at the maximum tillering and mature stage; and the As accumulation in rice (c) husk and (d) de-husked grains at the mature stage exposed to arsenic and different Cu amendments in soil ($n = 4$). Different letters indicate significant differences between different treatments ($p < 0.05$).

In rice husk and grains, both inorganic As species and (dimethylarsinic acid) DMA(V) are detected (**Figure IV-3e and IV-3f**). Interestingly, all three forms of Cu significantly decreased As(III) and DMA(V) in rice husk, but CuONPs and CuOBPs significantly increased the As(V) concentration in the husk compared to rice plants from only As treatment, However, in rice grains, only Cu ions significantly inhibited As(III) accumulation, while all three forms of Cu significantly enhanced the DMA(V) concentration in the grains. To further look into the effects of different Cu amendments to the most toxic species: inorganic As(III) (Awasthi, et al. 2017), the ratio of As(III) to total As in rice tissues is presented in **Figure IV-5**. The ratio was unaffected in rice root

and shoot at the maximum tillering stage, but it was changed with the addition of Cu amendments at the mature stage depending on the rice tissues. In rice roots, all three forms of Cu enhanced the As(III) retention, but only the effect of Cu^{2+} was significant. The addition of all Cu amendments significantly lowered the As(III)/total As ratio in rice shoot, husk and grains, with the Cu ions showing the greatest inhibition of the As(III)/total As in the grains. Our results revealed that all forms of Cu fertilizers decreased As(III), the most toxic species of As, in aboveground tissues of rice. Different from the general expectations that CuONPs are more effective than conventional Cu ion fertilizers, our results indicate that Cu^{2+} fertilizer is more efficient in stimulating grain yield and lowering As accumulation in rice grains.

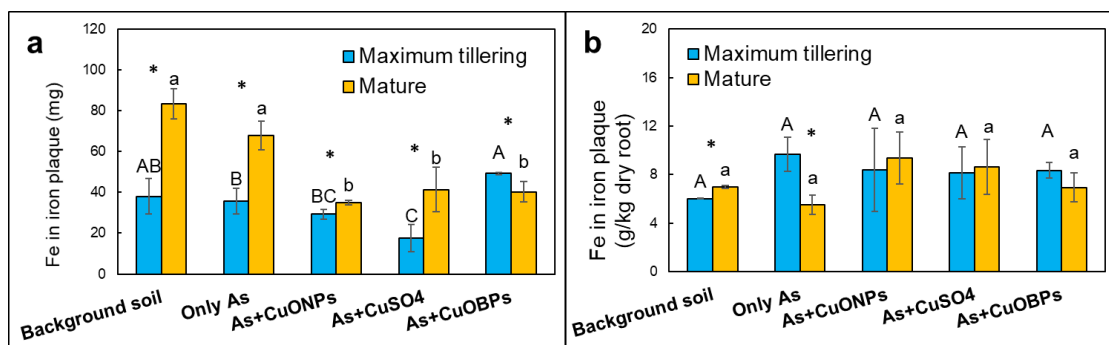


Figure IV-6. The (a) total mass of Fe and (b) amount of Fe normalized by root dry weight in the iron plaque at the maximum tillering and mature stage exposed to arsenic and different Cu amendments in soil ($n = 4$). Different letters indicate significant differences between different treatments ($p < 0.05$). Asterisks (*) indicate significant differences between maximum tillering and mature stages according to t-test.

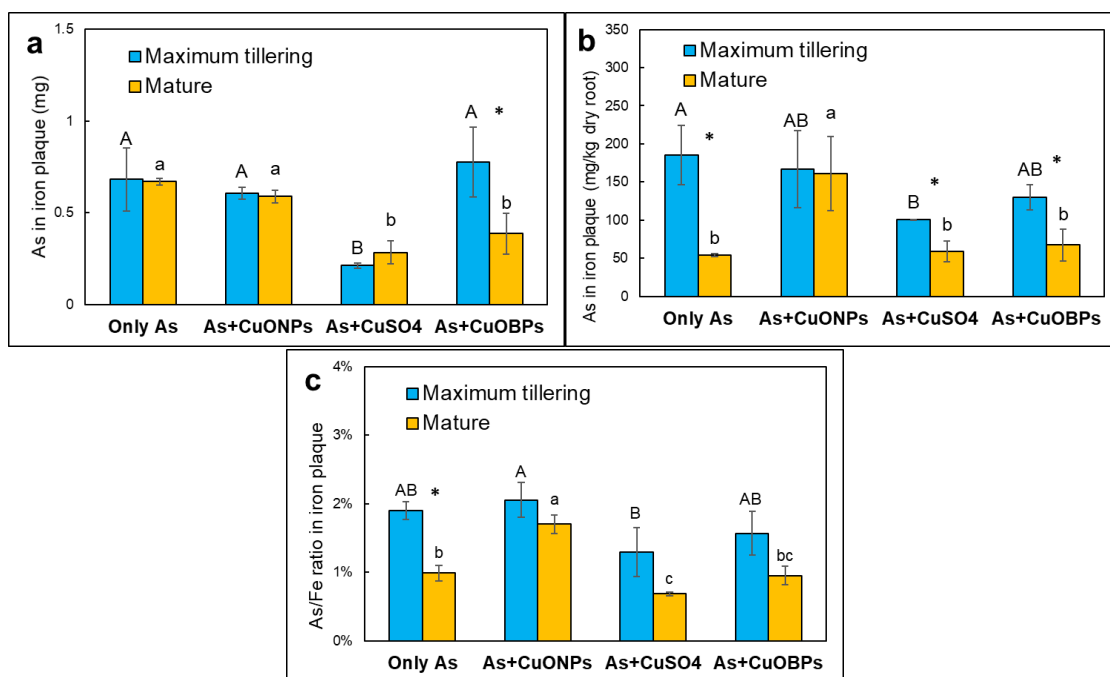


Figure IV-7. The (a) total mass of As, (b) amount of As normalized by root dry weight in the iron plaque, and (c) As/Fe ratio in the iron plaque at the maximum tillering and mature stage exposed to arsenic and different Cu amendments in soil ($n = 4$). Different letters indicate significant differences between different treatments ($p < 0.05$). Asterisks (*) indicate significant differences between maximum tillering and mature stages according to t-test.

Effects of Cu amendments on iron plaque formation

The formation of iron plaque is a key mechanism for lowering As bioavailability and uptake (Awasthi, et al. 2017; Liu, et al. 2006). The effect of different Cu fertilizers on iron plaque formation is presented in **Figure IV-6**. As alone did not affect the total mass of Fe in the DCB extraction, but the introduction of Cu amendments affected the formation of iron plaque, which varied with the form of Cu and the rice growth stages. Only Cu^{2+} significantly decreased the total Fe of iron plaque at the maximum tillering stage, while all three forms of Cu significantly lower the mass of the iron plaque at the mature stage compared to the plants treated with As alone. While the mass of iron

plaque continued to grow from the tillering stage to the mature stage for plants from the control and Cu^{2+} treatment, plants treated with CuONPs and CuOBPs had similar amount of iron plaque at both stages. This result might be stemmed from the shortened growth period of plants by CuONPs and CuOBPs, which lead to the reductive dissolution of iron plaque on the aged rice roots (Chen, et al. 2016b; Zhang, et al. 2012). Due to the significantly altered rice root biomass in different treatments and at different stages, the amount of Fe normalized by root dry weight in the iron plaque is presented in **Figure IV-6b**. The results indicated that the addition of As, or the combination of As and different Cu amendments did not change the density of iron plaque on the unit mass of plant roots. In other words, the observed differences in iron plaque formation from different treatments were mainly due to the altered root biomass by different treatments.

To further investigate the effects of Cu amendments on As retention in the iron plaque, the total mass of As and the amount of As normalized by root dry weight in the iron plaque is shown in **Figure IV-7a and 7b**. The addition of Cu^{2+} significantly lowered the normalized As concentration in the iron plaque at the maximum tillering stage, while the addition of CuONPs significantly increased it at the mature stage. Some previous studies suggested that concentrations of As in the iron plaque are positively correlated with the DCB-extractable Fe content in the iron plaque (Hu, et al. 2005). However, such correlation was not observed in this study (**Figure IV-7c**). The results further indicated that CuONPs significantly enhanced the ability of iron plaque to retain As at the mature stage, while Cu^{2+} inhibited the As retainment. The lowest As retention in the iron plaque and highest As concentration in the rice root of Cu^{2+} treated

rice plants suggested that Cu^{2+} lowered the As accumulation in rice grains mainly through the enhanced As(V) to As(III) reduction and stabilization process in rice root (Chen, et al. 2017b; Cui, et al. 2019; Gong, et al. 2020; Printz, et al. 2016). The promoted As retention in the iron plaque with the addition of CuONPs showed the nano-specific effects of CuONPs, indicating the effects of CuONPs on iron plaque maybe one of the main factors lowering the As uptake in this treatment.

Conclusions

In closing, our study showed that adding Cu amendments to a paddy soil containing high levels of As could markedly mitigate the As phytotoxicity, increase rice yield and lower As accumulation in rice tissues. In particular, conventional Cu salt amendment showed the most remarkable effect in reducing the total As accumulation in rice husk and grains, even though all three forms of Cu amendments significantly lowered the more hazardous As(III) in rice grains,. While the addition of Cu amendments did not affect the amount of iron plaque formed on unit weight rice root, they significantly altered the ability of iron plaque to retain As which varied with different forms of Cu fertilizers. Future studies should also evaluate the effects of different Cu fertilizers on the properties of iron plaque to further understand the relationship between the iron plaque properties and As accumulation. With the increasing application of nanotechnology in agriculture, our results suggested that more investigations are needed before we fully embrace nanotechnology. Close examination is

needed to evaluate whether nanofertilizer could be more effective than conventional salt fertilizers regarding the rice yield and As food safety concern.

CHAPTER V

SIMULTANEOUS MITIGATION OF ARSENIC AND CADMIUM
ACCUMULATION IN RICE (*ORYZA SATIVA L.*) SEEDLINGS BY SILICON
OXIDE NANOPARTICLES UNDER DIFFERENT WATER MANAGEMENT
SCHEMES*

Introduction

Rice (*Oryza sativa*) is the second largest cereal crop and a staple food for over half of the world's population. Many paddy soils around the world are co-contaminated by arsenic (As) and cadmium (Cd) from both geogenic and anthropogenic sources (Khanam, et al. 2020; Palansooriya, et al. 2020). In the United States, soil contains around 1 to 40 mg/kg of As and about 0.1 to 1 mg/kg of Cd (Chou and Harper 2007; Page, et al. 1987). Rice cultivated in polluted paddy soils could accumulate high concentrations of As and/or Cd in rice grains, depending on their bioavailability in soils (Khanam, et al. 2020). Exposure to both chemicals can cause a wide variety of human health problems (Huff, et al. 2007; Rahman, et al. 2008; Shen, et al. 2013). For example, long-term exposure to As could lead to skin, bladder, lung, and prostate cancer (Zhang, et al. 2002), and chronic exposure to Cd can lead to *Itai-Itai* disease, kidney failure and cancer (Huff, et al. 2007). Thus, it is imperative to explore effective approaches to

* Reprinted with permission from “Simultaneous mitigation of arsenic and cadmium accumulation in rice (*Oryza sativa L.*) seedlings by silicon oxide nanoparticles under different water management schemes.” by Wang, X., Jiang, J., Dou, F., Sun, W. and Ma, X., *Paddy and Water Environment* (2021): 1-16. Copyright [2021] by Springer.

simultaneously reduce both As and Cd accumulation in rice grains grown in As and Cd co-contaminated paddies.

Several previous studies have explored approaches to simultaneously control As and Cd accumulation in rice tissues through various agricultural management practices, such as the use of soil amendments and different water management schemes (Arao, et al. 2009; Honma, et al. 2016a; Honma, et al. 2016b; Li, et al. 2009; Suda and Makino 2018). Water management is one of the most common approaches to control As and Cd accumulation in rice grains. Two irrigation schemes are typically applied in rice cultivation including continuous flooding (CF) and alternate wetting and drying (AWD). CF is commonly practiced in the United States, while AWD is more popular in countries facing water shortage. An additional benefit of AWD is the lower As uptake by rice because aerobic condition during the drying period results in the oxidation of arsenite (As(III)) to arsenate (As(V)) which is less available to rice. However, AWD generally enhances the Cd uptake by rice due to the dissolution of cadmium sulfide (CdS) under an oxidizing condition (Honma, et al. 2016b; Sun, et al. 2014b). Opposite results were observed in CF irrigation that Cd uptake is effectively inhibited but As uptake is enhanced because inorganic As(III) is more mobile and bioavailable (Honma, et al. 2016b; Sun, et al. 2014b). This trade-off relationship makes it challenging to simultaneously control both Cd and As accumulation in rice in a co-contaminated paddy soil. A recent study showed that controlling soil pH at around 6.2 and Eh at -73 mV achieved the optimal trade-off of As and Cd accumulation in rice (Honma, et al. 2016a). However, soil properties of rice paddies can vary remarkably at different locations,

which renders it extremely difficult to control pH and Eh precisely to the optimal ranges for As and Cd control.

As such, soil amendments are often applied to co-contaminated rice paddies to lower As and/or Cd accumulation in rice. For example, A previous study showed that zero-valent iron combined with biochar could increase the formation of amorphous iron and iron plaque on rice root surface to immobilize Cd and As (Qiao, et al. 2018). Silicon (Si) is a beneficial element for rice and silicon amendments such as Si-potash fertilizer, Si-calcium fertilizer, sodium metasilicate (Na_2SiO_3) and rice straw generally lead to higher rice yield (Wang, et al. 2016). Previous studies also demonstrated that some Si amendments lowered As or Cd accumulation in rice (Li, et al. 2009; Nwugo and Huerta 2008; Tripathi, et al. 2013). The lower As uptake in rice caused by Si amendments was attributed to the competitive uptake between Si and inorganic As(III), a dominant As species in CF, due to their shared *Lsi1* transporter on root cell membranes, and the retarded crystallization of amorphous ferrihydrite in rice rhizosphere which has more adsorption sites for As than crystal iron oxide (Jones, et al. 2009; Limmer, et al. 2018). However, not all forms of silica had the same effect on plant As uptake. In fact, some studies showed that the addition of silicon fertilizers increased the plant available As in paddy soils (Wu, et al. 2016). The different solubility of silicon fertilizers was considered as a key factor in the different effects of silicon fertilizers on plant As uptake. In comparison, literature is more consistent on the effect of silicon fertilizers on the Cd uptake by rice (Ji, et al. 2017; Tripathi, et al. 2012). In general, the reduced Cd uptake in rice caused by Si fertilizers was ascribed to the suppressed expression of Cd transporters

OsLCT1 and *OsNramp5*, and the decreased stress in rice (Feng Shao, et al. 2017; Nwugo and Huerta 2008). Despite the encouraging results that some Si fertilizers could lower the accumulation of As and Cd in rice grains, different Si fertilizers (e.g. silicon salts vs. silicon in rice biomass) exhibited different effects on the accumulation of As or Cd in rice grains, and none of the evaluated Si amendments could lower As and Cd simultaneously (Wang, et al. 2016).

Silicon is the second most abundant element in the earth's crust, most of them are incorporated in stable Si-rich materials such as quartz and clay which cannot be used as effective Si-fertilizers (Hussain, et al. 2019). A previous study reported that both biochar and ashes derived from Si-rich rice husks resulted in reduced As availability (Leksungnoen, et al. 2019). However, the rice husk needed to generate adequate biochar or ashes to provide enough Si for rice growth was about 10 times higher than the rice husk residues produced in each crop cycle, making this approach less practical.

Recently, applications of nanotechnology in agriculture have received increasing attention due to the unique properties of nanoparticles. Silicon oxide nanoparticles (SiO₂ NPs) were shown to be more efficient in reducing As-induced phytotoxicity and its accumulation in plants than conventional Si amendments. SiO₂ NPs display limited dissolution in typical environmental conditions (Diedrich, et al. 2012), suggesting that SiO₂ NPs may behave differently from conventional Si amendments if they are used as a source of Si to promote rice growth. Interestingly, a recent study showed that zinc oxide nanoparticles (ZnO NPs), another widely explored nano-agrochemical, simultaneously lowered both As and Cd accumulation in rice tissues grown in a co-contaminated rice

paddy soil under flooded irrigation. This study also discussed the different behaviors of ZnO NPs and soluble Zn^{2+} , and concluded that ZnO NPs and soluble Zn^{2+} had different impact on the fate of As and Cd in rice paddies, likely due to their different transformation processes (Ma, et al. 2019). Interestingly, SiO_2 NPs have also been shown to lower either As or Cd in rice and other cereal crops such as wheat, likely through different mechanisms from conventional Si amendments due to the unique properties of nanoparticles (Ali, et al. 2019; Liu, et al. 2014). Consequently, it is imperative to explore whether SiO_2 NPs can simultaneously lower As and Cd accumulation in rice as a novel silicon amendment. Due to the significant role of water management on the fate and transport of As and Cd in rice paddies, the primary objectives of this study were to (1) investigate whether SiO_2 NPs can simultaneously lower As and Cd accumulation in rice and (2) how the interactions of SiO_2 NPs with As and Cd in co-contaminated rice paddy soils is affected by different water management schemes.

Materials and Methods

Chemicals and Nanoparticles Characterization

High purity sodium arsenite ($NaAsO_2 > 99.9\%$) and cadmium sulfate ($CdSO_4 > 99\%$) were purchased from Sigma Aldrich (St. Louis, MO). SiO_2 NPs dispersion in water (25 wt%) was purchased from US Research Nanomaterials, Inc (Houston, TX). The shape, size and crystal patterns of SiO_2 NPs were determined by a Hitachi H-9500 transmission electron microscope (TEM), equipped with an energy

dispersive X-ray spectroscopy (EDS). The crystal structure was determined by selected-area electron diffraction (SAED). The hydrodynamic size and zeta potential of SiO₂ NPs in tap water at 100 mg/L were measured with a dynamic light scattering (DLS) instrument (Malvern Zetasizer Nano-ZS90). Tap water was used in the characterization of SiO₂ NPs because tap water was used as the irrigation water in this study.

Pot Experiment

Universal montmorillonite clay (EP Minerals, Reno, NV) and organic top soil (Black Kow, Oxford, FL) were purchased from local stores. The clay soil was ground with an automatic continuous hammer mill grinder (LAB-PDR-GRIND1, EFK-II Supply). The top soil was sifted through a 2-mm sieve and then homogenized with the clay soil at a ratio of 2:3 (mass/mass). The detailed information of soil preparation and characterization were reported in a previously reported study (Liu, et al. 2018b). The high clay content soil was used in this study because clay-rich soil such as vertisol is dominant in southeastern Texas (Wang, et al. 1993).

Five different treatments were prepared including one negative control, one treatment with freshly added As and Cd at 5 mg/kg As and 1 mg/kg Cd respectively, and three other treatments with the same As and Cd concentrations but with the addition of SiO₂ NPs at 150, 500, or 2,000 mg Si/kg dry soil. To prepare the soils for different treatments, 100 mL solution with NaAsO₂ (50 mg/L As) and CdSO₄ (10 mg/L Cd) was first added to 10 kg dry soil to achieve a concentration of 5 mg As/kg dry soil and 1 mg Cd/kg dry soil. After the soil was homogenized, soil subsample equivalent to 300 g dry weight was transferred to each pot and saturated with either 500 mL tap water or

different concentrations of SiO₂ NPs solutions. SiO₂ NPs solutions were prepared at 90, 300 and 1,200 mg Si/L in tap water. The concentrations of As and Cd were chosen based on their corresponding background concentrations in U.S. soil and the detection limit in plants (Chou and Harper 2007; Page, et al. 1987). The concentrations for Si were selected based on the guidance of Si demand in rice, in which one is below the recommended demand, one is approximate to the recommended demand, and the other is above the recommended demand (Datnoff and Rodrigues 2005). Rice seeds were pre-soaked for 24 hours in deionized (DI) water and six of them were wet-seeded in each container with the prepared soils. The seedlings were thinned down to four in each container when the seedlings reached about 7 cm around two-leaf stage. The water level was maintained below the soil surface until seedlings reached 15 cm to initiate different water managements. Each of the five treatments had six replicates, with half of the replicates managed under CF irrigation and the other half under AWD scheme.

For CF irrigation, the soil in the pot was flooded by tap water to maintain 3-5 cm standing water above the soil surface during the growing period. For AWD irrigation, the soil at the beginning was flooded at the same depth as for CF and then the water was resupplied to the initial level after the water dropped to about 0.5 cm below the soil surface, which took about 4 days for each drying cycle. The watering cycle was repeated until the end of the experiment. Soil pH was measured daily by a pre-buried soil pH meter (MS02, Sonkir) in each pot. Soil redox potential (Eh) was determined daily using a combined platinum and silver/silver chloride electrode system (HI 3230B. Hanna

Instruments, Woonsocket, RI), with the electrode being inserted at approximately 1 cm below the soil surface.

Rice seedlings were gently removed from the soil 14 days after the water management was imposed and then were rinsed with DI water thoroughly. Roots and shoots were separated and weighed to obtain their fresh weight. Three randomly selected plants from each container were oven-dried to determine the dry biomass and the concentrations of total As, Cd and Si in rice tissue samples. The fourth seedling from each container was used for scanning electron microscope (SEM) analysis. The roots were thoroughly rinsed with DI water and tapped dry with a paper towel before they were examined under a Hitachi S-4800 field-emission scanning electron microscopy (FE-SEM), equipped with an X-ray energy dispersive spectroscopy (EDS).

Sampling and Analysis of the Soil Solution

Approximately 10 mL of soil solution was withdrawn right before the plant harvest with a soil solution sampler (1908D2.5L10K05, Soil Moisture Equipment Corp, Santa Barbara, CA) connected with a needle and a glass vacuum tube. The pH of the soil solution was measured immediately after sampling with a portable pH meter. The soil solution was then acidified with 10% HNO₃ at a sample/HNO₃ ratio of 9:1 (volume/volume), and filtered through a 0.2 μm filter. The total As, Cd and Si in the filtrate was measured with an inductively coupled plasma mass spectrometry (ICP-MS) (Perkin Elmer mod. DRCII, Waltham, MA).

Total Elements in Rice Plants

The total As, Cd and Si in rice tissues was determined by ICP-MS following strong acid digestion as previously reported by Ebbs et al (2016). Approximately 0.2 g of dry root and 0.3 g of dry shoot were added into a 5 mL HNO₃ solution (70% by volume) and sat overnight at room temperature for pre-digestion. They were then digested using a DigiPREP MS hot block digester (SCP science, Clark Graham, Canada) at 95 °C for 4 hours until all remaining tissues were fully dissolved. The digestate was then cooled to room temperature and further mixed with 3 mL of 30% H₂O₂ (w/v) and heated in the hot block at 95 °C for another 2 hours. This solution was then analyzed with an ICP-MS.

Statistical Analysis

Minitab was used to perform t-tests, one-way analysis of variance (ANOVA), and two-way ANOVA analyses on the data obtained. Two-way ANOVA was used to determine whether the two independent factors: SiO₂ NPs and water management are significant for the concerned parameters. One-way ANOVA was conducted to evaluate whether the dosage of SiO₂ NPs had a significant impact on the measured parameters under the same water management scenario. T-test was used to determine whether the measured parameters at the same SiO₂ NPs dosage were significantly different between the two water management schemes.

Results

SiO₂ Nanoparticle Characterization

TEM images showed that the SiO₂ NPs used in this study are predominantly spherical with an average size of 10 nm (**Figure V-1a**). The size was smaller than the 30 nm average size reported by the vendor. EDS analysis confirmed the purity of the SiO₂ NPs, with the trace amount of Au detected by EDS likely from the grid (**Figure V-1b**). The electron diffraction pattern suggested that the SiO₂ NPs are amorphous (**Figure V-1c**). The hydrodynamic size of SiO₂ NPs in 100 mg/L of solution was 48 ± 17 nm and the zeta potential of these nanoparticles in the same solution was about -27.8 ± 8.23 mV.

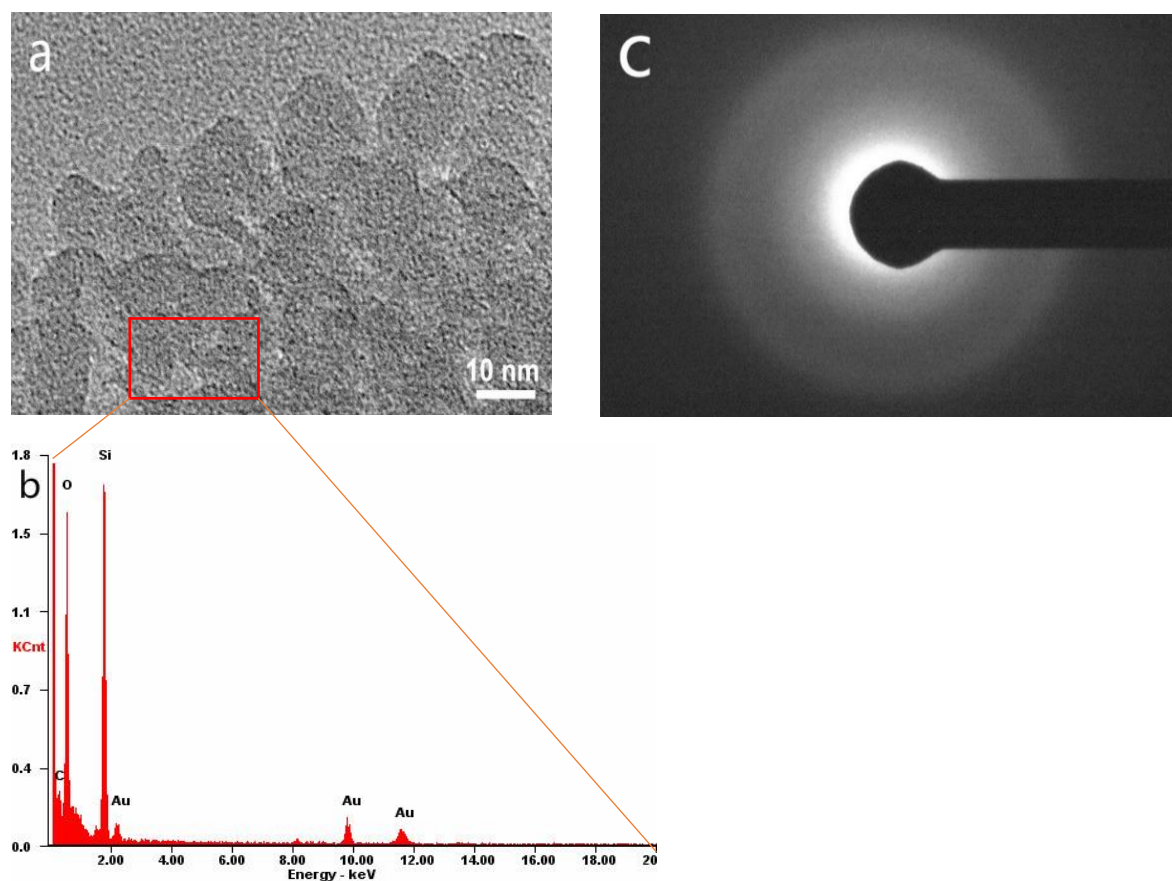


Figure V-1. SiO₂ NPs characterization. (a) HRTEM image, showing the size and shape of average SiO₂ NPs, (b) EDS spectrum of SiO₂ NPs at the selected area in red box, and (c) electron diffraction pattern of SiO₂ NPs.

Soil Redox Potential (Eh) and pH

The Eh values of CF scheme decreased from around +230 mV to -230 mV five days after the flooding initiated and stabilized at this level, while the Eh values of AWD treatments fluctuated between +230 mV and -70 mV (**Figure V-2**). The measured pH values were around 7.1-7.6 for completely flooded soil and 7.4-7.8 for soil under AWD during the growth period.

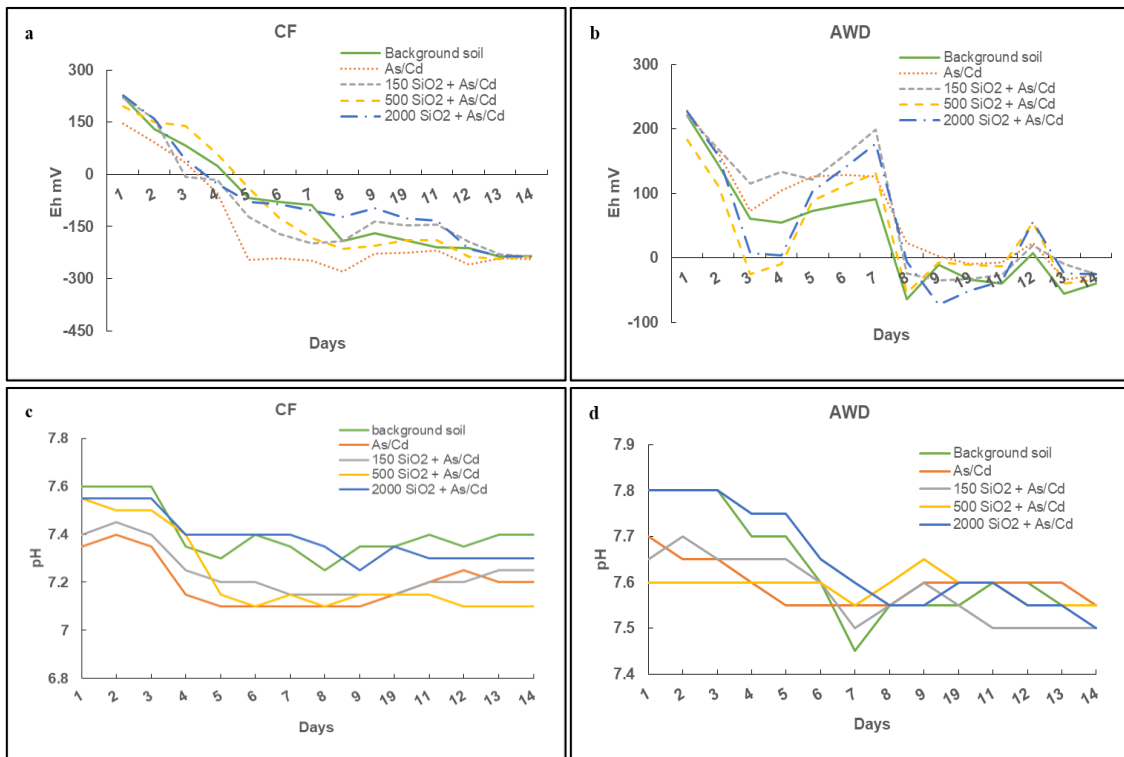


Figure V-2. Redox potential (a and b) and pH (c and d) of soil in different water management: CF (a and c) and AWD (b and d) exposed to 1 mg/kg of As with 5 mg/kg of Cd alone or As and Cd with 150 mg/kg, 500 mg/kg or 2000 mg/kg of SiO₂ NPs.

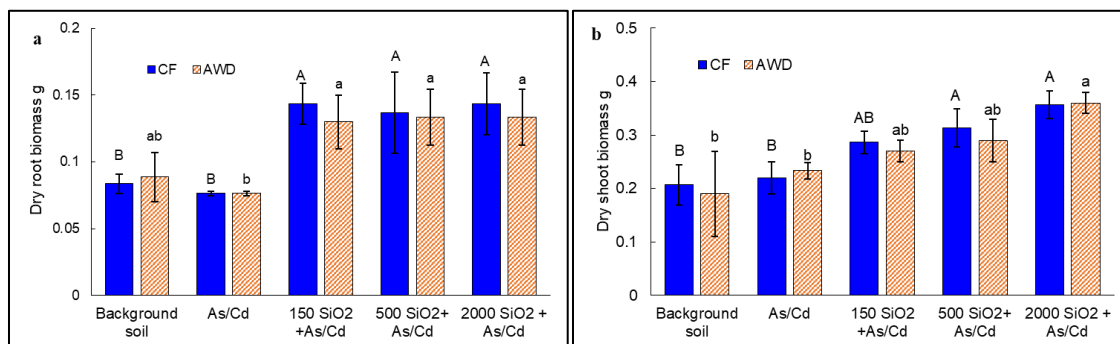


Figure V-3. Dry biomass of rice tissues under different level of SiO₂ NPs treatment and different water management schemes. Root biomass (a) and shoot biomass (b) of rice plants treated with different combination of 1 mg/kg of As with 5 mg/kg of Cd and 150 mg/kg, 500 mg/kg or 2000 mg/kg of SiO₂ NPs under two different water managements: CF and AWD. Values represent mean \pm SD (n=3). Different letters indicate significant differences ($p \leq 0.05$) according to one-way ANOVA followed by Tukey's test.

Table V-1. Results of two-way ANOVA test. P-values of significant effects of different concentration of SiO₂ NPs and/or different water management and interaction between them are highlighted in bold.

	SiO ₂ NPs	Water Management	Interaction
Dry root biomass	0.003	0.562	0.973
Dry shoot biomass	<0.001	0.604	0.624
Total As in rice root	0.005	0.023	0.56
Total As in rice shoot	0.22	<0.001	0.011
Total Cd in rice root	<0.001	0.413	0.012
Total Cd in rice shoot	<0.001	0.322	<0.001
Total Si in rice root	<0.001	0.021	0.001
Total Si in rice shoot	0.102	0.020	0.001
Total As in soil solution	0.006	<0.001	0.006
Total Cd in soil solution	<0.001	<0.001	<0.001
Total Si in soil solution	0.099	0.004	0.035

Rice Plant Biomass

Coexistence of As and Cd at the levels used in this study did not affect the rice biomass compared with rice grown in the control soil under both water management

schemes. The addition of SiO₂ NPs generally increased the biomass of rice roots and shoots. However, the biomass increase was dependent upon the concentration of SiO₂ NPs and the water management (**Figure V-3 and Table V-1**). The dry root biomass increased by 87.8%, 79.0% and 87.8% in the co-presence of 150, 500 and 2,000 mg/kg SiO₂ NPs under CF, and by 70.3%, 74.7% and 74.7% under AWD, compared to the As and Cd alone treatment under each irrigation scheme. The addition of SiO₂ NPs at 150, 500, and 2,000 mg/kg significantly increased the dry shoot biomass by 30.3%, 42.4% and 62.1% under CF, and 15.7%, 24.2% and 54.3% under AWD, compared to rice only exposed to As and Cd under the same irrigation conditions. Overall, the enhanceive role of SiO₂ NPs on rice biomass was more pronounced for rice seedlings under CF than under AWD irrigation. The root biomass change caused by SiO₂ NPs did not follow a positive dose-response relationship while the shoot biomass did. The interactive effects of water management and SiO₂ NPs on rice biomass were insignificant.

Accumulation of As in Rice Tissues

Two-way ANOVA analyses indicated that both SiO₂ NPs and water management significantly affected total As concentration in rice roots, but their interaction was insignificant (**Table V-1**). The addition of SiO₂ NPs reduced As concentration in rice roots by 32%-43% under CF and 21%-35% under AWD irrigation (**Figure V-4**). The co-presence of SiO₂ NPs at the tested concentrations slightly reduced As concentration in rice shoots under both irrigation schemes, except for the treatment with 2,000 mg/kg SiO₂ NPs under AWD, which significantly increased As concentration in rice shoot by 83.3%, compared to rice seedlings treated with only As and Cd under AWD.

Surprisingly, there is no significant difference of As accumulation in rice root and shoot between CF and AWD in all treatments, except that As concentration in rice shoots was significantly higher under CF than that under AWD irrigation at 500 mg/kg SiO₂ NPs according to the t-test. The translocation rate of As (total As in shoot / total As in root) did not significantly change with the addition of SiO₂ NPs under either irrigation scheme, except that 2,000 mg/kg SiO₂ NPs significantly increased As translocation rate under AWD compared treatments without the addition of SiO₂ NPs.

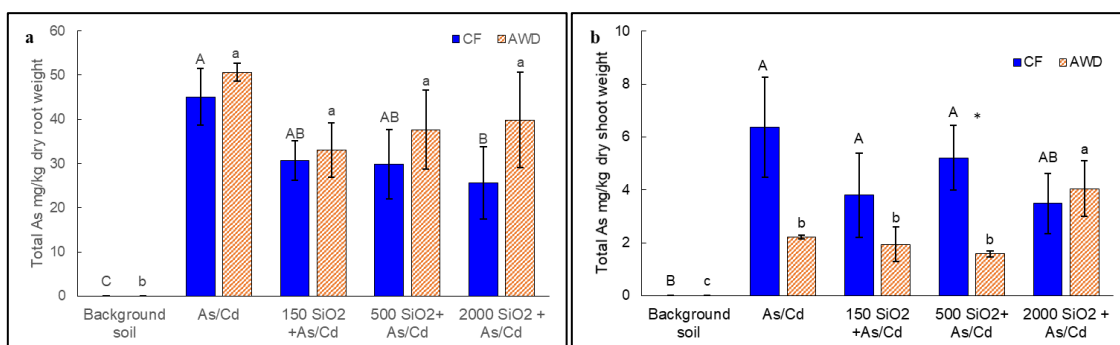


Figure V-4. Total arsenic in rice root (a) and shoot (b) exposed to 1 mg/kg of As with 5 mg/kg of Cd alone or As and Cd with 150 mg/kg, 500 mg/kg or 2000 mg/kg of SiO₂ NPs under two different water managements: CF and AWD. Values represent mean \pm SD (n=3). Different letters indicate significant differences ($p \leq 0.05$) according to one-way ANOVA followed by Tukey's test. Asterisks (*) indicate significant differences between water management at a particular Si concentration level, according to t-test.

Accumulation of Cd in Rice Tissues

As expected, Cd concentrations in rice tissues were higher under AWD than under CF irrigation when treated with Cd and As alone (**Figure V-5**). SiO₂ NPs and its interaction with water management significantly affected Cd concentrations in rice tissues according to the results of two-way ANOVA (**Table V-1**). The addition of SiO₂ NPs at 500 and 2,000 mg/kg significantly reduced Cd concentration in rice roots under

both water managements but increased Cd translocation rate from root to shoot. Consequently, significant Cd reduction in rice shoots was only observed under AWD irrigation. In particular, Cd in rice shoots under AWD irrigation was 50% lower than that in rice shoots under CF irrigation at 500 mg/kg SiO₂ NPs, or in rice shoots exposed to As and Cd alone under AWD. In summary, SiO₂ NPs displayed significant impact on As and Cd accumulation in rice seedlings and the net effect depended on the concentration of SiO₂ NPs and the irrigation schemes. Under AWD irrigation, the addition of 500 mg/kg SiO₂ NPs, or the recommended Si level, led to simultaneous reduction of As and Cd in rice shoots.

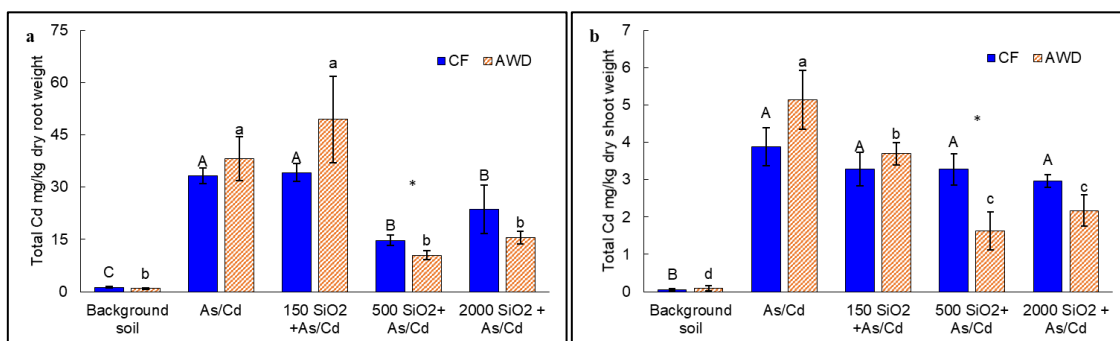


Figure V-5. Total cadmium in rice root (a) and shoot (b) exposed to 1 mg/kg of As with 5 mg/kg of Cd alone or As and Cd with 150 mg/kg, 500 mg/kg or 2000 mg/kg of SiO₂ NPs under two different water managements: CF and AWD. Values represent mean \pm SD (n=3). Different letters indicate significant differences ($p \leq 0.05$) according to one-way ANOVA followed by Tukey's test. Asterisks (*) indicate significant differences between water management at a particular Si concentration level, according to t-test.

Accumulation of Si in Rice Tissues

Compared with rice seedlings grown in the background soil, elevated As and Cd concentration had minimal effect on Si concentration in rice roots, but significantly increased Si concentration in rice shoots under CF condition (**Figure V-6**). By comparison, the addition of As and Cd did not affect the Si concentration in rice root and

shoot under AWD irrigation. Surprisingly, the addition of up to 2,000 mg/kg of SiO₂ NPs significantly lowered Si concentration in rice roots at all tested concentrations regardless of the water management scenarios, with a greater reduction under AWD than that under CF at higher SiO₂ NPs concentrations (500 and 2,000 mg/kg). The addition of SiO₂ NPs had no effect on Si concentrations in rice shoots under both water management schemes.

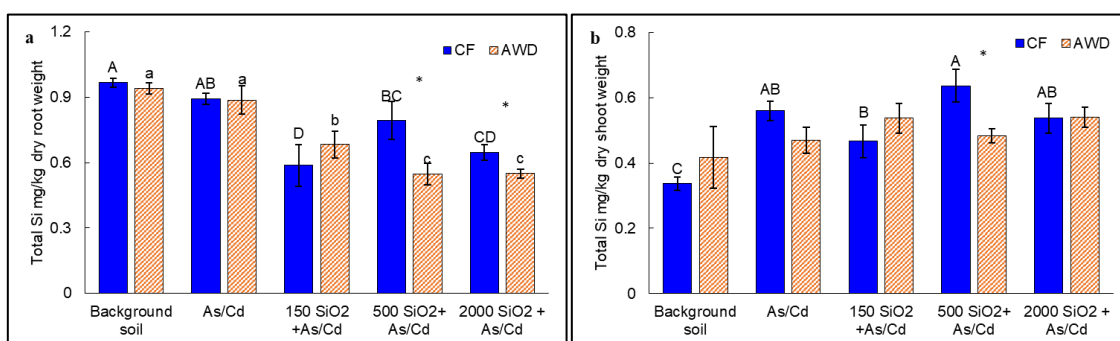


Figure V-6. Concentration of element Si in rice root (a) and shoot (b) exposed to 1 mg/kg of As with 5 mg/kg of Cd alone or As and Cd with 150 mg/kg, 500 mg/kg or 2000 mg/kg of SiO₂ NPs under two different water managements: CF and AWD. Values represent mean \pm SD (n=3). Different letters indicate significant differences ($p \leq 0.05$) according to one-way ANOVA followed by Tukey's test. Asterisks (*) indicate significant differences between water management at a particular Si concentration level, according to t-test.

Soil solution Chemistry

Significant interactions of SiO₂ NPs and water managements were observed in terms of As and Cd concentrations in soil solution according to two-way ANOVA (**Table V-1**). The concentration of As in soil solution under CF irrigation was significantly higher with the addition of SiO₂ NPs, with higher SiO₂ NPs resulting in the greater As concentration in soil solution (**Figure V-7a**). In contrast, the As concentration in soil solution was unaffected by SiO₂ NPs under AWD. SiO₂ NPs markedly increased

Cd concentration in soil solution at 150 mg/kg but significantly decreased Cd concentration at 2,000 mg/kg under CF compared with the As and Cd alone treatment (Figure V-7b). However, the Cd concentration in soil solution under AWD irrigation slightly decreased with the co-presence of higher concentration of SiO₂ NPs (500 mg/kg and 2,000 mg/kg). Highly intriguingly, significantly lower dissolved Cd was observed under AWD irrigation than that under CF irrigation with the addition of 150 and 500 mg/kg SiO₂ NPs.

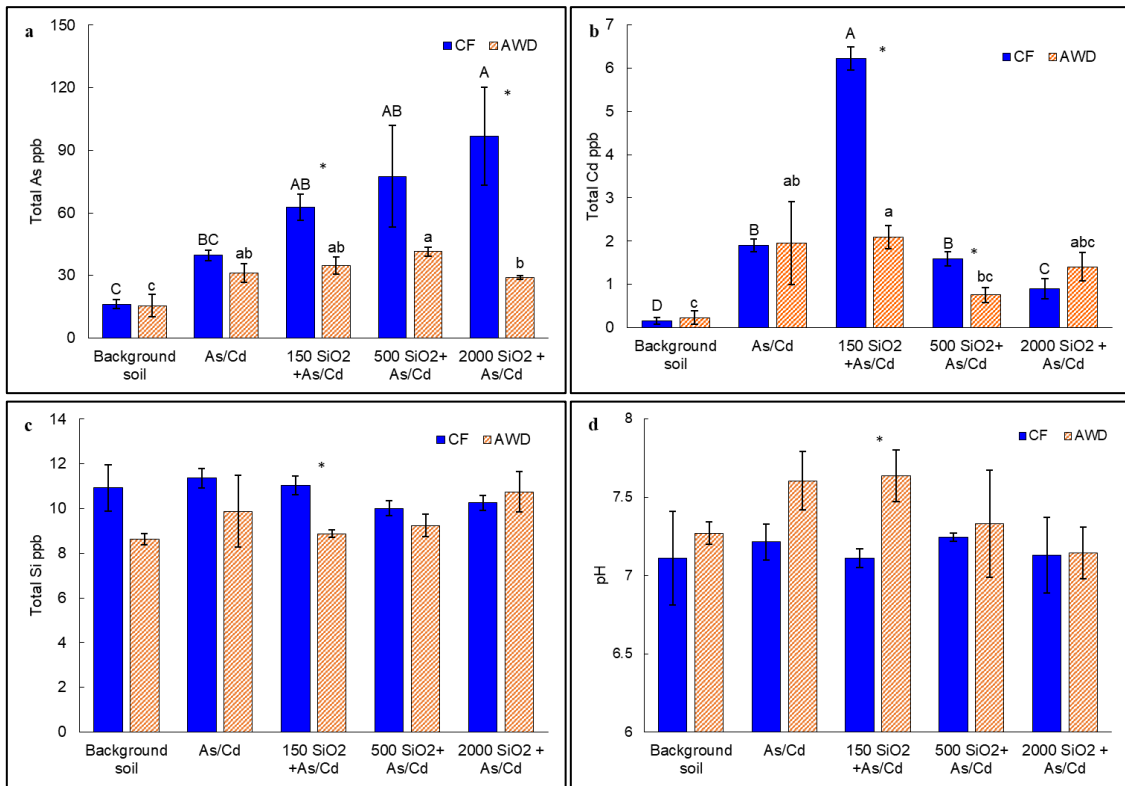


Figure V-7. Concentration of element As (a), Cd (b) and Si (c) in soil solution and pH (d) of soil solution extracted from the soil exposed to 1 mg/kg of As with 5 mg/kg of Cd alone or As and Cd with 150 mg/kg, 500 mg/kg or 2000 mg/kg of SiO₂ NPs under two different water managements: CF and AWD. Values represent mean ± SD (n=3). Different letters indicate significant differences (p ≤ 0.05) according to one-way ANOVA followed by Tukey's test. Asterisks (*) indicate significant differences between water management at a particular Si concentration level, according to t-test.

No significant differences in Si concentration in soil solution was observed among different treatments (**Figure V-7c**). At 150 mg/kg, the dissolved Si concentration under AWD was significantly higher than that under CF. Soil solution in all treatments under CF irrigation had a pH values in the range of 7.11-7.21, while slightly higher pH values were observed under AWD, ranging from 7.27 to 7.63 (**Figure V-7d**).

SEM of Rice Root

Rice roots grown in the background soil and in soil with freshly added As and Cd alone or with 150 mg/kg SiO₂ NPs showed appreciable Si aggregation on the root surface under both irrigation conditions (**Figures V-8 a-f**), even though less aggregation was generally observed under AWD than that under CF. Interestingly, there was less aggregates on root surface at higher concentrations of SiO₂ NPs, but large amount of dumb-bell-shaped silica body was noticed on the root surface cells (**Figures V-8 g, h and j**), except for rice treated with 2000 mg/kg SiO₂ NPs under CF condition. An EDS analysis indicated that the Si in the surface aggregates and silica bodies might come from different sources (**Figure V-9**). The Si aggregates composed of elements C, O, Fe, Na, Mg, Al, Si, P, S, Cl, K and Ca (**Figure V-9b**), consistent with background Si minerals while silica bodies (**point B in Figure V-9a**) contained predominantly elements Si, O and C (**Figure V-9c**), which is more aligned with the SiO₂ NPs added to the treatment systems.

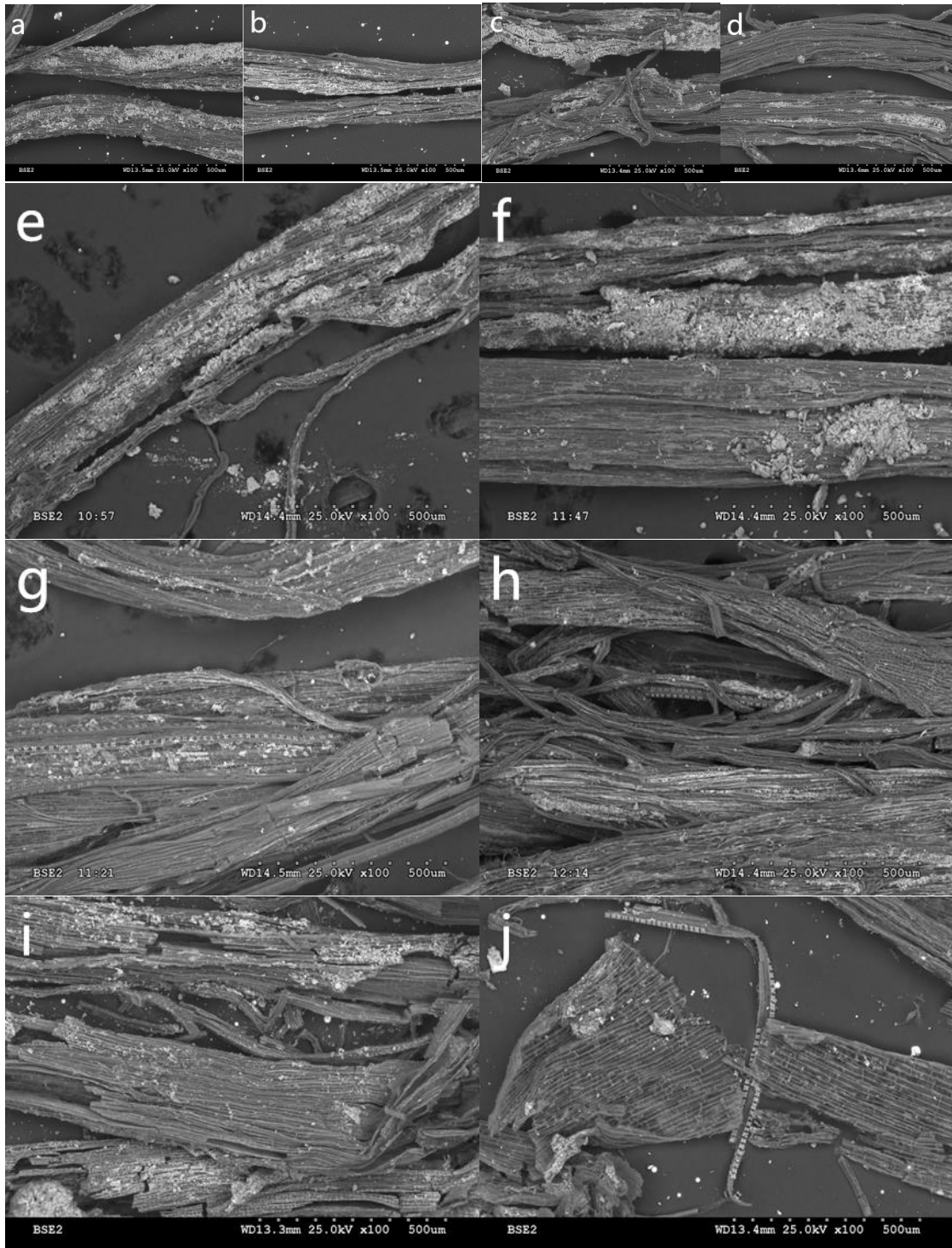


Figure V-8. Scanning electron micrographs (SEM) of rice root under various condition: (a) control under CF (b) control under AWD (c) As and Cd without SiO₂ NPs under CF, (d) As and Cd without SiO₂ NPs under AWD. (e) As and Cd with 150 mg/kg SiO₂ NPs

under CF, (f) As and Cd with 150 mg/kg SiO₂ NPs under AWD. (g) As and Cd with 500 mg/kg SiO₂ NPs under CF, (h) As and Cd with 500 mg/kg SiO₂ NPs under AWD. (i) As and Cd with 2000 mg/kg SiO₂ NPs addition under CF, (j) As and Cd with 2000 mg/kg SiO₂ NPs addition under AWD.

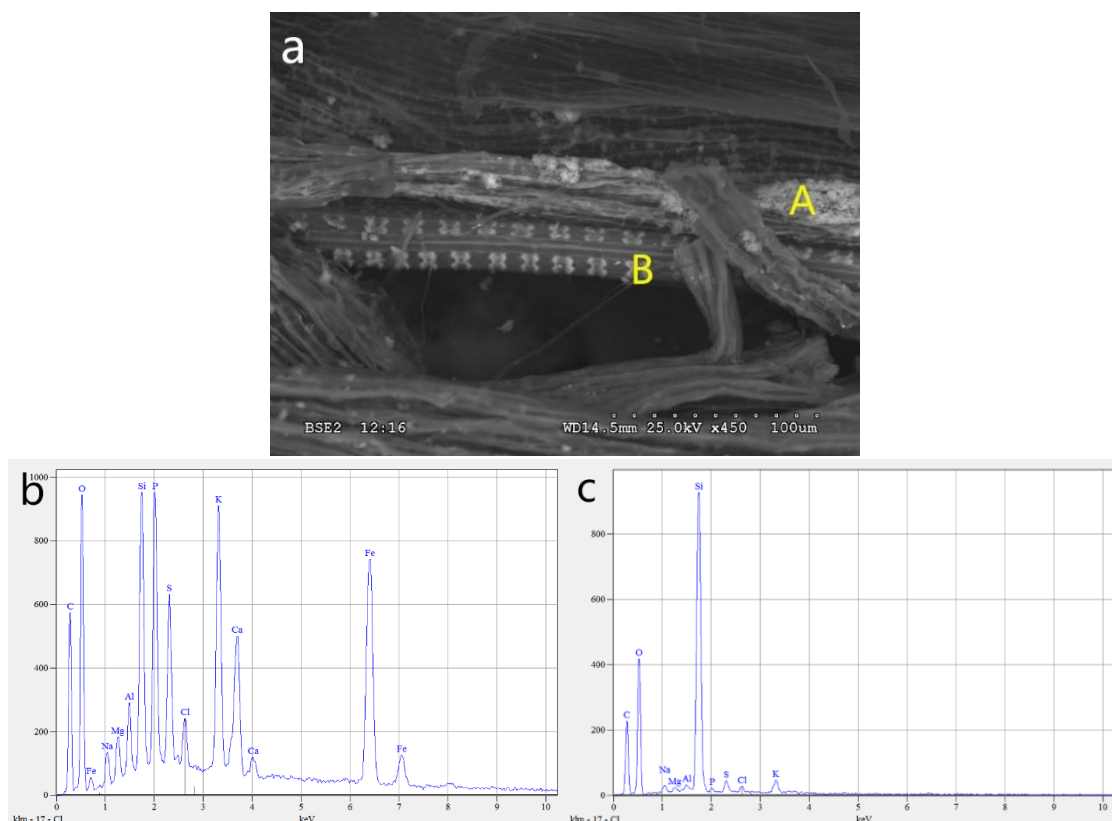


Figure V-9. (a) SEM of rice root in the presence of 500 mg/kg SiO₂ NPs under CF. (b and c) Energy dispersive X-ray (EDX) spectra taken from the point A and B in figure 8a.

Discussion

Simultaneous reduction of As and Cd in rice can dramatically reduce food safety risks from dietary consumption of tainted rice grains, which threatens the public health of over half of the global population. From numerous research over the past decade, nanotechnology has shown promises to address many imminent challenges in agriculture such as reduced effectiveness of conventional agrochemicals, widespread crop and soil-

borne diseases, and environmental degradation due to excessive uses of agrochemicals. Recently, we have shown that several engineered nanoparticles such as cerium oxide nanoparticles and copper oxide nanoparticles interacted closely with co-existing heavy metal(loid)s, resulting in lower uptake of these co-existing poisonous pollutants in plant tissues (Wang, et al. 2019b; Wang, et al. 2018). In particular, a previous study demonstrated that zinc oxide nanoparticles (ZnO NPs), different from its soluble ionic form, simultaneously lowered both As and Cd in rice shoots, suggesting that nano-agricultural chemicals might be a promising solution to address widespread food safety issues stemmed from heavy metals pollution (Ma, et al. 2019). However, the concerns about potential Zn phytotoxicity hinder its broad applications in agriculture. Therefore, search for safe alternative nano-agricultural chemicals that can simultaneously lower As and Cd in rice without negatively affecting rice growth is of great interest. In addition, the previous study was only conducted under CF condition, and with only one concentration (Ma, et al. 2019). In this study, we explored the potential of SiO₂ NPs as an alternative form of nano-agricultural chemical for simultaneous control of As and Cd in rice tissues at multiple concentrations and under different water management schemes. Our results showed that SiO₂ NPs can be another promising nano-agricultural chemical to simultaneously decrease As and Cd accumulation in rice tissues at the right combination of dosage (e.g. 500 mg/kg of SiO₂) and water management schemes. Importantly, the optimal concentration of SiO₂ NPs found in this study aligned well with the recommended Si guidance, suggesting that no additional Si beyond the physiological demand of rice is needed to reap the benefit of lowered As and Cd accumulation in rice grains.

SiO₂ NPs and Cd Accumulation in Rice Tissues

The addition of SiO₂ NPs at the recommended Si level (500 mg/kg) resulted in significantly lower Cd in rice roots under both water management schemes. The lower Cd concentration in rice roots could be due to the adsorption of Cd on the negatively charged surface of SiO₂ NPs which could be retained in soil by forming less bioavailable aggregates due to homo- and/or hetero-aggregation with other colloidal particles in the soil pore water. This assumption is supported by that observation that Cd in the pore water with 150 mg/kg of SiO₂ NPs was significantly higher than in other treatments (**Figure V-7**), but the Cd concentration in plant roots from this treatment was not significantly different from plants treated with only As and Cd, indicating that the Cd in soil pore water was probably not in the free standing Cd²⁺ format. SiO₂ NPs also significantly reduced Cd concentration in rice shoots under AWD irrigation, but not under CF irrigation. The reason is partly because that Cd uptake in completely flooded rice shoots was already low since Cd under the anaerobic condition was not bioavailable to rice, regardless of the addition of SiO₂ NPs. Under AWD irrigation, the lower Cd in rice shoots was attributed to the formation of silica bodies in root cell walls as shown in the SEM images (**Figure V-9**), which could reduce the root-to-shoot transfer of Cd. A silica body is a mature silica cell with observable dumbbell-shaped silicon deposition formed via biosilicification (Zhang, et al. 2013), which might be a sign of increased cell wall lignification of rice roots, resulting in the thickening of the cell walls (Isa, et al. 2010). The silica body has been shown to adsorb bi- and tri-valent metals, and reduce the root-to-shoot transfer and accumulation of Cd in rice shoots (Li, et al. 2014). Even

though reports on the formation of silica bodies in rice roots are relatively rare, there are plenty of reports showing the formation of silica bodies in the cell walls of rice shoots at high concentrations of silicon amendments because high concentrations of silicon will interact with polysaccharides of cell walls and form SiO₂ colloids which eventually develop into three-dimensional silica bodies (Ali, et al. 2019; Cui, et al. 2017). The introduction of SiO₂ NPs as the silicon source may allow fast and significant buildup of SiO₂ in the root cell walls of rice to form silica bodies. The SEM-EDS analysis confirmed that silicon bodies were predominantly formed from SiO₂ NPs rather than the background Si. In addition to the physical adsorption, the formation of silica body could potentially stimulate pectin formation in rice root border cells, and further inhibit Cd uptake because pectin was reported to decrease heavy metal accumulation (Cui, et al. 2020; Nagayama, et al. 2019). Moreover, the exposure to SiO₂ NPs might also inhibit Cd transporters *OsLCT1* and *OsNramp5* to decrease Cd uptake by rice, thus, causing an overall reduction of Cd accumulation in rice shoot tissues (Cui, et al. 2017).

SiO₂ NPs and As Accumulation in Rice Tissues

The impact of SiO₂ NPs on the accumulation of As in rice tissues was less pronounced than its impact on Cd. The addition of SiO₂ NPs caused a steady increase of As in the soil solution from CF treatments. However, the increase of soluble As in soil solution did not result in higher As accumulation in rice roots as expected. In fact, the As concentration in rice roots was either unaffected at lower SiO₂ NP concentrations or significantly lowered at 2,000 mg/kg of SiO₂ NPs at CF. Several processes might have contributed to the lower As concentration in rice roots in the presence of high

concentrations of SiO₂ NPs. A recent study showed that SiO₂ NPs inhibited the expression of As(III) transporters *Lsi1* and *Lsi2*, a predominant As species under CF, leading to lower As accumulation in rice roots (Cui, et al. 2020). In addition, the lower As concentrations in rice roots might be partially attributed to the adsorption of As on suspended amorphous SiO₂ NPs in solution. Our previous studies have demonstrated substantial adsorption of inorganic As species on metal oxide nanoparticles such as cerium oxide nanoparticles (Sharifan, et al. 2018). Even though this part of As might be detected in soil solution as “soluble” As because the sampling of pore water solution did not distinguish the truly dissolved As and the As adsorbed on the suspended SiO₂ NPs in this study. It is possible that such As-SiO₂ complex is not readily bioavailable for rice uptake even though they suspended in pore water. This assumption is supported by the observation that low Si concentration in rice tissues was observed after the addition of SiO₂ NPs under CF.

In addition to the physiological properties of roots, rhizosphere chemistry has a substantial impact on the uptake of As by rice plants. In particular, the formation of iron plaque can significantly reduce the uptake of As by rice roots. However, the impact of iron plaque in this study was expected to be low because the rice seedlings were only six weeks old at termination and significant buildup of iron plaque was not expected. The EDS analysis revealed considerable amounts of Fe in Si aggregates on rice root surface at low SiO₂ NPs concentrations (**Figure V-8**), suggesting that there is significant clay mineral deposition on root surface, in which the aluminum or/and magnesium was substituted by iron. The addition of SiO₂ NPs at high concentrations appeared to inhibit

the deposition of clay minerals on root surface. Instead, it facilitated the formation of silica bodies in root cells. Compared with the Si-Fe aggregates formed from background clay minerals, the adsorption of negatively charged or neutral As onto the negatively charged silicon bodies in root cell walls was lower, leading to low As concentration in rice roots under CF at the highest SiO₂ NPs concentration.

The addition of SiO₂ NPs did not affect As concentration in rice shoots under CF irrigation, but As accumulation in rice shoots under AWD irrigation decreased insignificantly with the increase of SiO₂ NPs concentration from 0 to 500 mg/kg. However, the As concentration in rice shoots increased dramatically at 2,000 mg/kg even though the As concentration in rice root showed minimal change compared with other treatments, suggesting that the root-to-shoot transport of arsenate (As(V)) was improved by the presence of high concentrations of SiO₂ NPs, possibly through an enhanced expression of phosphate transporters. Overall, the impact of SiO₂ NP amendment was relatively mild for As, compared with its impact on Cd accumulation in rice seedlings. Water management scheme is an important consideration in determining the impact of SiO₂ NPs amendment on the accumulation of As and Cd in rice tissues (**Figures V-4 and 5**). Without the SiO₂ NPs addition, AWD could potentially be a great scheme to apply to the paddy field as it generally lowered the As concentration in rice shoot and did not affect rice seedling biomass and Cd accumulation in the rice seedling compared to under CF. Specifically, the present study demonstrated that SiO₂ NPs at the recommended fertilizer level under AWD can result in lower accumulation of both As and Cd in rice seedlings because SiO₂ NPs significantly inhibited Cd accumulation in

rice shoots while As levels can be maintained low under AWD. Together with our previous studies with ZnO NPs and a few other metal oxide nanoparticles, the results of this study suggest that metal oxide nanoparticles in agrochemicals can lead to substantial and simultaneous reduction of As and Cd in rice tissues while conferring their intended benefits, opening doors for broader applications of nano-agrochemicals in agriculture.

Conclusions

In summary, the present study has demonstrated that a combined strategy to include both water management and SiO₂ NPs addition might have a significant impact on As and Cd bioavailability and accumulation in rice plants. This study for the first time demonstrated that SiO₂ NPs could be a potential candidate for simultaneous As and Cd control in rice paddies with the proper water management strategies. The results also showed that addition of SiO₂ NPs as a Si amendment can result in the formation of silica bodies in rice root cell walls which inhibit the passive uptake of As and Cd. Such a phenomenon was not reported for other Si amendments. While the authors are aware that the experimental duration of this study is shorter than what is desired, we argue that the results still contain enlightening information for the scientific community to continue to explore the applications and implications of nanotechnology for sustainable agriculture. Future investigations covering the whole life cycle of rice in field conditions will generate more convincing evidence that SiO₂ NPs, a possible soil amendment at the current recommended level, can also potentially confer food safety benefits by lowering the accumulation of As and Cd in rice grains. However, it is worth mentioning that the

interactions of SiO₂ NPs and co-existing metal(loid)s are complicated and the affected processes could have contradicting effects on the net accumulation of As and Cd by rice seedlings. Current efforts should focus on understanding how SiO₂ NPs affect the individual processes involved in the uptake of As and Cd by rice. Specifically, the uptake of As and Cd involve both regulated trafficking by various transporters and passive diffusion through root cell membranes. While this study reports one of the first evidences that SiO₂ NPs alter As and Cd diffusion through cell membrane by forming silica bodies, detailed studies on the impact of SiO₂ NPs on the expression of As and Cd transporters need to be elucidated at different field conditions. Detailed understanding of the physical and chemical interactions of SiO₂ NPs with As and Cd in rice paddies, the physiological adjustments of plant root cells due to the addition of SiO₂ NPs and the response of soil microorganisms to SiO₂ NPs also require attention because the microbial community in rice paddies plays a marked role in As speciation. Even though our previous studies have demonstrated the importance of adsorption of metalloids on nanoparticle surfaces, quantitative determination of the adsorption of As and Cd on the surface of SiO₂ NPs under different redox and pH conditions will shed light on the significance of this process. Finally, it will be important to compare SiO₂ NPs with other forms of Si amendments so as to gain more insights into the unique role of nanotechnology in agriculture.

CHAPTER VI

PREDICTION OF PLANT UPTAKE AND TRANSLOCATION OF ENGINEERED METALLIC NANOPARTICLES BY MACHINE LEARNING*

Introduction

Breakthroughs in nanotechnology in the past decades have dramatically changed the landscape of modern science and technology. Engineered nanoparticles (ENPs) are now incorporated into a wide range of industrial and commercial products such as agricultural products, household appliances and biomedical materials (Acharya and Pal 2020; Nikolova and Chavali 2020; Wang, et al. 2019a). The enthusiasm for applying nanotechnology in agriculture is especially high because of the rising global population, low food security and worsening climate change (White and Gardea-Torresdey 2018). There has been a global push to intentionally apply ENPs to plants as nanofertilizers, nanopesticides and nanodelivery systems to enhance agricultural productivity (Chhipa 2017; Kah 2015; Kah, et al. 2018; Xin, et al. 2020). Agricultural soils are also a primary sink for ENPs incidentally introduced into the environment after the disposal of ENP-containing commercial products. Therefore, plants exposure to ENPs are highly likely, causing some food safety concerns over the potential uptake and accumulation of ENPs by food crops. Metallic nanoparticles (NPs) are important candidates for agricultural

* Reprinted with permission from “Prediction of Plant Uptake and Translocation of Engineered Metallic Nanoparticles by Machine Learning.” by Wang, X., Liu, L., Zhang, W. and Ma, X., 2021. *Environmental Science & Technology*, 55, 11, 7491–7500. Copyright [2021] by ACS Publications.

applications (Sun, et al. 2021). Even though studies on the extent and mechanisms of plant uptake of ENPs have been conducted for over a decade, questions remain that how likely are ENPs been taken up by plant roots and translocated to plant shoots (Ma and Yan 2018). It is also unclear what factors govern the plant uptake and accumulation of ENPs (Liu, et al. 2020). Answers to these questions are important because they will provide key insights into the sustainable applications of ENPs in agriculture.

Unfortunately, answers to these questions are still elusive due to the enormous discrepancies in the literature with regard to the extent of plant uptake of ENPs, arising mostly from the huge differences of plant species, properties of ENPs and growth conditions used in previous studies (Lv, et al. 2019).

Machine learning (ML) has displayed unparalleled capability for result predictions, anomaly detection, feature importance identification and new materials and medicine design without prior assumption on data distribution (Hsieh, et al. 2019; Ke, et al. 2020; Khan, et al. 2021; Liu and Wang 2019; Masmoudi, et al. 2020; Ribeiro, et al. 2020). With the rapid advancement of ML, its popularity among environmental scientists and engineers is growing. Artificial neural network (ANN) is a supervised algorithm that has been successfully used in a variety of applications including the prediction of plant uptake of organic contaminants and heavy metals (Bagheri, et al. 2019; Raza, et al. 2019). An ANN comprises parallel systems consisting of processing elements (PEs) or neurons, which are assembled at different layers and connected through several links or weights (Hsieh, et al. 2019). The neural network calculates its output at epochs, and compares it with each input vector's expected and measured output to compute the error.

Back propagation neural network (BPNN) is a classical ANN designed for the non-linear exclusive disjunction (XOR), and has been effectively used in complex high dimensional problems (Shah, et al. 2012). Examples of successful applications of ANN in plant contaminant studies include the prediction of cadmium uptake by Brassica in the copresence of cerium oxide nanoparticles (Rossi, et al. 2019); enhanced heavy metal uptake by *Sinapis alba L* (Jaskulak, et al. 2020); and prediction of the root concentration factor (RCF) (Bagheri, et al. 2020) and transpiration stream concentration factor (TSCF) of organic contaminants (Bagheri, et al. 2021). While ML is a data-driven model, the results may reveal new insights into the physical science in a modeling system, given proper feature interpretation. The large variety of ENPs, plant species, and growth conditions make ML a potentially powerful tool to predict the plant uptake of ENPs based on the properties of ENPs and plant species.

The plant uptake and translocation of ENPs can be described by the root concentration factor (RCF) and translocation factor (TF) of ENPs. RCF represents the capacity of plant roots to take up ENPs from the environment, and TF describes the ability of the *in-planta* transfer of ENPs from roots to shoots. The two factors are defined as shown below:

$$RCF = \frac{\text{Concentration of ENPs in plant roots (mg/kg dry weight)}}{\text{Concentration of ENPs in the growth media } \left(\frac{\text{mg}}{\text{L}}\right) \text{ or } \left(\frac{\text{mg}}{\text{kg}}\right)} \quad (1)$$

$$TF = \frac{\text{Concentration of ENPs in plant shoot (mg/kg dry weight)}}{\text{Concentration of ENPs in plant root (mg/kg dry weight)}} \quad (2)$$

Our objectives were (1) to evaluate the feasibility of BPNN to predict plant uptake and accumulation of metallic ENPs in both hydroponic and soil systems; (2) to identify key factors governing the uptake and accumulation of metallic ENPs by terrestrial plants; and (3) to develop mathematical equations to estimate RCF and TF for different ENPs and plant species from selected quantifiable properties of ENPs. The results are expected to accelerate the innovation and applications of nanotechnology in agriculture because the potential ENP uptake by different plant species at different growth conditions are critical considerations in the application of nanotechnology in agriculture.

Materials and Methods

Data collection and processing

Data for plant uptake and translocation of ENPs were extracted from peer-reviewed publications since 2011, when the earliest studies on plant uptake of ENPs were reported. The publications were identified by searching “nanoparticles, plant accumulation and hydroponic” for hydroponic studies and “nanoparticles, plant accumulation and soil” for soil studies in Google Scholar, resulting in around 400 and 300 data sets for the hydroponic and soil studies, respectively. The RCF and TF were calculated based on the concentrations of ENP elements in plant roots, shoots and media directly reported in the literature or extrapolated from the published figures. Key input properties of ENPs were used as reported or from their referred citations. Among these publications, only studies focused-on terrestrial plant uptake of metallic nanoparticles

from root exposure in a hydroponic system or in a well-characterized soil system were included. We excluded carbon-based nanomaterials because precise quantification of carbon nanomaterials in plant tissues was rare. For hydroponic studies, some studies lasted for several weeks, which requires the replenishment of transpired growth media during exposure. However, the exact volume of replenished solution was often missing in these publications, rendering it impossible to know the actual mass of ENP exposure. As a result, only those studies that did not require replenishment due to a short period of exposure or those that replenished the transpired solutions with water were included for hydroponic studies. For the soil system, only studies that provided at least the basic soil characterization information such as the percentage of organic matter and clay were included. To avoid the impact of outliers, a comprehensive data cleaning was performed by trimming off the lowest and highest 5% of independent variables (Carson, et al. 1996; Winston 2014). The remaining 90% of the data, or 114 sets for RCF and 88 sets for TF in hydroponic systems, and 130 sets for RCF and 106 sets for TF in soil systems were used for the ANN modeling. The frequency of different ENPs and plant subclass used in previous experimental studies before and after data cleaning is shown in **Figure VI-1 and 2**.

Prior to the ANN modeling, the data were randomized by stochastic process and normalized to ranges from 0 to 1 as follows (Wang, et al. 2008):

$$x_{norm} = \frac{x - x_{min}}{x_{max} - x_{min}} \quad (3)$$

$$x = x_{norm} \times (x_{max} - x_{min}) + x_{min} \quad (4)$$

where, x_{norm} is the normalized dimensionless variable, x is the observed value, x_{min} is the minimum value, and x_{max} is the maximum value of the variable. The randomized and normalized data were divided into three groups for model training (70%), cross validation (CV) (15%), and testing (15%).

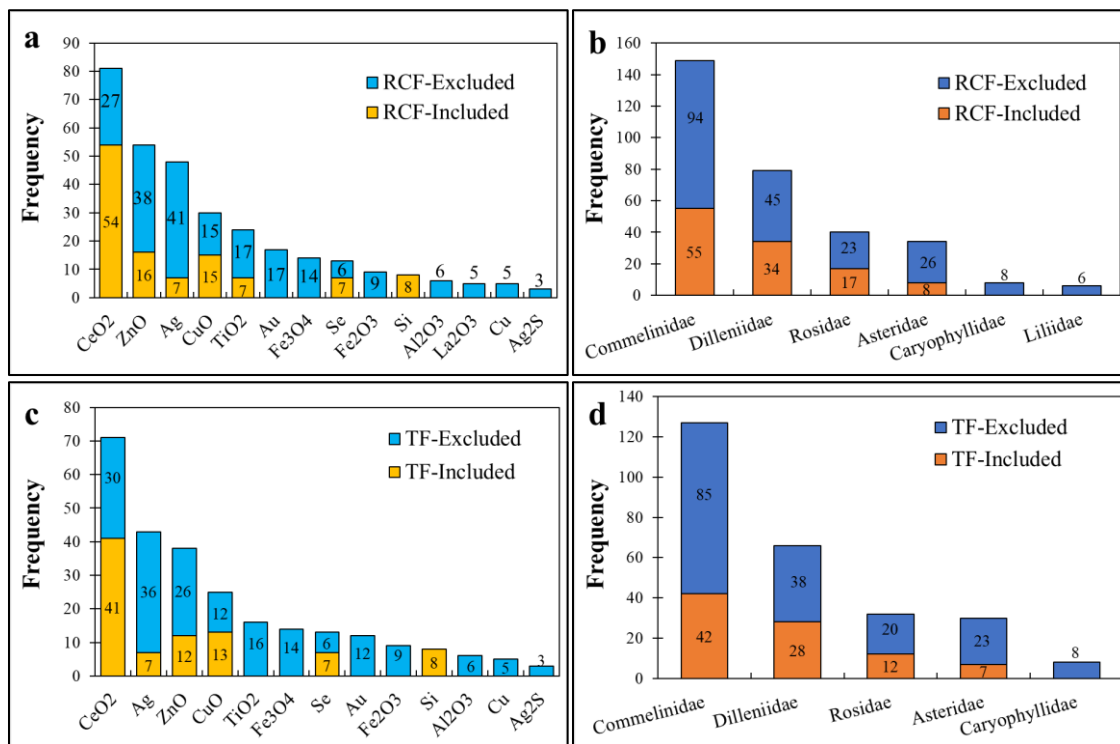


Figure VI-1. Frequency of (a) ENPs composition for RCF; (b) Plant subclass for RCF; (c) ENPs composition for TF; and (d) Plant subclass for TF in the hydroponic systems. Included refers to the dataset used in the modeling after cleaning. Excluded refers to the raw dataset that was not included in the modeling.

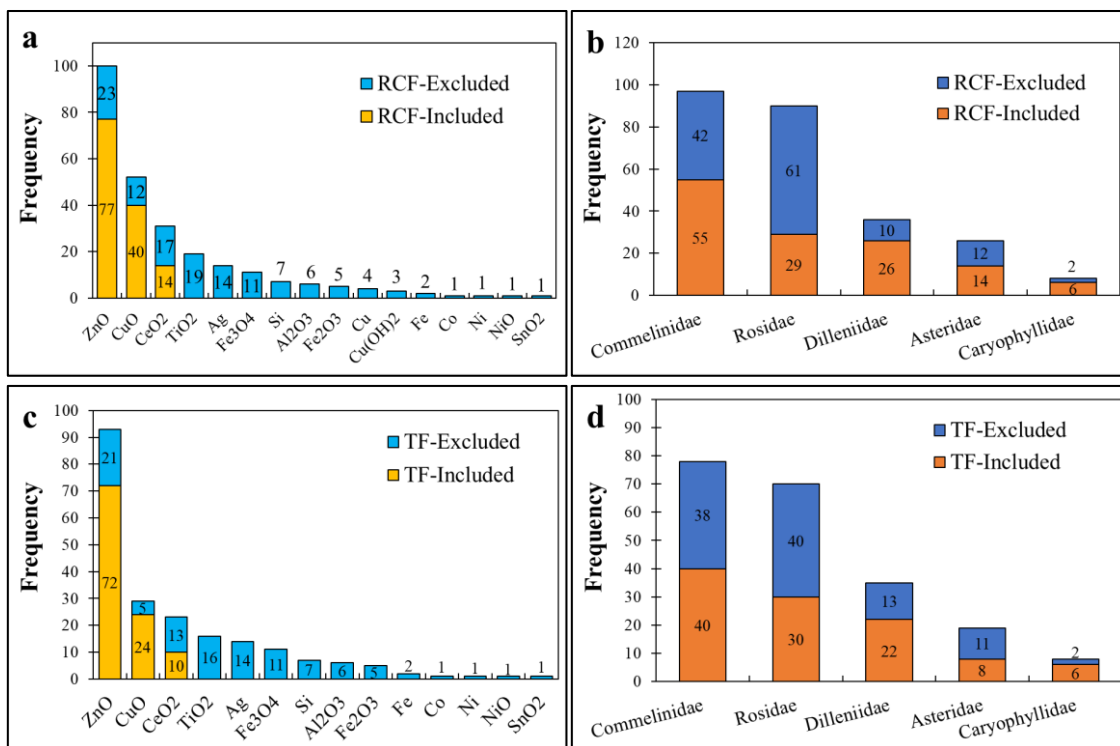


Figure VI-2. Frequency of (a) ENPs composition for RCF; (b) Plant subclass for RCF; (c) ENPs composition for TF; and (d) Plant subclass for TF in the soil system. Included refers to the dataset used in the modeling after cleaning. Excluded refers to the raw dataset that was not included in the modeling.

Back propagation neural network (BPNN)

The classical BPNN algorithm was used to predict RCF and TF of metallic nanoparticles in both hydroponic and soil systems. The model was developed by NeuroSolution 7.1 from NeuroDimension, Inc (Gainesville, FL, US). The BPNN model consisted of an input layer, two hidden layers and an output layer. The maximum epoch was set at 1000 with 0.01 learning rate. Online update and the Levenberg-Marquardt gradient search method with an early stopping callback were employed to prevent overfitting. The activation function used in this study was the sigmoid function. The

model accuracy was determined by R^2 . Plant classification at the level of subclass, ENPs exposure time (only for RCF) and three predominant physicochemical properties of ENPs: composition, size and surface charge were used as input variables in the hydroponic system. They were chosen because experimental studies suggested that they are all important factors affecting plant ENP uptake and translocation (Ma and Quah 2016; Ma, et al. 2014; Quah, et al. 2015; Spielman-Sun, et al. 2017; Sun, et al. 2014a; Wang, et al. 2018). Soil organic matter (SOM) and clay content were included as additional input variables in the soil system because they have been shown to affect the accumulation of ENPs in plants (Majumdar, et al. 2016; Moghaddasi, et al. 2017; Theng and Yuan 2008). The numerical input and output parameters and the ranges of these parameters are summarized in **Table VI-1**.

Sensitivity analysis (SA)

Sensitivity analysis (SA) was performed to determine the relative importance of different input features to the two output parameters. The network output was computed by the input mean \pm minimum/maximum* 1/50 to 50/50 while fixing all other inputs at their respective means (Memarian, et al. 2013). This process was repeated to determine the model sensitivity to each numerical input (Principe, et al. 2005). The sensitivity index was calculated according to equation (5).

$$Sensitivity\ index = \sqrt{\frac{1}{N} \sum_{i=1}^N (y_i - \mu)^2} \quad (5)$$

where, y_i is the varied output in the i^{th} step, μ is the average of varied output, and N is the number of steps (101 in this study). Smaller change of the output suggests a less significant role of the input in the model (Hsieh, et al. 2019).

Table VI-1. Characteristics of input and output numerical variables in the dataset.

Growth system	Input numerical variables	Min	Max	Output variables	Min	Max
Hydroponic	Size (nm)	6	86	RCF	0.55	700.00
	Surface Charge (mV)	-51.57	8.90			
	Exposure Time (days)	0.21	42.00			
	Size (nm)	6	86	TF	9.62E-07	0.47
	Surface Charge (mV)	-51.57	8.90			
Soil	Size (nm)	8	68	RCF	0.072	16.00
	Surface Charge (mV)	-52.00	50.40			
	Exposure Time (days)	7.00	131.00			
	SOM (%)	0.04	12.70			
	Clay (%)	3.70	39.00			
	ENPs Initial Concentration (mg/kg soil)	1.00	1000.00			
	Size (nm)	8	68	TF	0.017	1.77
	Surface Charge (mV)	-52.00	13.80			
	SOM (%)	0.04	12.70			
	Clay (%)	3.70	39.00			
	ENPs Initial Concentration (mg/kg soil)	0.01	900.00			

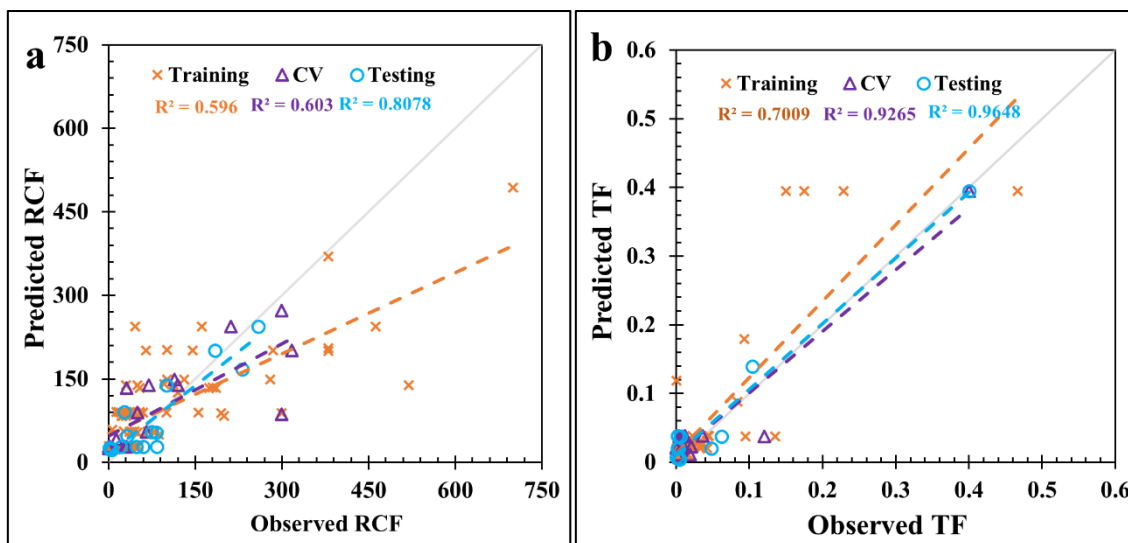


Figure VI-3. ANN simulation correlation in model training/CV/testing stage of (a) RCF, and (b) TF in hydroponic system.

Results and Discussion

BPNN simulation on the plant uptake of ENPs in hydroponic systems

In the hydroponic system, we used plant subclass, time of exposure, and the composition, size and surface charge of ENPs as model descriptors. Our results demonstrate that BPNN produced satisfactory predictions for both RCF ($R^2_{\text{testing}} = 0.8078$) and TF ($R^2_{\text{testing}} = 0.9648$), **Figure VI-3**, suggesting that the selected descriptors are appropriate. The diagonal gray lines in the figure represent 100% accurate prediction by the BPNN algorithm of the measured RCF and TF. The relatively poor simulation of RCF may derive from two reasons. First, the inherent inaccuracy of RCF measurement for ENPs can be a primary factor because by definition, RCF is the ratio of the concentration of ENPs in plant roots over the concentration of ENPs in the growth media. However, a majority of the literature that reported the concentration of ENPs did not distinguish ENPs and their ionic counterparts in plant roots. Therefore, the reported

concentrations of ENPs in plant roots are actually the total concentration of ENP elements. This could cause large errors for highly soluble ENPs such as AgNPs and ZnONPs because the mechanisms for plant uptake of ENPs and their dissolved ions can be markedly different (Dang, et al. 2020; Garcia-Gomez, et al. 2015). For example, metal ions may enter into plant root cells through various protein channels embedded in root membrane, but such pathway is unlikely for ENPs, most of which are much larger than the openings of these channels. In addition, few studies distinguished ENPs attached to the root surface from those accumulated in plant root matrix when the ENP concentrations in plant roots were reported. Previous studies have demonstrated that repeated rinse with deionized water alone would not remove ENPs adsorbed on root surface (Zhou, et al. 2011). ENPs typically experience intense aggregation in liquid media and the extent of aggregation depends on the properties of ENPs such as the surface charge and the composition of the growth media (Badawy, et al. 2010; Dunphy Guzman, et al. 2006; Keller, et al. 2010). Different nutrient solutions and different strength of nutrient solutions were used in different studies which affected ENP aggregation in those media. For cerium oxide nanoparticles, phosphate has been shown to be a main factor affecting its uptake due to the formation of precipitable cerium phosphate (Lin and Xing 2008; Ma, et al. 2015; Rui, et al. 2015). We postulate that the hydrodynamic size of ENPs in the media during or after the exposure would be a better descriptor than the primary particle size. However, the relatively loose requirement on ENP characterization in earlier publications and the lack of information on the hydrodynamic sizes for many publications hinder our effort to verify this hypothesis.

Future investigations may explore the potential use of the hydrodynamic size as a descriptor when more experimental data become available. We suggest that *in-situ* and post-characterization of ENPs should be performed in future studies to provide deeper insights into the interactions of ENPs and plants.

BPNN simulation on the plant uptake of ENPs in soil systems

Due to the critical roles of SOM and clay contents in plant uptake of ENPs, the percentages of SOM and clay content were added as two additional descriptors in soil systems (Majumdar, et al. 2016; Moghaddasi, et al. 2017; Theng and Yuan 2008). BPNN algorithm yielded an acceptable prediction of TF ($R^2_{\text{training}} = 0.8261$) but the prediction of RCF was poor, especially for the training set ($R^2_{\text{training}} = 0.4894$), **Figure VI-4a and b**. The results exhibited the complex interactions between ENPs and plant roots in the rhizosphere soil because the poor fitting indicated that the selected invariables could not fully capture the relationship between the input and output and additional input variables are needed to describe the reactions in plant rhizosphere. Previous studies have shown that ENPs undergo homo- and heteroaggregation in soil pore water (Schultz, et al. 2018), attach to soil mineral particles (Cornelis, et al. 2014; Zhang, et al. 2018), and interact with soil microbial community which reciprocally affect plant uptake of ENPs (Stowers, et al. 2018). To capture the effect of these physical, chemical and biological processes, we added one more descriptor in the BPNN model in soil: the initial concentration of ENPs because the interactions of ENPs with soil components are often concentration dependent. By adding an additional descriptor, the accuracy of BPNN

simulation was notably improved for both RCF ($R^2_{\text{training}} = 0.7895$) and TF ($R^2_{\text{training}} = 0.9050$) for the training dataset, **Figure VI-4c and d.**

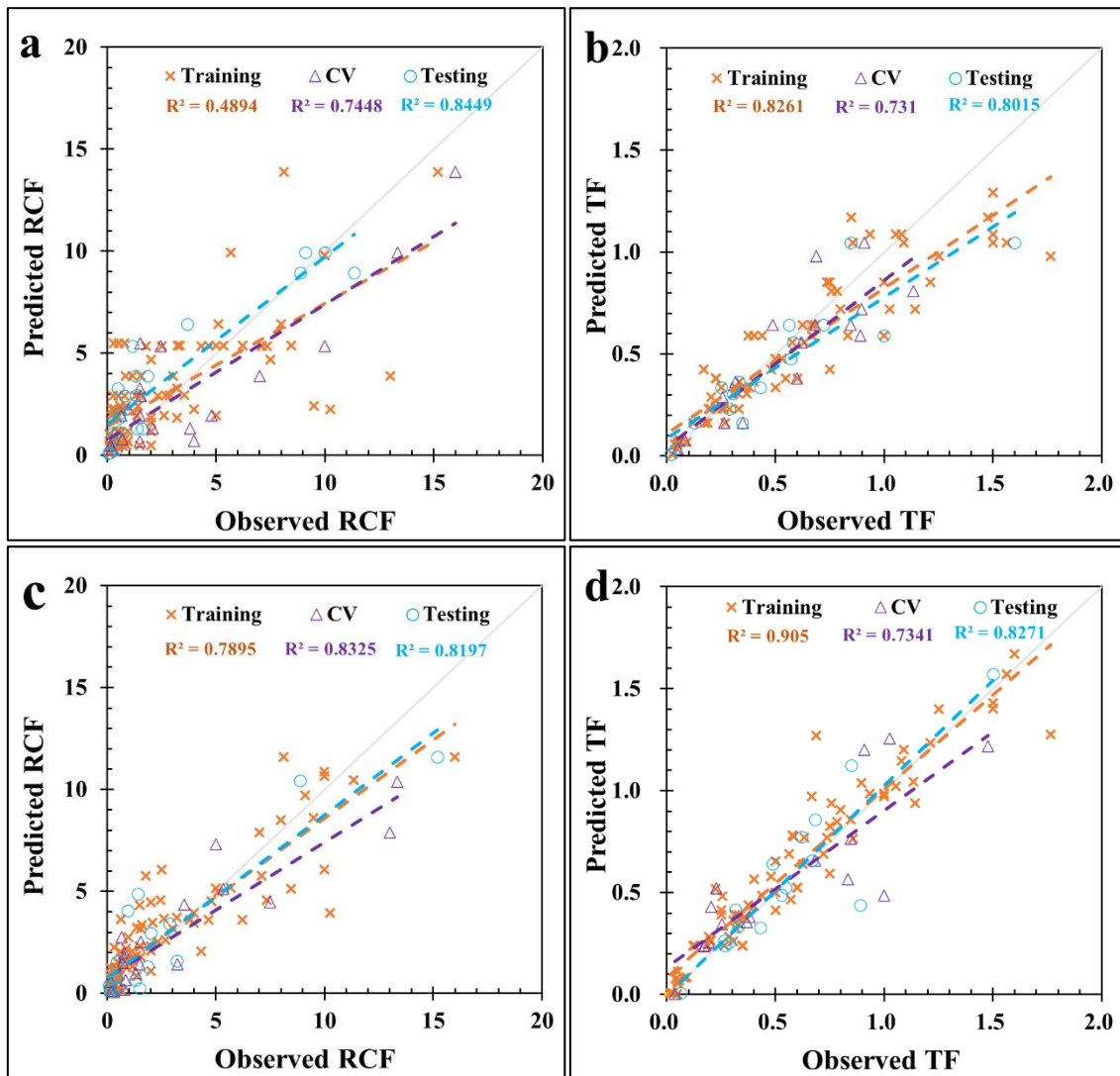


Figure VI-4. ANN simulation correlation in model training/CV/testing stage without input “ENPs initial concentration” of (a) RCF, and (b) TF; and with input “ENPs initial concentration” of (c) RCF, and (d) TF in soil system.

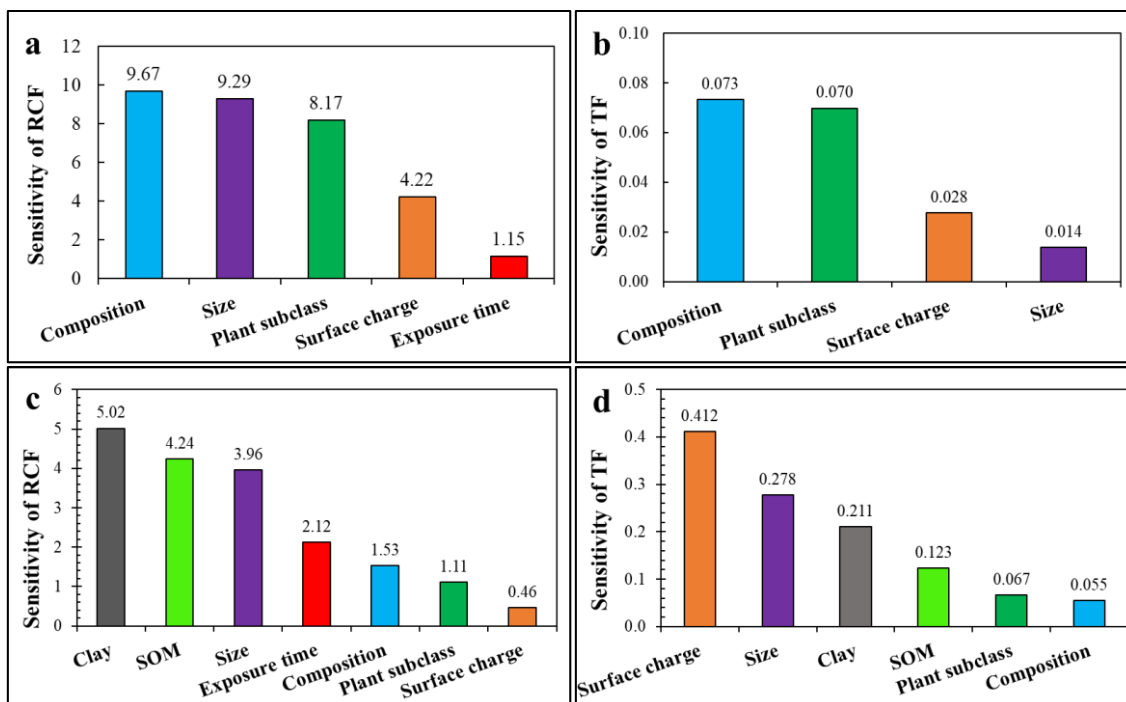


Figure VI-5. Sensitivity analysis index of each input descriptor for (a) RCF model and (b) TF model in hydroponic system; and (c) RCF model and (d) TF model in soil system.

Sensitivity analysis on the input variables

Figure VI-5 shows the relative importance of different descriptors for both RCF and TF in different growth systems. The composition of ENPs carries a greater weight in governing RCF and TF in hydroponic systems, followed by their size and surface charge. Based on the literature, pure metal ENPs generally had higher RCF than metal oxide ENPs, **Figure VI-6a**. It is unclear whether this trend reveals inherently different behaviors of pure metal ENPs and metal oxide ENPs, or it is simply a coincidence. A similar pattern with regard to the effect of the ENP composition on TF was not observed. Plant type is also an important factor for both RCF and TF. **Figure VI-6** illustrates the variations of RCF and TF with different ENPs and plant subclasses in hydroponic systems. At present, comprehensive studies on the plant uptake and accumulation of

ENPs by different plant species are still limited. A survey of the literature showed that most plant species used in studies in ENP plant interactions fall into four subclasses, with the plant subclass Asteridea exhibiting highest ENP accumulation in their roots, followed by Dilleniidae, Commelinidea, and Rosidae. The impact of plant subclasses on TF differed from their influence on RCF. This is understandable because the TF is associated with the *in-planta* transfer of ENPs, which is more affected by the structure of xylem in plant roots and shoots and the transpiration rate of plants while the RCF depends more on the architectural structure of roots, composition of root exudates and the biogeochemical conditions in the rhizosphere (e.g. the presence or absence of phosphate). The properties of root exudates vary significantly for different plant species at different growth stages and these differences might be an important reason for the varying RCF and TF values observed in the literature. It should be mentioned that the trend displayed in **Figure VI-6** with regard to the effect of plant species ignored the variations of the properties of ENPs and growth conditions. Therefore, the figure is only a general illustration of the role of the ENP composition and plant species, it does not necessary mean that plants associated with higher RCF and TF will have the highest accumulation of metallic ENPs in actual studies. For plant commonly used in the study of plant uptake of ENPs, lettuce, tomatoes and sunflowers belong to Asteridea, while cucumber, pumpkins and radish are common Dilleniidae plants. Commelinidea are monocot plants including wheat, rice and corn. Rosidae primarily include leguminous plants such as kidney beans.

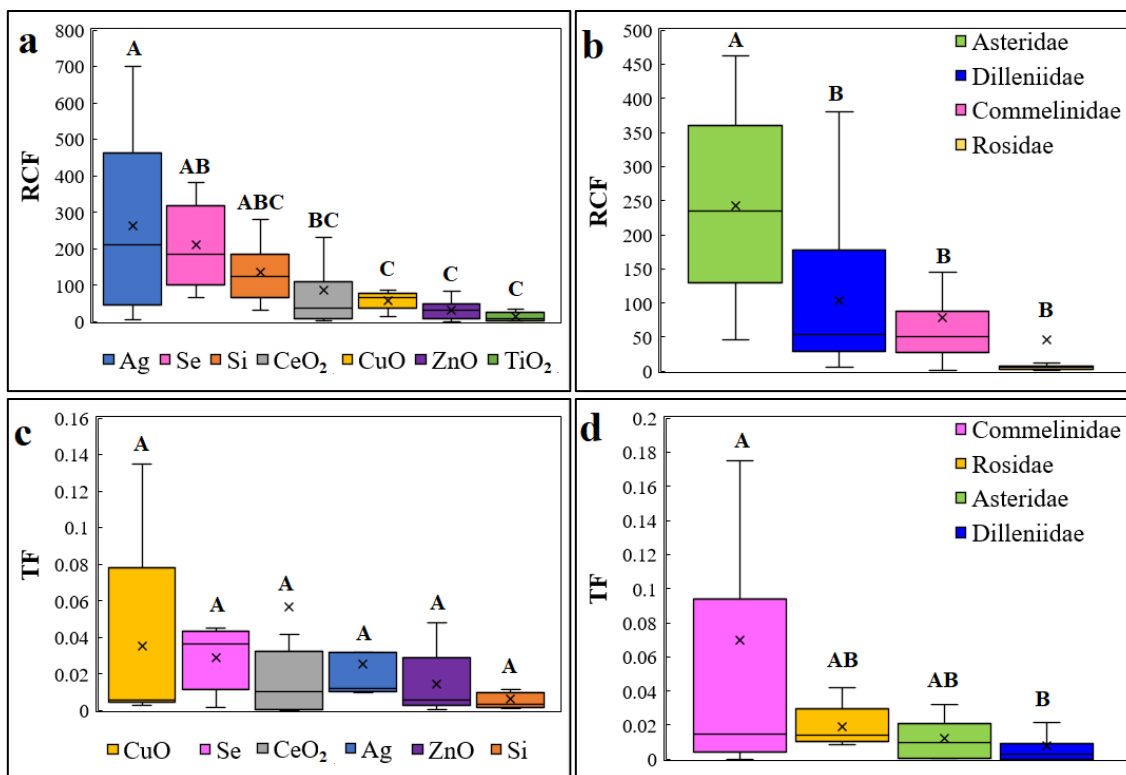


Figure VI-6. Boxplot of cleaned dataset showing (a) RCF by ENPs composition; (b) RCF by plant subclass; (c) TF by NPs composition; and (d) TF by plant subclass in hydroponic system. The cross marker represents the data means and the lines indicated data medians.

Different from the hydroponic system, soil properties play a dominant role in the RCF of ENPs, **Figure VI-5c**, suggesting that complex interactions of ENPs with soil particles dictate the plant uptake and accumulation of ENPs in soil systems. This result underscores the importance of fully characterizing soil properties in studies concerning the plant uptake of ENPs, and demonstrates the striking differences between hydroponic and soil systems. While hydroponic studies generate important insights into the ENP plant interactions, the results cannot be directly extrapolated to soil systems due to the pronounced role of soil clay minerals and organic matter (Dimkpa 2018; Gao, et al. 2019). After ENPs enter into the root tissues, their upward transport to shoots would be

expectedly less affected by soil properties, consistent with the results from the SA analysis, **Figure VI-5d**. Two ENP properties, the surface charge and size, govern the TF of ENPs in soil systems. The importance of these two ENP properties on plant uptake and transport of ENPs have been reported in the literature previously. For example, positively charged ENPs resulted in greater accumulation in roots but lower upward transport from roots to shoots compared with the negatively charged ENPs (Spielman-Sun, et al. 2019; Zhu, et al. 2012). Electrostatic attraction between positively charged ENPs and negatively charged root surface was likely the main reason for elevated RCF. Electrostatic attraction reduced TF because most of these ENPs are adsorbed to the root surface rather than penetrate into the root matrix, and their translocation to the shoots was limited, resulting in smaller TF.

Neither the composition of ENPs nor the plant subclasses is dominant in the soil system. The less significant role of ENP composition in the study might arise from the fact that only limited types of ENPs were investigated in ENP plant studies in soil systems so far. For the three most commonly investigated ENPs, however, a clear pattern was observed between ENP compositions and their RCF and TF, **Figure VI-7 a and c**. The higher RCF and TF for ZnONPs, followed by CuONPs and then CeO₂NPs correlate well with their dissolution rates, suggesting that in the soil system, a significant percentage of RCF and TF for these ENPs might be contributed by their corresponding ions. Supporting the sensitivity analysis, plant subclasses did not make much difference in the RCF and TF values of ENPs in soil systems, **Figure VI-7 b and d**. The results confirmed that in a soil system, the properties of soil and its interactions with ENPs are

controlling factors for ENP plant uptake while the properties of ENPs are more important for ENP transport from root to shoot.

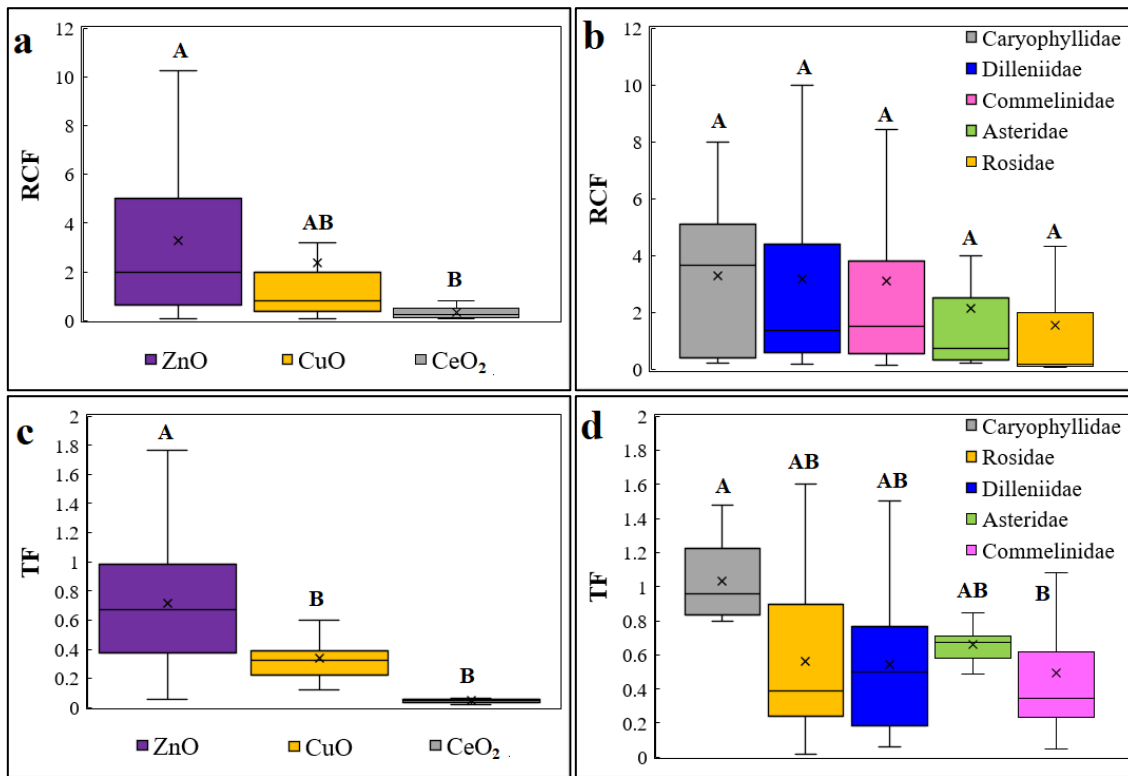


Figure VI-7. Boxplot of cleaned dataset showing (a) RCF by ENPs composition; (b) RCF by plant subclass; (c) TF by ENPs composition; and (d) TF by plant subclass in soil system. The cross marker represents the data means and the lines indicated data medians.

Conclusion

In closing, our results demonstrate that machine learning could be an effective tool to predict the uptake and translocation of ENPs by plants. The BPNN model and SA revealed the key factors dictating the ENP accumulation in plant tissues. In a soil system, the model confirmed the critical role of soil properties. Even though there are some concerns, applications of nanotechnology are expected to continue to expand in agriculture. A predictive model that enables the estimation of the accumulation of

specific ENPs in specific plant species will allow researchers and farmers to match ENPs and plant species in such a way that they can reap the unique benefits provided by nanotechnology, but avoid the potential food safety concerns due to the accumulation of ENPs in food crops. This approach will also benefit the study of ecosystem health when plants are accidentally exposed to ENPs. Currently, foliar application of nanomaterials becomes more popular than root application because of its lower demand for nanomaterials and easier application. Future efforts can be extended to evaluate the accumulation of ENPs in plants from foliar exposure by machine learning. Finally, it is important to underscore that while ML promises to be a powerful tool for environmental investigation, it is a data-driven method. The application of ML must be accompanied with extensive model interpretation to gain new insights into underlying mechanisms of concerned processes.

CHAPTER VII

CONCLUSIONS AND RECOMMENDATIONS

Conclusions

This dissertation has comprehensively evaluated the effects of three metallic nanoparticles on soil chemical properties, and their effect on the uptake of co-contaminants by rice. The results demonstrated that the concerned ENPs displayed complex and distinctive effects on the soil chemical properties, varied with their composition, soil types, exposure duration and specific chemical properties. Compared with ZnO NPs and CuO NPs, their respective ionic counterparts showed a better performance in increasing the rice yield and lowering the total As and As(III) accumulation in rice grains, indicating that the use of ENPs as nanofertilizer should be more closely examined. Our studied also demonstrated significant impact of ZnO NPs and CuO NPs on the formation and properties of iron plaque, which played a crucial role in governing the total As accumulation in rice grains. Furthermore, simultaneous decrease of As and Cd in rice tissues was achieved with the addition of 500 mg/kg SiO₂ NPs combined with AWD irrigation schemes in short term studies. In terms the accumulation of ENPs in plants, machine learning was used to successfully predict the RCF and TF based on key properties of ENPs and plants. The compositions and properties of ENPs dictate their uptake in hydroponic systems, while soil properties, in particular, the clay content and soil organic matter are more dominant factors affecting

ENP plant uptake in soil systems. Overall, this study shed light on the sustainable application of nanotechnology in agriculture.

Recommendations

While this study has significantly advanced our understanding on the impact of ENPs on the soil health, and uptake and accumulation of co-existing As and Cd in rice grains, many questions remain. From the aspect of soil health, this study is one of the earliest research focusing on the effects of different ENPs on soil chemical properties. Future studies should continue to evaluate the effects of different soil amendments on other chemical properties of soil, such as phytoavailable micronutrients and other heavy metal concentrations. In addition, even though the soil biological properties were broadly investigated, most previous studies only investigated the impact of ENPs on the bacterial community. However, soil contains a diverse group of biotas including fungi, nematodes, insects and earthworms. They all play an important role in maintaining the ecological functions of soil and are subject to the impact of soil amendments, which needs to be further investigated.

While this study has demonstrated the impact of three metallic nanoparticles on the uptake and accumulation of As in rice, only one concentration was used for each nanoparticle. The concentration effects of different amendments should be examined to provide guidance for safe and economic applications of ENPs. In addition, the properties of ENPs such as their shape and surface charge have been shown as key parameters affecting their fate and impact in soil plant systems. Therefore, how ENPs with different

properties affect their interactions with coexisting As and other contaminants deserve further investigation. This study showed for the first time that soil amendments significantly affect the properties of iron plaque, which in turn modifies the plant uptake of As and its speciation in plant tissues. However, the impact of different soil amendments on the properties of iron plaque and the microbial community in the iron plaque are still elusive and worth additional examining in the future. Even though simultaneous reduction of As and Cd was observed in our study in the combination of SiO₂ NPs application and water management, long-term experiments extending the whole life cycle of rice in the paddy field should further be conducted to gain more insight into the application of SiO₂ NPs and other forms of Si amendments. Considering that ENPs affect soil chemical properties which may lead to different bioavailability of As and Cd, detailed studies on the bioavailability of As and Cd after ENP applications under different pH and redox conditions will provide better understanding of the long-term impact of nanoagrichemicals.

Finally, the use of machine learning to predict the plant uptake of ENPs was proved to be effective but still at the early stage. Future efforts should be extended to evaluate the uptake and accumulation of ENPs with more extensive dataset and model interpretation to gain an in-depth understanding of the concerned processes. Machine learning can also be used to predict how the presence of ENPs or other soil amendments affects the plant uptake of As and other co-contaminants. From this perspective, the improvement of the data quantity and quality should be made to further making machine learning a powerful tool.

REFERENCES

Acharya, Amitabha, and Probir Kumar Pal

2020 Agriculture nanotechnology: Translating research outcome to field applications by influencing environmental sustainability. *NanoImpact* 19:100232.

Ali, Shafaqat, et al.

2019 Silicon nanoparticles enhanced the growth and reduced the cadmium accumulation in grains of wheat (*Triticum aestivum* L.). *Plant Physiology and Biochemistry* 140:1-8.

Anawar, HM, A Garcia-Sanchez, and I Santa Regina

2008 Evaluation of various chemical extraction methods to estimate plant-available arsenic in mine soils. *Chemosphere* 70(8):1459-1467.

Arao, Tomohito, et al.

2009 Effects of water management on cadmium and arsenic accumulation and dimethylarsinic acid concentrations in Japanese rice. *Environmental Science & Technology* 43(24):9361-9367.

Awasthi, Surabhi, et al.

2017 The Journey of Arsenic from Soil to Grain in Rice. *Frontiers in Plant Science* 8(1007).

Bacha, RE, and LR Hossner

1977 Characteristics of coatings formed on rice roots as affected by iron and manganese additions. *Soil Science Society of America Journal* 41(5):931-935.

Badawy, Amro M El, et al.

2010 Impact of environmental conditions (pH, ionic strength, and electrolyte type) on the surface charge and aggregation of silver nanoparticles suspensions. *Environmental science & technology* 44(4):1260-1266.

Bagheri, Majid, et al.

2020 Examining plant uptake and translocation of emerging contaminants using machine learning: Implications to food security. *Science of The Total Environment* 698:133999.

Bagheri, Majid, et al.

2019 A deeper look at plant uptake of environmental contaminants using intelligent approaches. *Science of The Total Environment* 651:561-569.

Bagheri, Majid, et al.

2021 Investigating plant uptake of organic contaminants through transpiration stream concentration factor and neural network models. *Science of The Total Environment* 751:141418.

Bala, Reetu, Anu Kalia, and Salwinder Singh Dhaliwal

2019 Evaluation of Efficacy of ZnO Nanoparticles as Remedial Zinc Nanofertilizer for Rice. *Journal of Soil Science and Plant Nutrition* 19(2):379-389.

Başar, H

2009 Methods for estimating phytoavailable metals in soils. *Communications in Soil Science and Plant Analysis* 40(7-8):1087-1105.

Ben-Moshe, Tal, et al.

2013 Effects of metal oxide nanoparticles on soil properties. *Chemosphere* 90(2):640-646.

Blanco-Canqui, Humberto, et al.

2013 Soil organic carbon: The value to soil properties. *Journal of Soil and Water Conservation* 68(5):129A-134A.

Bokhtiar, SM, et al.

2012 Effects of silicon on yield contributing parameters and its accumulation in abaxial epidermis of sugarcane leaf blades using energy dispersive x-ray analysis. *Journal of plant nutrition* 35(8):1255-1275.

Bowen, GD, and AD Rovira

1999 The rhizosphere and its management to improve plant growth. *Advances in agronomy* 66:1-102.

Bünemann, Else K., et al.

2018 Soil quality – A critical review. *Soil Biology and Biochemistry* 120:105-125.

Burt, Rebecca

2014 Soil survey field and laboratory methods manual: United States Department of Agriculture.

Carson, Richard T, et al.

1996 Contingent valuation and revealed preference methodologies: comparing the estimates for quasi-public goods. *Land economics* 72:80-99.

Castiglione, Monica Ruffini, et al.

2016 Root responses to different types of TiO₂ nanoparticles and bulk counterpart in plant model system *Vicia faba* L. *Environmental and experimental botany* 130:11-21.

Cervantes-Avilés, Pabel, Xiangning Huang, and Arturo A. Keller

2021 Dissolution and aggregation of metal oxide nanoparticles in root exudates and soil leachate: Implications for nanoagrochemical application. *Environmental Science & Technology*.

Chai, Hankui, et al.

2015 The effect of metal oxide nanoparticles on functional bacteria and metabolic profiles in agricultural soil. *Bulletin of environmental contamination and toxicology* 94(4):490-495.

Chen, C. C., J. B. Dixon, and F. T. Turner

1980 Iron coatings on rice roots: Morphology and models of development. *Soil Science Society of America Journal* 44(5):1113-1119.

Chen, Jing, et al.

2018 Phytotoxicity and bioaccumulation of zinc oxide nanoparticles in rice (*Oryza sativa* L.). *Plant Physiology and Biochemistry* 130:604-612.

Chen, Junren, et al.

2016a Organic acid compounds in root exudation of Moso Bamboo (*Phyllostachys pubescens*) and its bioactivity as affected by heavy metals.

Environmental Science and Pollution Research 23(20):20977-20984.

Chen, Manjia, et al.

2016b Dynamics of the microbial community and Fe (III)-reducing and dechlorinating microorganisms in response to pentachlorophenol transformation in paddy soil. Journal of hazardous materials 312:97-105.

Chen, Y., et al.

2017a Arsenic Transport in Rice and Biological Solutions to Reduce Arsenic Risk from Rice. Frontiers in Plant Science 8:11.

Chen, Yanshan, et al.

2017b Arsenic transport in rice and biological solutions to reduce arsenic risk from rice. Frontiers in plant science 8:268.

Chen, Zheng, et al.

2005 Direct evidence showing the effect of root surface iron plaque on arsenite and arsenate uptake into rice (*Oryza sativa*) roots. New Phytologist 165(1):91-97.

Cheng, Hao, et al.

2012 Interactions among Fe^{2+} , S^{2-} , and Zn^{2+} tolerance, root anatomy, and radial oxygen loss in mangrove plants. Journal of Experimental Botany 63(7):2619-2630.

Chhipa, Hemraj

2017 Nanofertilizers and nanopesticides for agriculture. *Environmental chemistry letters* 15(1):15-22.

Chou, C-H, and Carolyn Harper

2007 Toxicological profile for arsenic.

Cornelis, Geert, et al.

2014 Fate and bioavailability of engineered nanoparticles in soils: a review. *Critical Reviews in Environmental Science and Technology* 44(24):2720-2764.

Cui, Jianghu, et al.

2020 Silica nanoparticles inhibit arsenic uptake into rice suspension cells via improving pectin synthesis and the mechanical force of the cell wall. *Environmental Science: Nano*.

Cui, Jianghu, et al.

2017 Silica nanoparticles alleviate cadmium toxicity in rice cells: mechanisms and size effects. *Environmental Pollution* 228:363-369.

Cui, Jin-li, et al.

2019 Distribution and speciation of copper in rice (*Oryza sativa* L.) from mining-impacted paddy soil: Implications for copper uptake mechanisms. *Environment international* 126:717-726.

Dang, Fei, et al.

2020 Uptake kinetics of silver nanoparticles by plant: relative importance of particles and dissolved ions. *Nanotoxicology* 14(5):654-666.

Das, Suvendu, et al.

2019 Silicate fertilizer amendment alters fungal communities and accelerates soil organic matter decomposition. *Frontiers in Microbiology* 10(2950).

Datnoff, Lawrence E, and FA Rodrigues

2005 The role of silicon in suppressing rice diseases: American Phytopathological Society.

Deng, Rui, et al.

2017 Nanoparticle interactions with co-existing contaminants: joint toxicity, bioaccumulation and risk. *Nanotoxicology* 11(5):591-612.

Di Bonito, Marcello, et al.

2008 Overview of selected soil pore water extraction methods for the determination of potentially toxic elements in contaminated soils: operational and technical aspects. *In Environmental Geochemistry*. Pp. 213-249: Elsevier.

Diedrich, Tamara, et al.

2012 The Dissolution Rates of SiO₂ Nanoparticles As a Function of Particle Size. *Environmental science & technology* 46(9):4909-4915.

Dimkpa, Christian O

2018 Soil properties influence the response of terrestrial plants to metallic nanoparticles exposure. *Current Opinion in Environmental Science & Health* 6:1-8.

Dimkpa, Christian O, et al.

2015 Nano-CuO and interaction with nano-ZnO or soil bacterium provide evidence for the interference of nanoparticles in metal nutrition of plants.

Ecotoxicology 24(1):119-129.

Ding, Changfeng, et al.

2019 Changes in the pH of paddy soils after flooding and drainage: Modeling and validation. Geoderma 337:511-513.

Domingos, Rute F, et al.

2013 Agglomeration and dissolution of zinc oxide nanoparticles: role of pH, ionic strength and fulvic acid. Environmental Chemistry 10(4):306-312.

Duhan, Joginder Singh, et al.

2017 Nanotechnology: The new perspective in precision agriculture. Biotechnology Reports 15:11-23.

Duiker, Sjoerd W, et al.

2003 Iron (hydr) oxide crystallinity effects on soil aggregation.

Duncan, Elliott, and Gary Owens

2019 Metal oxide nanomaterials used to remediate heavy metal contaminated soils have strong effects on nutrient and trace element phytoavailability. Science of The Total Environment 678:430-437.

Dunphy Guzman, Katherine A, Michael P Finnegan, and Jillian F Banfield

2006 Influence of surface potential on aggregation and transport of titania nanoparticles. Environmental science & technology 40(24):7688-7693.

Ebbs, Stephen D., et al.

2016 Accumulation of zinc, copper, or cerium in carrot (*Daucus carota*) exposed to metal oxide nanoparticles and metal ions. *Environmental Science: Nano* 3(1):114-126.

Elhaj Baddar, Zeinah, and Jason M Unrine

2018 Functionalized-ZnO-nanoparticle seed treatments to enhance growth and zn content of wheat (*Triticum aestivum*) seedlings. *Journal of agricultural and food chemistry* 66(46):12166-12178.

Elisa, AA, et al.

2016 Alleviating aluminum toxicity in an acid sulfate soil from Peninsular Malaysia by calcium silicate application. *Solid Earth* 7(2):367.

Fayiga, Abioye O, and Uttam K Saha

2017 Nanoparticles in biosolids: effect on soil health and crop growth. *Annals of Environmental Science and Toxicology* 2(2):059-067.

Feng Shao, Ji, et al.

2017 Silicon reduces cadmium accumulation by suppressing expression of transporter genes involved in cadmium uptake and translocation in rice. *Journal of experimental botany* 68(20):5641-5651.

French, Rebecca A, et al.

2009 Influence of ionic strength, pH, and cation valence on aggregation kinetics of titanium dioxide nanoparticles. *Environmental science & technology* 43(5):1354-1359.

Frommer, Jakob, et al.

2011 Biogeochemical processes and arsenic enrichment around rice roots in paddy soil: results from micro - focused X - ray spectroscopy. *European Journal of Soil Science* 62(2):305-317.

Fu, You-Qiang, et al.

2016 Identification, separation and component analysis of reddish brown and non-reddish brown iron plaque on rice (*Oryza sativa*) root surface. *Plant and soil* 402(1-2):277-290.

Gao, Xiaoyu, et al.

2018 CuO nanoparticle dissolution and toxicity to wheat (*Triticum aestivum*) in rhizosphere soil. *Environmental science & technology* 52(5):2888-2897.

Gao, Xiaoyu, et al.

2019 Effect of soil organic matter, soil pH, and moisture content on solubility and dissolution rate of CuO NPs in soil. *Environmental science & technology* 53(9):4959-4967.

Garcia-Gomez, C, et al.

2015 Integrating ecotoxicity and chemical approaches to compare the effects of ZnO nanoparticles, ZnO bulk, and ZnCl₂ on plants and microorganisms in a natural soil. *Environmental Science and Pollution Research* 22(21):16803-16813.

Garg, N., and P. Singla

2011 Arsenic toxicity in crop plants: physiological effects and tolerance mechanisms. *Environmental Chemistry Letters* 9(3):303-321.

Gong, Bing, et al.

2020 Interactions of arsenic, copper, and zinc in soil-plant system: Partition, uptake and phytotoxicity. *Science of The Total Environment* 745:140926.

Greger, Maria, Tommy Landberg, and Marek Vaculík

2018 Silicon influences soil availability and accumulation of mineral nutrients in various plant species. *Plants* 7(2):41.

Guan, Xiangyu, et al.

2020 CuO nanoparticles alter the rhizospheric bacterial community and local nitrogen cycling for wheat grown in a Calcareous soil. *Environmental Science & Technology* 54(14):8699-8709.

Guo, Binglin, et al.

2019 Attachment of cerium oxide nanoparticles of different surface charges to kaolinite: Molecular and atomic mechanisms. *Environmental research* 177:108645.

Hansel, Colleen M, et al.

2001 Characterization of Fe plaque and associated metals on the roots of mine-waste impacted aquatic plants. *Environmental Science & Technology* 35(19):3863-3868.

Hansel, Colleen M, et al.

2002 Spatial and temporal association of As and Fe species on aquatic plant roots. *Environmental Science & Technology* 36(9):1988-1994.

Hoang, Trung Viet, et al.

2019 Heat stress transcription factor OsSPL7 plays a critical role in reactive oxygen species balance and stress responses in rice. *Plant Science* 289:110273.

Hochella, Michael F, et al.

2019 Natural, incidental, and engineered nanomaterials and their impacts on the Earth system. *Science* 363(6434).

Honma, Toshimitsu, et al.

2016a Optimal soil Eh, pH, and water management for simultaneously minimizing arsenic and cadmium concentrations in rice grains. *Environmental science & technology* 50(8):4178-4185.

Honma, Toshimitsu, et al.

2016b Effects of soil amendments on arsenic and cadmium uptake by rice plants (*Oryza sativa* L. cv. Koshihikari) under different water management practices. *Soil Science and Plant Nutrition* 62(4):349-356.

Hsieh, Sheng-Hsin, et al.

2019 Sensitivity analysis on the rising relation between short-term rainfall and groundwater table adjacent to an artificial recharge lake. *Water* 11(8):1704.

Hu, Y., et al.

2005 Sequestration of As by iron plaque on the roots of three rice (*Oryza sativa* L.) cultivars in a low-P soil with or without P fertilizer. *Environ Geochem Health* 27(2):169-76.

Huang, Guoyong, et al.

2020 Variations of dissolved organic matter and Cu fractions in rhizosphere soil induced by the root activities of castor bean. *Chemosphere*:126800.

Huff, James, et al.

2007 Cadmium-induced cancers in animals and in humans. *International journal of occupational and environmental health* 13(2):202-212.

Hughes, Michael F.

2002 Arsenic toxicity and potential mechanisms of action. *Toxicology Letters* 133(1):1-16.

Hussain, Afzal, et al.

2019 Seed priming with silicon nanoparticles improved the biomass and yield while reduced the oxidative stress and cadmium concentration in wheat grains. *Environmental Science and Pollution Research* 26(8):7579-7588.

Imtiaz, Muhammad, et al.

2016 Silicon occurrence, uptake, transport and mechanisms of heavy metals, minerals and salinity enhanced tolerance in plants with future prospects: A review. *Journal of Environmental Management* 183:521-529.

Isa, Mami, et al.

2010 Silicon enhances growth independent of silica deposition in a low-silica rice mutant, *lsi1*. *Plant and Soil* 331(1):361-375.

Islam, Shofiqul, et al.

2016 Arsenic accumulation in rice: consequences of rice genotypes and management practices to reduce human health risk. *Environment international* 96:139-155.

Jaskulak, Marta, Anna Grobelak, and Franck Vandebulcke

2020 Modeling and optimizing the removal of cadmium by *Sinapis alba* L. from contaminated soil via Response Surface Methodology and Artificial Neural Networks during assisted phytoremediation with sewage sludge. *International Journal of Phytoremediation* 22(12):1321-1330.

Ji, Xionghui, et al.

2017 Effect of silicon fertilizers on cadmium in rice (*Oryza sativa*) tissue at tillering stage. *Environmental Science and Pollution Research* 24(11):10740-10748.

Jia, Yan, et al.

2014 Arsenic uptake by rice is influenced by microbe-mediated arsenic redox changes in the rhizosphere. *Environmental science & technology* 48(2):1001-1007.

Jianfeng, MA, and Eiichi Takahashi

1991 Effect of silicate on phosphate availability for rice in a P-deficient soil. *Plant and Soil* 133(2):151-155.

Jobbágy, Esteban G, and Robert B Jackson

2000 The vertical distribution of soil organic carbon and its relation to climate and vegetation. *Ecological applications* 10(2):423-436.

Jones, Adele M, et al.

2009 The effect of silica and natural organic matter on the Fe (II)-catalysed transformation and reactivity of Fe (III) minerals. *Geochimica et Cosmochimica Acta* 73(15):4409-4422.

Joško, Izabela, et al.

2019 Long-term effect of ZnO and CuO nanoparticles on soil microbial community in different types of soil. *Geoderma* 352:204-212.

Kah, Melanie

2015 Nanopesticides and nanofertilizers: emerging contaminants or opportunities for risk mitigation? *Frontiers in chemistry* 3:64.

Kah, Melanie, et al.

2018 A critical evaluation of nanopesticides and nanofertilizers against their conventional analogues. *Nature nanotechnology* 13(8):677.

Kah, Melanie, Nathalie Tufenkji, and Jason C. White

2019 Nano-enabled strategies to enhance crop nutrition and protection. *Nature Nanotechnology* 14(6):532-540.

Kaya, Cengiz, et al.

2009 Mitigation effects of silicon on maize plants grown at high zinc. *Journal of Plant Nutrition* 32(10):1788-1798.

Ke, Yi-Yu, et al.

2020 Artificial intelligence approach fighting COVID-19 with repurposing drugs. *Biomedical journal* 43(4):355-362.

Keller, Arturo A, et al.

2010 Stability and aggregation of metal oxide nanoparticles in natural aqueous matrices. *Environmental science & technology* 44(6):1962-1967.

Khan, Mohsin Ali, et al.

2021 Compressive strength of fly-fsh-based geopolymer concrete by gene expression programming and random forest. *Advances in Civil Engineering* 2021:6618407.

Khan, Zahra Saeed, et al.

2020 Effects of silicon nanoparticles on growth and physiology of wheat in cadmium contaminated soil under different soil moisture levels. *Environmental Science and Pollution Research* 27(5):4958-4968.

Khanam, Rubina, et al.

2020 Metal (loid) s (As, Hg, Se, Pb and Cd) in paddy soil: Bioavailability and potential risk to human health. *Science of the Total Environment* 699:134330.

Kouhi, Seyed Mousa Mousavi, et al.

2015 Comparative effects of ZnO nanoparticles, ZnO bulk particles, and Zn²⁺ on *Brassica napus* after long-term exposure: changes in growth, biochemical compounds, antioxidant enzyme activities, and Zn bioaccumulation. *Water, Air, & Soil Pollution* 226(11):1-11.

Lambers, Hans, et al.

2009 Plant-microbe-soil interactions in the rhizosphere: an evolutionary perspective. *Plant and soil* 321(1-2):83-115.

Landa, Premysl, et al.

2016 Effect of metal oxides on plant germination: phytotoxicity of nanoparticles, bulk materials, and metal ions. *Water, Air, & Soil Pollution* 227(12):448.

Lee, Chia-Hsing, et al.

2013 Iron plaque formation and its effect on arsenic uptake by different genotypes of paddy rice. *Plant and soil* 363(1):231-241.

Lehmann, Johannes, et al.

2020a The concept and future prospects of soil health. *Nature Reviews Earth & Environment* 1(10):544-553.

Lehmann, Johannes, et al.

2020b Persistence of soil organic carbon caused by functional complexity. *Nature Geoscience* 13(8):529-534.

Leifeld, Jens, Kristy Klein, and Chloé Wüst-Galley

2020 Soil organic matter stoichiometry as indicator for peatland degradation. *Scientific Reports* 10(1):1-9.

Leksungnoen, Parapond, et al.

2019 Biochar and ash derived from silicon-rich rice husk decrease inorganic arsenic species in rice grain. *Science of The Total Environment* 684:360-370.

Li, RY, et al.

2009 Mitigation of arsenic accumulation in rice with water management and silicon fertilization. *Environmental Science & Technology* 43(10):3778-3783.

Li, Zimin, Zhaoliang Song, and Jean-Thomas Cornelis

2014 Impact of rice cultivar and organ on elemental composition of phytoliths and the release of bio-available silicon. *Frontiers in Plant Science* 5(529).

Limmer, Matthew A, et al.

2018 Silicon-rich amendments in rice paddies: Effects on arsenic uptake and biogeochemistry. *Science of the total environment* 624:1360-1368.

Lin, Daohui, and Baoshan Xing

2008 Root uptake and phytotoxicity of ZnO nanoparticles. *Environmental Science & Technology* 42(15):5580-5585.

Liu, Chuanping, et al.

2014 Effects of nanoscale silica sol foliar application on arsenic uptake, distribution and oxidative damage defense in rice (*Oryza sativa* L.) under arsenic stress. *Rsc Advances* 4(100):57227-57234.

Liu, Jing, Birendra Dhungana, and George P. Cobb

2018a Copper oxide nanoparticles and arsenic interact to alter seedling growth of rice (*Oryza sativa japonica*). *Chemosphere* 206:330-337.

Liu, Jing, et al.

2021a Mobility of arsenic in the growth media of rice plants (*Oryza sativa* subsp. *japonica*. 'Koshihikari') with exposure to copper oxide nanoparticles in a life-cycle greenhouse study. *Science of The Total Environment* 774:145620.

Liu, Jing, et al.

2018b Physiological effects of copper oxide nanoparticles and arsenic on the growth and life cycle of rice (*Oryza sativa japonica* ‘Koshihikari’).

Environmental science & technology 52(23):13728-13737.

Liu, Jing, et al.

2019 Distribution and speciation of copper and arsenic in rice plants (*Oryza sativa japonica* ‘Koshihikari’) treated with copper oxide nanoparticles and arsenic during a life cycle. Environmental science & technology 53(9):4988-4996.

Liu, Li-Wei, and Yu-Min Wang

2019 Modelling Reservoir Turbidity Using Landsat 8 Satellite Imagery by Gene Expression Programming. Water 11(7):1479.

Liu, W - J, et al.

2004 Do phosphorus nutrition and iron plaque alter arsenate (As) uptake by rice seedlings in hydroponic culture? New Phytologist 162(2):481-488.

Liu, W. J., et al.

2006 Arsenic sequestration in iron plaque, its accumulation and speciation in mature rice plants (*Oryza sativa* L.). Environmental Science & Technology 40(18):5730-5736.

Liu, Yang, et al.

2020 Can the properties of engineered nanoparticles be indicative of their functions and effects in plants? Ecotoxicology and Environmental Safety 205:111128.

Liu, Yangzhi, et al.

2021b A new strategy using nanoscale zero-valent iron to simultaneously promote remediation and safe crop production in contaminated soil. *Nature Nanotechnology* 16(2):197-205.

Lv, Jitao, Peter Christie, and Shuzhen Zhang

2019 Uptake, translocation, and transformation of metal-based nanoparticles in plants: recent advances and methodological challenges. *Environmental Science: Nano* 6(1):41-59.

Ma, Huanhuan, et al.

2020a Formation of iron plaque on roots of *Iris pseudacorus* and its consequence for cadmium immobilization is impacted by zinc concentration. *Ecotoxicology and environmental safety* 193:110306.

Ma, X, and B Quah

2016 Effects of surface charge on the fate and phytotoxicity of gold nanoparticles to *Phaseolus vulgaris*. *Journal of Food Chemistry & Nanotechnology* 2:57-65.

Ma, X. M., et al.

2014 Interactions Between Engineered Nanoparticles (ENPs) and Plants: Phytotoxicity, Uptake and Accumulation. *Science of the Total Environment* 481:635-635.

Ma, Xingmao, et al.

2019 Simultaneous reduction of arsenic (As) and cadmium (Cd) accumulation in rice by zinc oxide nanoparticles. *Chemical Engineering Journal*:123802.

—

2020b Simultaneous reduction of arsenic (As) and cadmium (Cd) accumulation in rice by zinc oxide nanoparticles. *Chemical Engineering Journal* 384:123802.

Ma, Xingmao, and Jun Yan

2018 Plant uptake and accumulation of engineered metallic nanoparticles from lab to field conditions. *Current Opinion in Environmental Science & Health* 6:16-20.

Ma, Yuhui, et al.

2015 Where does the transformation of precipitated ceria nanoparticles in hydroponic plants take place? *Environmental science & technology* 49(17):10667-10674.

Majumdar, Sanghamitra, et al.

2016 Soil organic matter influences cerium translocation and physiological processes in kidney bean plants exposed to cerium oxide nanoparticles. *Science of the Total Environment* 569:201-211.

Malwal, Deepika, and P Gopinath

2017 Efficient adsorption and antibacterial properties of electrospun CuO-ZnO composite nanofibers for water remediation. *Journal of hazardous materials* 321:611-621.

Manrique, LA, CA Jones, and PT Dyke

1991 Predicting cation - exchange capacity from soil physical and chemical properties. *Soil Science Society of America Journal* 55(3):787-794.

Marin, AR, PH Masscheleyn, and WH Patrick

1993 Soil redox-pH stability of arsenic species and its influence on arsenic uptake by rice. *Plant and Soil* 152(2):245-253.

Martinson, Carol A, and KJ Reddy

2009 Adsorption of arsenic (III) and arsenic (V) by cupric oxide nanoparticles. *Journal of Colloid and Interface Science* 336(2):406-411.

Masmoudi, Sahar, et al.

2020 A machine-learning framework for predicting multiple air pollutants' concentrations via multi-target regression and feature selection. *Science of the Total Environment* 715:136991.

McDonald, Kyle J, Brandon Reynolds, and KJ Reddy

2015 Intrinsic properties of cupric oxide nanoparticles enable effective filtration of arsenic from water. *Scientific reports* 5:11110.

Memarian, Hadi, Siva Kumar Balasundram, and Mohamad Tajbakhsh

2013 An expert integrative approach for sediment load simulation in a tropical watershed. *Journal of Integrative Environmental Sciences* 10(3-4):161-178.

Mishra, Sandhya, et al.

2017 Integrated approach of agri-nanotechnology: challenges and future trends. *Frontiers in plant science* 8:471.

Moghaddasi, Sahar, et al.

2017 Bioavailability of coated and uncoated ZnO nanoparticles to cucumber in soil with or without organic matter. *Ecotoxicology and environmental safety* 144:543-551.

Mushtaq, Ayesha, et al.

2018 Engineered Silica Nanoparticles and silica nanoparticles containing Controlled Release Fertilizer for drought and saline areas. *IOP conference series: materials science and engineering*, 2018. Vol. 414, pp. 012029. IOP Publishing.

Muthukumararaja, TM, and MV Sriramachandrasekharan

2012 Effect of zinc on yield, zinc nutrition and zinc use efficiency of lowland rice. *Journal of Agricultural Technology* 8(2):551-561.

Nagayama, Teruki, et al.

2019 Changes in the distribution of pectin in root border cells under aluminum stress. *Frontiers in Plant Science* 10(1216).

Nardi, S, et al.

2000 Soil organic matter mobilization by root exudates. *Chemosphere* 41(5):653-658.

Nelson, DW, and L_E Sommers

1983 Total carbon, organic carbon, and organic matter. *Methods of soil analysis: Part 2 chemical and microbiological properties* 9:539-579.

Nikolova, Maria P, and Murthy S Chavali

2020 Metal oxide nanoparticles as biomedical materials. *Biomimetics* 5(2):27.

Nwugo, Chika C, and Alfredo J Huerta

2008 Effects of silicon nutrition on cadmium uptake, growth and photosynthesis of rice plants exposed to low-level cadmium. *Plant and Soil* 311(1-2):73-86.

Page, AL, AC Chang, and EA Mohamed

1987 Cadmium levels in soils and crops. *The United States scope* 31:120-122.

Palansooriya, Kumuduni Niroshika, et al.

2020 Soil amendments for immobilization of potentially toxic elements in contaminated soils: A critical review. *Environment international* 134:105046.

Parada, J, et al.

2019 The nanotechnology among US: are metal and metal oxides nanoparticles a nano or mega risk for soil microbial communities? *Critical reviews in biotechnology* 39(2):157-172.

Parfitt, RL, DJ Giltrap, and JS Whitton

1995 Contribution of organic matter and clay minerals to the cation exchange capacity of soils. *Communications in soil science and plant analysis* 26(9-10):1343-1355.

Peng, Cheng, et al.

2018 Iron plaque: A barrier layer to the uptake and translocation of copper oxide nanoparticles by rice plants. *Environmental science & technology* 52(21):12244-12254.

Peng, Cheng, et al.

2020 Bioavailability and translocation of metal oxide nanoparticles in the soil-rice plant system. *Science of The Total Environment* 713:136662.

Peng, Cheng, et al.

2017 Fate and transformation of CuO nanoparticles in the soil–rice system during the life cycle of rice plants. *Environmental Science & Technology* 51(9):4907-4917.

Pigna, Massimo, et al.

2015 Arsenic in the soil environment: mobility and phytoavailability. *Environmental Engineering Science* 32(7):551-563.

Principe, J, et al.

2005 NeuroSolutions–Documentation. NeuroDimension, Inc.: Gainesville, FL.

Printz, Bruno, et al.

2016 Copper trafficking in plants and its implication on cell wall dynamics. *Frontiers in plant science* 7:601.

Punshon, T., et al.

2017 Understanding Arsenic Dynamics in Agronomic Systems to Predict and Prevent Uptake by Crop Plants. *Science of the Total Environment* 581:209-220.

Qaswar, Muhammad, et al.

2020 Soil nutrients and heavy metal availability under long-term combined application of swine manure and synthetic fertilizers in acidic paddy soil. *Journal of Soils and Sediments* 20(4):2093-2106.

Qiao, Jiang-tao, et al.

2018 Simultaneous alleviation of cadmium and arsenic accumulation in rice by applying zero-valent iron and biochar to contaminated paddy soils. *Chemosphere* 195:260-271.

Quah, Bryan, et al.

2015 Phytotoxicity, uptake, and accumulation of silver with different particle sizes and chemical forms. *Journal of Nanoparticle Research* 17(6):1-13.

Rahman, M Azizur, et al.

2008 Straighthead disease of rice (*Oryza sativa* L.) induced by arsenic toxicity. *Environmental and experimental botany* 62(1):54-59.

Rai, Prabhat Kumar, et al.

2018 Nanoparticle-plant interaction: Implications in energy, environment, and agriculture. *Environment international* 119:1-19.

Rajput, Vishnu D, et al.

2018a Effects of zinc-oxide nanoparticles on soil, plants, animals and soil organisms: a review. *Environmental Nanotechnology, Monitoring & Management* 9:76-84.

Rajput, Vishnu D, et al.

2018b Effect of nanoparticles on crops and soil microbial communities. *Journal of Soils and Sediments* 18(6):2179-2187.

Rameshraddy, et al.

2017 Zinc oxide nano particles increases Zn uptake, translocation in rice with positive effect on growth, yield and moisture stress tolerance. *Indian Journal of Plant Physiology* 22(3):287-294.

Rastogi, Anshu, et al.

2017 Impact of metal and metal oxide nanoparticles on plant: A critical review. *Frontiers in Chemistry* 5(78).

Raza, Akber, et al.

2019 A machine learning approach for predicting defluorination of per-and polyfluoroalkyl substances (PFAS) for their efficient treatment and removal. *Environmental Science & Technology Letters* 6(10):624-629.

Ribeiro, Victor Henrique Alves, et al.

2020 A novel dynamic multi-criteria ensemble selection mechanism applied to drinking water quality anomaly detection. *Science of The Total Environment* 749:142368.

Rooney, Corinne P., Fang-Jie Zhao, and Steve P. McGrath

2006 Soil factors controlling the expression of copper toxicity to plants in a wide range of European soils. *Environmental Toxicology and Chemistry* 25(3):726-732.

Rossi, Lorenzo, et al.

2019 Using artificial neural network to investigate physiological changes and cerium oxide nanoparticles and cadmium uptake by *Brassica napus* plants. *Environmental Pollution* 246:381-389.

Rousk, Johannes, et al.

2012 Comparative toxicity of nanoparticulate CuO and ZnO to soil bacterial communities. *PloS one* 7(3):e34197.

Rui, Yukui, et al.

2015 Transformation of ceria nanoparticles in cucumber plants is influenced by phosphate. *Environmental Pollution* 198:8-14.

Samarajeewa, AD, et al.

2020 Ecotoxicological effects of copper oxide nanoparticles (nCuO) on the soil microbial community in a biosolids-amended soil. *Science of The Total Environment*:143037.

Schultz, Carolin L, et al.

2018 Influence of soil porewater properties on the fate and toxicity of silver nanoparticles to *Caenorhabditis elegans*. *Environmental toxicology and chemistry* 37(10):2609-2618.

Seshadri, B, NS Bolan, and R Naidu

2015 Rhizosphere-induced heavy metal (loid) transformation in relation to bioavailability and remediation. *Journal of soil science and plant nutrition* 15(2):524-548.

Seybold, CA, RB Grossman, and TG Reinsch

2005 Predicting cation exchange capacity for soil survey using linear models. *Soil Science Society of America Journal* 69(3):856-863.

Seyfferth, Angelia L, et al.

2010 Arsenic localization, speciation, and co-occurrence with iron on rice (*Oryza sativa* L.) roots having variable Fe coatings. *Environmental science & technology* 44(21):8108-8113.

Shah, Habib, et al.

2012 Global hybrid ant bee colony algorithm for training artificial neural networks. *International Conference on Computational Science and Its Applications*, 2012, pp. 87-100. Springer.

Sharifan, Hamidreza, et al.

2018 Investigation on the modification of physicochemical properties of cerium oxide nanoparticles through adsorption of Cd and As(III)/As(V). *ACS Sustainable Chemistry & Engineering* 6(10):13454-13461.

Shen, Shengwen, et al.

2013 Arsenic binding to proteins. *Chemical reviews* 113(10):7769-7792.

Shen, Zhaoyi, et al.

2015 Ecotoxicological effect of zinc oxide nanoparticles on soil microorganisms. *Frontiers of Environmental Science & Engineering* 9(5):912-918.

Shi, Jiyan, et al.

2018 Effects of copper oxide nanoparticles on paddy soil properties and components. *Nanomaterials* 8(10):839.

Shi, Shulin, et al.

2016 OsHAC1; 1 and OsHAC1; 2 function as arsenate reductases and regulate arsenic accumulation. *Plant Physiology* 172(3):1708-1719.

Shrivastava, Anamika, et al.

2020 Arsenic mitigation in rice grain loading via alternative irrigation by proposed water management practices. *Chemosphere* 238:124988.

Simonin, Marie, et al.

2016 Titanium dioxide nanoparticles strongly impact soil microbial function by affecting archaeal nitrifiers. *Scientific reports* 6(1):1-10.

Spielman-Sun, Eleanor, et al.

2019 Nanoparticle surface charge influences translocation and leaf distribution in vascular plants with contrasting anatomy. *Environmental Science: Nano* 6(8):2508-2519.

Spielman-Sun, Eleanor, et al.

2017 Impact of surface charge on cerium oxide nanoparticle uptake and translocation by wheat (*Triticum aestivum*). *Environmental Science & Technology* 51(13):7361-7368.

Stowers, Cheyenne, et al.

2018 Initial sterilization of soil affected interactions of cerium oxide nanoparticles and soybean seedlings (*Glycine max* (L.) Merr.) in a greenhouse study. *ACS Sustainable Chemistry & Engineering* 6(8):10307-10314.

Suda, Aomi, and Tomoyuki Makino

2018 Attenuation of inorganic arsenic and cadmium in rice grains using by-product iron materials from the casting industry combined with different water management practices. *Soil science and plant nutrition* 64(4):503-511.

Sun, Dequan, et al.

2014a Uptake and cellular distribution, in four plant species, of fluorescently labeled mesoporous silica nanoparticles. *Plant cell reports* 33(8):1389-1402.

Sun, Liming, et al.

2014b Water management practices affect arsenic and cadmium accumulation in rice grains. *The Scientific World Journal* 2014.

Sun, Qi, Jianmei Li, and Tao Le

2018a Zinc oxide nanoparticle as a novel class of antifungal agents: current advances and future perspectives. *Journal of agricultural and food chemistry* 66(43):11209-11220.

Sun, Sheng - Kai, et al.

2018b Decreasing arsenic accumulation in rice by overexpressing Os NIP 1; 1 and Os NIP 3; 3 through disrupting arsenite radial transport in roots. *New Phytologist* 219(2):641-653.

Sun, Wenjie, et al.

2020 Impacts of metallic nanoparticles and transformed products on soil health. *Critical Reviews in Environmental Science and Technology*:973-1002.

Sun, Wenjie, et al.

2021 Impacts of metallic nanoparticles and transformed products on soil health. *Critical Reviews in Environmental Science and Technology* 51(10):973-1002.

Syu, Chien-Hui, et al.

2013 Arsenic sequestration in iron plaque and its effect on As uptake by rice plants grown in paddy soils with high contents of As, iron oxides, and organic matter. *Soil Science and Plant Nutrition* 59(3):463-471.

Taylor, Gregory J, and AA Crowder

1983 Use of the DCB technique for extraction of hydrous iron oxides from roots of wetland plants. *American Journal of Botany* 70(8):1254-1257.

Theng, Benny KG, and Guodong Yuan

2008 Nanoparticles in the soil environment. *Elements* 4(6):395-399.

Tolaymat, Thabet, et al.

2017 Analysis of metallic and metal oxide nanomaterial environmental emissions. *Journal of cleaner production* 143:401-412.

Torn, Margaret S, et al.

1997 Mineral control of soil organic carbon storage and turnover. *Nature* 389(6647):170-173.

Tourinho, Paula S, et al.

2012 Metal - based nanoparticles in soil: Fate, behavior, and effects on soil invertebrates. *Environmental Toxicology and Chemistry* 31(8):1679-1692.

Tripathi, Durgesh Kumar, et al.

2012 Rice seedlings under cadmium stress: effect of silicon on growth, cadmium uptake, oxidative stress, antioxidant capacity and root and leaf structures. *Chemistry and Ecology* 28(3):281-291.

Tripathi, Preeti, et al.

2013 Silicon mediates arsenic tolerance in rice (*Oryza sativa* L.) through lowering of arsenic uptake and improved antioxidant defence system. *Ecological engineering* 52:96-103.

Tu, S. X., L. Ma, and T. Luongo

2004 Root exudates and arsenic accumulation in arsenic hyperaccumulating *pteris vittata* and non-hyperaccumulating *nephrolepis exaltata*. *Plant and Soil* 258(1-2):9-19.

Verma, Yukti, et al.

2021 Interaction of zinc oxide nanoparticles with soil: Insights into the chemical and biological properties. *Environmental Geochemistry and Health*:1-14.

Vives-Peris, Vicente, et al.

2020 Root exudates: from plant to rhizosphere and beyond. *Plant Cell Reports* 39(1):3-17.

Waalewijn-Kool, Pauline L, et al.

2013 Sorption, dissolution and pH determine the long-term equilibration and toxicity of coated and uncoated ZnO nanoparticles in soil. *Environmental pollution* 178:59-64.

Wang, HD, et al.

1993 Ferrihydrite, lepidocrocite, and goethite in coatings from east Texas vertic soils. *Soil Science Society of America Journal* 57(5):1381-1386.

Wang, Hong-Yan, et al.

2016 Mitigation of cadmium and arsenic in rice grain by applying different silicon fertilizers in contaminated fields. *Environmental Science and Pollution Research* 23(4):3781-3788.

Wang, Shengsen, et al.

2019a Biochar-supported nZVI (nZVI/BC) for contaminant removal from soil and water: a critical review. *Journal of hazardous materials* 373:820-834.

Wang, Tiangen, and John H Peverly

1999 Iron oxidation states on root surfaces of a wetland plant (*Phragmites australis*). *Soil Science Society of America Journal* 63(1):247-252.

Wang, Xiaoxuan, et al.

2021 Elucidating the impact of three metallic nanoagrichemicals and their bulk and ionic counterparts on the chemical properties of bulk and rhizosphere soils in rice paddies. *Environmental Pollution* 290:118005.

Wang, Xiaoxuan, Wenjie Sun, and Xingmao Ma

2019b Differential impacts of copper oxide nanoparticles and Copper (II) ions on the uptake and accumulation of arsenic in rice (*Oryza sativa*). *Environmental Pollution*.

Wang, Xiaoxuan, et al.

2018 Elucidating the effects of cerium oxide nanoparticles and zinc oxide nanoparticles on arsenic uptake and speciation in rice (*Oryza sativa*) in a hydroponic system. *Environmental Science & Technology* 52(17):10040-10047.

Wang, Xin, et al.

2015 Recent advances in arsenic bioavailability, transport, and speciation in rice. *Environmental Science and Pollution Research* 22(8):5742-5750.

Wang, Yi, et al.

2020 Improvement of nutrient elements and allicin content in green onion (*Allium fistulosum*) plants exposed to CuO nanoparticles. *Science of The Total Environment* 725:138387.

Wang, Yu-Min, Seydou Traore, and Tienfuan Kerh

2008 Monitoring event-based suspended sediment concentration by artificial neural network models. *WSEAS Transactions on Computers* 5(7):359-368.

White, Jason C, and Jorge Gardea-Torresdey

2018 Achieving food security through the very small. *Nature nanotechnology* 13(8):627-629.

Winston, Wayne

2014 *Microsoft Excel 2013 Data Analysis and Business Modeling: Data Analysis and Business Modeling*: Pearson Education.

Woolson, EA, JH Axley, and PC Kearney

1971 Correlation between available soil arsenic, estimated by six methods, and response of corn (*Zea mays* L.). Soil Science Society of America Journal 35(1):101-105.

Wu, Chuan, et al.

2016 Effect of silicate on arsenic fractionation in soils and its accumulation in rice plants. Chemosphere 165:478-486.

Wu, Fan, et al.

2020a Effects of zinc oxide nanoparticles on arsenic stress in rice (*Oryza sativa* L.): germination, early growth, and arsenic uptake. Environmental science and pollution research international.

Wu, Qianhua, et al.

2021 Regulatory mechanism of copper oxide nanoparticles on uptake of different species of arsenic in rice. Nanomaterials 11(9):2228.

Wu, Xinyi, et al.

2020b Application of TiO₂ nanoparticles to reduce bioaccumulation of arsenic in rice seedlings (*Oryza sativa* L.): A mechanistic study. Journal of Hazardous Materials:124047.

Xin, Xiaoping, et al.

2020 Nano-enabled agriculture: from nanoparticles to smart nanodelivery systems. Environmental Chemistry 17(6):413-425.

Xu, Chen, et al.

2015 Distinctive effects of TiO₂ and CuO nanoparticles on soil microbes and their community structures in flooded paddy soil. *Soil Biology and Biochemistry* 86:24-33.

Xu, Jiming, et al.

2017 OsHAC4 is critical for arsenate tolerance and regulates arsenic accumulation in rice. *New Phytologist* 215(3):1090-1101.

Xu, X. Y., S. P. McGrath, and F. J. Zhao

2007 Rapid reduction of arsenate in the medium mediated by plant roots. *New Phytologist* 176(3):590-599.

Yan, Shiwei, et al.

2021 Zinc oxide nanoparticles alleviate the arsenic toxicity and decrease the accumulation of arsenic in rice (*Oryza sativa* L.). *BMC Plant Biology* 21(1):150.

Yang, Judy Q., et al.

2021 4D imaging reveals mechanisms of clay-carbon protection and release. *Nature Communications* 12(1):622.

Yang, Xu-Jian, Zhihong Xu, and Hong Shen

2018 Drying–submergence alternation enhanced crystalline ratio and varied surface properties of iron plaque on rice (*Oryza sativa*) roots. *Environmental Science and Pollution Research* 25(4):3571-3587.

Yuan, Peng, et al.

2021 Ferrous ions inhibit Cu uptake and accumulation via inducing iron plaque and regulating the metabolism of rice plants exposed to CuO nanoparticles.

Environmental Science: Nano 8(5):1456-1468.

Zabrieski, Zac, et al.

2015 Pesticidal activity of metal oxide nanoparticles on plant pathogenic isolates of *Pythium*. *Ecotoxicology* 24(6):1305-1314.

Zavala, Yamily J., et al.

2008 Arsenic in rice: II. Arsenic speciation in USA grain and implications for human health. *Environmental Science & Technology* 42(10):3861-3866.

Zhang, Chaochun, et al.

2013 Do lignification and silicification of the cell wall precede silicon deposition in the silica cell of the rice (*Oryza sativa* L.) leaf epidermis? *Plant and soil* 372(1-2):137-149.

Zhang, Chunhua, et al.

2012 Iron oxidation-reduction and its impacts on cadmium bioavailability in paddy soils: a review. *Frontiers of Environmental Science & Engineering* 6(4):509-517.

Zhang, Qiqiong, Zhongzheng Yan, and Xiuzhen Li

2020 Ferrous iron facilitates the formation of iron plaque and enhances the tolerance of *Spartina alterniflora* to artificial sewage stress. *Marine Pollution Bulletin* 157:111379.

Zhang, Wei, et al.

2019 Impact of ZnO nanoparticles on Cd toxicity and bioaccumulation in rice (*Oryza sativa* L.). *Environmental Science and Pollution Research* 26(22):23119-23128.

Zhang, Weihua, et al.

2002 Arsenic speciation and distribution in an arsenic hyperaccumulating plant. *Science of the Total Environment* 300(1-3):167-177.

Zhang, Weilan, et al.

2018 Impact of nanoparticle surface properties on the attachment of cerium oxide nanoparticles to sand and kaolin. *Journal of environmental quality* 47(1):129-138.

Zhao, Fang-Jie, et al.

2013 Arsenic methylation in soils and its relationship with microbial arsM abundance and diversity, and as speciation in rice. *Environmental science & technology* 47(13):7147-7154.

Zhou, Dongmei, et al.

2011 Quantifying the adsorption and uptake of CuO nanoparticles by wheat root based on chemical extractions. *Journal of Environmental Sciences* 23(11):1852-1857.

Zhu, Zheng-Jiang, et al.

2012 Effect of surface charge on the uptake and distribution of gold nanoparticles in four plant species. *Environmental science & technology* 46(22):12391-12398.